

Crosslinked Polymers from Pyrolysis of Lignocellulosic Biomass

by

Mehul Ravindra Barde

A dissertation submitted to the Graduate Faculty of
Auburn University
in partial fulfillment of the
requirements for the Degree of
Doctor of Philosophy

Auburn, Alabama
December 15, 2018

Keywords: Bio-oil, crosslinked polymers, BioNovolac,
epoxy resins, cyanate esters, polyacrylates

Copyright 2018 by Mehul Ravindra Barde

Approved by

Dr. Maria L. Auad, Chair, Director of Center for Polymers and Advanced Composites and
Professor of Chemical Engineering, Auburn University, Auburn, AL

Dr. Sushil Adhikari, Director of Center for Bioenergy and Bioproducts and Professor of
Biosystems Engineering, Auburn University, Auburn, AL

Dr. Bryan Beckingham, Assistant Professor of Chemical Engineering, Auburn University,
Auburn, AL

Dr. Brian Via, Director of Forest Products Development Center and Regions Professor of Forest
Products, Auburn University, Auburn, AL

Abstract

Present research is aimed at the development of crosslinked polymers from biomass pyrolysis oil. Crosslinked polymers are high performance materials employed in a wide range of applications and are most commonly derived from petrochemicals. With the increasing depletion of petroleum and the climate change, the focus is shifted toward biomass-based polymers. Biomass has a great variety due to a vast number and types of plant species. Moreover, lignocellulosic biomass offers challenges for the development of materials due to its complex chemical nature. Pyrolysis of biomass efficiently breaks down biomass components to simpler organic compounds with differing functionalities which can be used for the development of novel monomers and polymers. For the current study, bio-oil was obtained from the fast pyrolysis of lignocellulosic biomass. Gas-chromatography-mass spectroscopy (GC-MS) was carried out for detection of compounds in the bio-oil. The hydroxyl number was measured using ^{31}P -Nuclear magnetic resonance (^{31}P -NMR) spectroscopy. Different monomeric structures were synthesized from bio-oil by reacting with specific reagents.

In chapter two, bio-oil was co-reacted with phenol and formaldehyde to produce bio-novolac resin. Glycidylation was performed on α -resorcylic acid to product another bio-based epoxy – GDGB. Semi-interpenetrating polymer networks (semi-IPN) of bio-novolac and GDGB were developed by crosslinking GDGB in immediate presence of bio-novolac. Differential scanning calorimetry (DSC) and dynamic mechanical analysis (DMA) were used for measuring glass transition temperature, storage modulus, loss modulus, $\tan \delta$ and active chains density.

In chapter 3, bio-oil and bio-novolac were glycidylated to form epoxidized bio-oil and epoxidized bio-novolac monomers which were crosslinked by an amine hardener – Jeffamine T-403. The thermo-mechanical performance of bio-oil-derived epoxy and novolac polymers was comparable to their conventional analogues.

In chapter 4 cyanate esters were produced from bio-oil organic phase and from bio-oil-derived biphenol (ORG-biphenol). Crosslinked cyanate esters from ORG-biphenol yielded higher glass transition temperature than bisphenol-A-cyanate ester.

In the final chapter, the aqueous phase of bio-oil was used for monomer synthesis. Methacrylation reaction was performed on bio-oil aqueous phase to produce a mixture of methacrylic monomers. Methacrylated aqueous bio-oil and acrylated epoxidized soybean oil were copolymerized to form crosslinked thermoset materials with sub-ambient glass transition temperatures.

Soxhlet extraction with refluxing dichloromethane was used for assessing mass retention of crosslinked materials. Morphology of the polymers was observed with scanning electron microscopy (SEM). Bio-oil based crosslinked polymers developed in this research study are sustainable and can be potentially applied in the fields of composites, coatings, adhesives, elastomers and packaging.

Keywords: Bio-oil, crosslinked polymers, BioNovolac, epoxy resins, cyanate esters, polyacrylates

Acknowledgments

Present research study is funded by US Department of Agriculture-National Institute of Food and Agriculture (USDA-NIFA-2015-67021-22842), National Science foundation - Center of Excellence in Nano-Bio Materials derived from Biorenewable and Waste Resources (NSF-CREST) and NSF-CREST Center for Sustainable Lightweight Materials (C-SLAM) award #1735971. I express my utmost gratitude to my research advisor and mentor Dr. Maria L. Auad for providing me the opportunity, guidance and motivation to pursue doctoral research in polymer science. I am thankful to the advisory committee members, Dr. Sushil Adhikari, Dr. Bryan Beckingham and Dr. Brian Via, for contributing their precious time and efforts in evaluating and improving current research project. I wish to sincerely thank Dr. Andrew Adamczyk for serving as the University Reader for the current dissertation. I would like to thank Department of Polymer and Fiber Engineering, Center for Polymers and Advanced Composites and Department of Chemical Engineering, at Samuel Ginn College of Engineering, Auburn University, Auburn for the research facilities, funds and administration. I thank Dr. Charles Edmunds, Dr. Nicole Labbè, Dr. Ramsis Farag, Dr. Bernal Sibaja, Dr. Yusuf Celikbag, Dr. Eldon Triggs, Dr. Zhouhong Wang, Dr. Michael Meadows, Dr. Michael Miller, Dr. Ming Chen, Dr. George Cheng for their noteworthy help, contributions and suggestions in progress of this research. I would like to extend my gratitude to the chair of Department of Chemical Engineering Dr. Mario Eden. I am very thankful to all my course instructors who helped me achieve more knowledge. I wholeheartedly thank my research colleagues and close friends for

their strong support throughout my graduate studies. I am thankful to the coffee, the elixir of my life, which made Ph.D. a beautiful journey. I am extremely indebted to my dear parents Mrs. Pournima Barde and Mr. Ravindra Barde and my dear sister Dr. Madhura Barde for the inexpressible and perpetual love and support. Lastly, I am profoundly grateful to Chemistry, an integral and ever-evolving science, which has imparted the meaning to my life.

Table of Contents

Abstract	ii
Acknowledgments.....	iv
List of Tables	xi
List of Figures.....	xii
List of Abbreviations	xv
Chapter 1: Introduction	1
1.1. Crosslinked Polymers: Importance, demand and raw materials	1
1.2. Petroleum: Recent problems and future consequences	7
1.3. Biomass: A potential alternative and an optimistic solution	9
1.4. Chemical transformation of biomass for crosslinked polymers: Overview and challenges	9
1.5. Thermochemical transformation of biomass	10
1.5.1. Pyrolysis of biomass	11
1.5.2. Biomass liquefaction	13
1.6. Bio-oil: Properties and characterization	14
1.7. Advances in polymers from bio-oil	19
1.7.1. Phenol-Formaldehyde polymers	19
1.7.2. Epoxy resins	20
1.7.3. Polyurethanes	20
1.8. Research objectives	22

References	25
Chapter 2: Bio-novolac/epoxy semi-interpenetrating polymer networks (semi-IPN)	38
2.1. Introduction	38
2.2. Experimental section.....	42
2.2.1. Materials	42
2.2.2. Methods.....	42
2.2.2.1. Characterization of fast pyrolysis bio-oil.....	42
2.2.2.2. Synthesis of novolac and bionovolac resins	43
2.2.2.3. Synthesis of glycidyl 3,5-diglycidoxybenzoate (GDGB)	44
2.2.2.4. Determination of epoxy equivalent weight (EEW)	45
2.2.2.5. Crosslinking of thermoset polymer networks	45
2.2.2.6. FTIR spectroscopy	46
2.2.2.7. Evaluation of thermo-mechanical performance.....	46
2.2.3. Results and discussion	48
2.2.3.1. Characterization of fast pyrolysis bio-oil.....	48
2.2.3.2. Characterization of BioNovolac resins	51
2.2.3.3. Characterization of glycidyl 3,5-diglycidoxybenzoate (GDGB).....	53
2.2.3.4. Network Formation.....	54
2.2.3.5. Evaluation of thermo-mechanical performance.....	58
2.2.3.6. Morphology.....	61
2.3. Conclusions	63
References	64

Chapter 3: Crosslinked networks from epoxidized bio-novolac and epoxidized bio-oil .. 70

3.1. Introduction	70
3.2. Experimental section.....	72
3.2.1. Materials	72
3.2.2. Methods	72
3.2.2.1. Characterization of fast pyrolysis bio-oil.....	72
3.2.2.2. Synthesis of novolac and bio-novolac resins	73
3.2.2.3. Synthesis of epoxy resins.....	73
3.2.2.4. Crosslinking of epoxy resins.....	74
3.2.2.5. Evaluation of thermo-mechanical performance.....	76
3.2.2.5. Other techniques	76
3.2.3. Results and discussion	77
3.2.3.1. Characterization of fast pyrolysis bio-oil.....	77
3.2.3.2. Characterization of BioNovolac resins	77
3.2.3.3. Characterization of epoxy resins.....	77
3.2.3.4. Thermo-mechanical performance of epoxy resins and other techniques.....	82
3.3. Conclusions	88
References	89

Chapter 4: High performance cyanate esters from biomass pyrolysis oil 92

4.1. Introduction	92
4.2. Experimental section.....	96
4.2.1. Materials	96
4.2.2. Methods	97

4.2.2.1. Fast pyrolysis of pine	97
4.2.2.2. Characterization of ORG-bio-oil	97
4.2.2.3. FTIR spectroscopy	98
4.2.2.4. Synthesis of ORG-biphenol	99
4.2.2.5. Synthesis of cyanate esters.....	99
4.2.2.6. Crosslinking of cyanate esters	102
4.2.2.7. Dynamic mechanical analysis.....	102
4.2.2.8. Morphology.....	102
4.2.3. Results and discussion	102
4.2.3.1. Characterization of ORG-bio-oil, ORG-biphenol and the cyanate esters.....	102
4.2.3.2. Thermo-mechanical performance of cyanate esters	106
4.2.3.3. Morphology of crosslinked cyanate esters.....	109
4.3. Conclusions	111
References	112
Chapter 5: Crosslinked acrylic polymers from aqueous phase of biomass pyrolysis oil and acrylated epoxidized soybean oil	118
5.1. Introduction	118
5.2. Experimental section.....	120
5.2.1. Materials	120
5.2.2. Methods	120
5.2.2.1. Fast pyrolysis of pine	120
5.2.2.2. Characterization of AQ-bio-oil.....	121
5.2.2.3. Synthesis and characterization of methacrylated aqueous bio-oil (MeABO)..	122
5.2.2.4. Polymerization of methacrylated monomers with AESO.....	123

5.2.2.5. Soxhlet extraction	126
5.2.2.6. Morphology.....	127
5.2.2.7. Dynamic mechanical analysis.....	127
5.2.3. Results and discussion	127
5.2.3.1. Characterization of AQ-bio-oil.....	127
5.2.3.2. Characterization of MeABO.....	129
5.2.3.3. FTIR spectroscopy of polymers.....	132
5.2.3.4. Soxhlet extraction	133
5.2.3.5. Morphology.....	134
5.2.3.6. Dynamic mechanical analysis.....	137
5.3. Conclusions	140
References	142
General Conclusions.....	148

List of Tables

Table 1.1: Market share of commonly used thermoset polymers	3
Table 1.2: Thermoset polymers: Chemistry and applications	5
Table 1.3: Differentiation between liquefaction and pyrolysis.....	13
Table 2.1: Hydroxyl content determined by ³¹ P-NMR technique	49
Table 2.2: Thermo-mechanical properties of thermosets	60
Table 3.1: Hydroxyl number measured by ³¹ P-NMR spectroscopy for (a) bio-oil and epoxidized bio-oil, (b) novolac and epoxidized novolac, (c) bio-novolac and epoxidized bio-novolac.....	81
Table 3.2: Epoxy equivalent weights of epoxy resins	82
Table 3.3: Thermo-mechanical properties of crosslinked epoxy resins	83
Table 4.1: Cyanate esters: Commercial products and properties.....	95
Table 4.2: Properties of ORG-bio-oil	103
Table 4.3: ³¹ P-NMR spectroscopy of ORG-bio-oil and ORG-biphenol.....	105
Table 5.1: Preparation of MeABO/AESO blends.....	124
Table 5.2: Properties of AQ-bio-oil	128
Table 5.3: ³¹ P-NMR spectroscopy of AQ-bio-oil, c-AQ-bio-oil and MeABO	132
Table 5.4: Thermo-mechanical properties of crosslinked polyacrylate samples	137

List of Figures

Figure 1.1: Schematic of molecular development of (a) thermoplastic polymer, (b) thermoset polymer.....	2
Figure 1.2: Auger-type pyrolysis reactor equipped with condensers	12
Figure 1.3: Pyrolysis products of lignin.....	15
Figure 1.4: Pyrolysis products of cellulose.....	16
Figure 1.5: Pyrolysis products of hemicelluloses	17
Figure 1.6: Research overview	22
Figure 2.1: Synthesis of (a) Novolac resin, (b) BioNovolac resin.....	44
Figure 2.2: Glycidylation of α -resorcylic acid.....	45
Figure 2.3: Compositional analysis of bio-oil by GC-MS	48
Figure 2.4: ^{31}P -NMR spectrum of bio-oil.....	50
Figure 2.5: FTIR spectra of (a) novolac (b) 50% BioNovolac and (c) bio-oil. Notes: ar – aromatic, ph – phenolic, oop – out of plane bending, al – aliphatic	51
Figure 2.6: BioNovolac extent of conversion.....	52
Figure 2.7: FTIR spectra of (a) α -resorcylic acid, (b) GDGB	53
Figure 2.8: Crosslinking of GDGB by DMAP	54
Figure 2.9: Grafting of BioNovolac and GDGB networks.....	55
Figure 2.10: FTIR spectra of (a) uncured GDGB (b) cured GDGB (c) cured GDGB: 50% BioNovolac 50:50 and (d) 50% BioNovolac	56
Figure 2.11: Species responsible for IR peak at 1652 cm^{-1} in cured networks.....	57
Figure 2.12: Curing of 50% BioNovolac, with and without DMAP	58

Figure 2.13: Glass transition temperature of semi-IPNs with (a) 10% BioNovolac (b) 50% BioNovolac	59
Figure 2.14: SEM Photographs (a) cured GDGB (b) cured GDGB:50% BioNovolac (50:50) (c) uncured 50% BioNovolac	62
Figure 3.1: Glycidylation of phenolic substrates	75
Figure 3.2: FTIR spectra of (a) bio-oil (b) epoxidized bio-oil.....	78
Figure 3.3: FTIR spectra of (a) bio-novolac (b) epoxidized bio-novolac.....	79
Figure 3.4: FTIR spectra of (a) novolac (b) epoxidized novolac.....	80
Figure 3.5: Storage modulus of crosslinked epoxy resins	84
Figure 3.6: SEM photographs of crosslinked thermosets: (a) epoxidized novolac, (b) epoxidized bio-novolac (EBN), (c) EBN:GDGB 50:50, (d) epoxidized bio-oil.....	87
Figure 4.1: Synthesis of bisphenol-A based cyanate ester (BPA-CE) and its crosslinked network..	93
Figure 4.2: Synthesis of ORG-biphenol, ORG-bio-oil-CE and ORG-biphenol-CE.....	101
Figure 4.3: GC-MS analysis of ORG-bio-oil.....	103
Figure 4.4: FTIR spectra of (a) ORG-bio-oil, (b) ORG-bio-oil-CE, (c) ORG-biphenol, (d) ORG-biphenol-CE, (e) bisphenol-A and (f) BPA-CE.....	106
Figure 4.5: Thermo-mechanical properties of cyanate esters: (a) storage modulus, (b) $\tan \delta$	107
Figure 4.6: SEM photographs of fractured surface of crosslinked materials: (a) BPA-CE, (b) ORG-bio-oil-CE and (c) ORG-biphenol-CE	109
Figure 5.1: Methacrylation of c-AQ-bio-oil	123
Figure 5.2: Polymerization of MeABO	124
Figure 5.3: Polymerization of AESO.....	125
Figure 5.4: Polymerization of MeABO and AESO	126
Figure 5.5: Chromatogram of AQ-bio-oil.....	128
Figure 5.6: ^{31}P -NMR spectra of c-AQ-bio-oil	129
Figure 5.7: FTIR spectra of (a) c-AQ-bio-oil (b) MeABO.....	130

Figure 5.8: $^1\text{H-NMR}$ spectra of (a) MeABO, (b) c-AQ-bio-oil.....	131
Figure 5.9: FTIR spectroscopy of (a) monomer blends of MeABO and AESO, (b) polymeric systems of MeABO and AESO.....	133
Figure 5.10: Morphology by scanning electron microscopy (a) poly(MeABO), (b) poly(75:25A), (c) poly(50:50A), (d) poly(25:75A) and (e) poly(AESO)	134
Figure 5.11: Glass transition temperature of crosslinked acrylates: Effects of copolymerization and crosslinking	140

List of Abbreviations

AESO	Acrylated Epoxidized Soybean Oil
AHEW	Active Hydrogen Equivalent Weight
AQ	Aqueous
ASTM	American Society for Testing and Materials
ATR	Attenuated Total Reflection
BHT	Butylated hydroxy toluene
BPA	Bisphenol-A
CE	Cyanate Ester
DMA	Dynamic Mechanical Analysis
DMAP	4-(Dimethylamino)pyridine
DSC	Differential Scanning Calorimetry
EBN	Epoxidized Bio-Novolac
EBO	Epoxidized Bio-oil
EEW	Epoxy Equivalent Weight
EN	Epoxidized Novolac
FTIR	Fourier Transform Infrared
GC-MS	Gas Chromatography-Mass Spectroscopy
GDGB	Glycidyl 3,5-diglycidoxybenzoate
IPN	Interpenetrating Polymer Network

MeABO	Methacrylated Aqueous Bio-oil
NHND	N-hydroxy-5-norbornene-2,3-dicarboximide
NIST	National Institute of Standards and Technology
NMR	Nuclear Magnetic Resonance
ORG	Organic
ppm	parts per million
PTFE	poly(tetrafluoroethylene)
SEM	Scanning Electron Microscopy
TAN	Total acid number
TMDP	2-Chloro-4,4,5,5-tetramethyl-1,3,2-dioxaphospholane

Chapter 1

Introduction

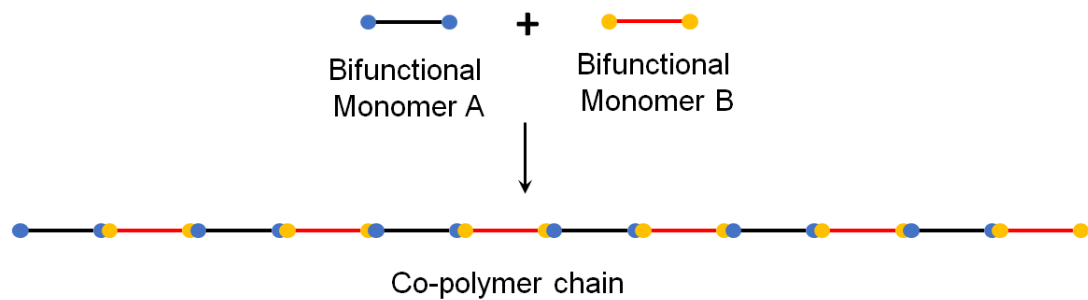
1.1. Crosslinked polymers: Importance, demand and raw materials

Innovation has been a prime factor in the development of polymers since their early developments. The current polymer industry observes a steady and lucrative growth due to the global demands arising out of higher performance requirements, major financial investments and ever-evolving breakthroughs in materials sciences. Polymeric materials are universally used in a vast range of household and industrial applications. Moreover, the global production of polymeric resins and fibers was around 380 million metric tons in the year 2015.[1] Although polymeric materials have penetrated almost every aspect of the modern life, they are primarily dependent on petroleum resources until today.

Polymers can be categorized into thermoplastics and thermosets based on their thermal treatments and properties. At molecular level, the macromolecular chains of thermoplastic polymers can mobilize on supplying energy and hence, thermoplastics can be molten, re-designed and thus, are often easily recyclable. On the other hand, polymeric chains present in thermoset polymers are chemically bonded, thereby providing a restriction to the molecular movement despite subjecting to moderate amount of energy. As a result, thermoset polymers do not melt and dissolve.[2] The chemical bonds connecting the polymeric chains are called crosslinks or crosslinking points; whereas the process of formation of the three-dimensional network by bonding of polymer chains is called crosslinking. The distinguishing aspect of thermoset polymers is that at least one

monomer possesses more than two functionalities which results in functional molecular branches that lead to crosslinked network formation as depicted in Figure 1.1. In most of the cases, the reaction between two multi-functional monomers or the reaction between a functional polymer and a multi-functional monomer (often called as crosslinking agent) is necessary.

(a) Characteristics of thermoplastic polymers



(b) Characteristics of thermoset polymers

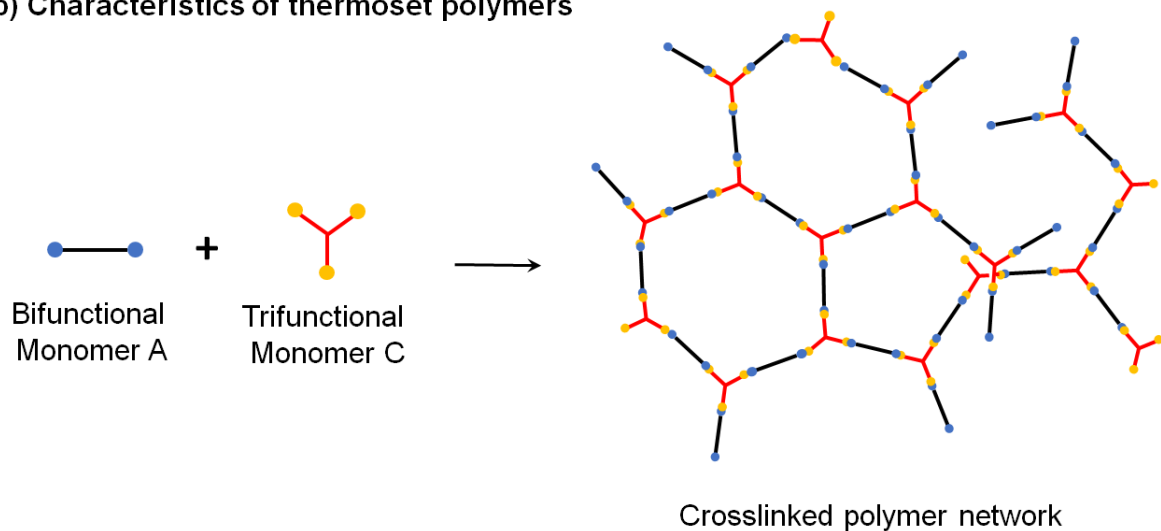


Figure 1.1: Schematic of molecular development of (a) thermoplastic polymer, (b) thermoset polymer.

The crosslinked network of thermoset polymers imparts higher thermal, mechanical and chemical properties than otherwise non-crosslinked analogues. Depending on the type of functionality, the structure of the repeating unit and the degree of crosslinking, thermoset polymers can have a wide range of properties. Thermoset polymers include a range of polymers

such as polyester, epoxy, phenol-formaldehyde, urea-formaldehyde, melamine-formaldehyde, polyurethane, vinyl ester, cyanate ester, bismaleimides, silicone polymers etc. The distribution of polymers is displayed in Table 1.1, depending on the type and region in which they are consumed.

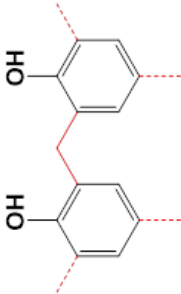
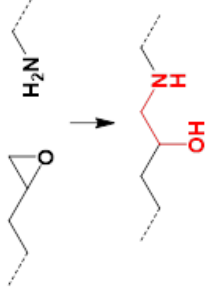
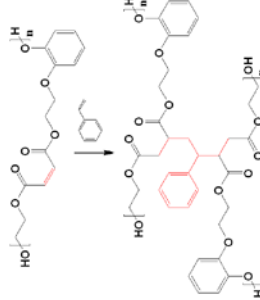
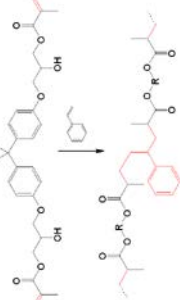
Table 1.1: Market share of commonly used thermoset polymers [3]

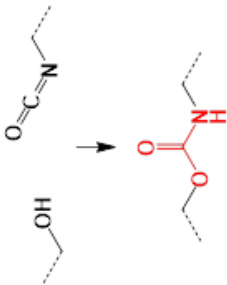
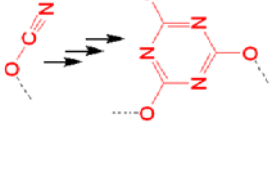
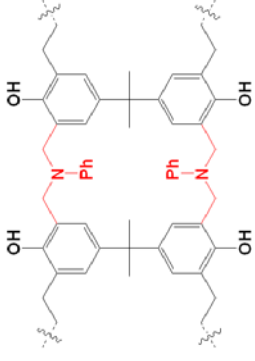
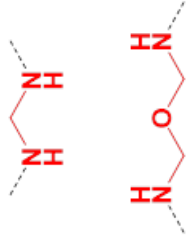
Thermoset Polymer	Annual Consumption (%)	
	USA	Worldwide
Polyurethane	36	31
Unsaturated polyesters	22	20
Phenolic resins	20	18
Amino resins	18	25
Epoxy	4	6

Resin is the typical term for easily processible, pre-polymeric thermoset. Resins appear in the forms of viscous liquids or solids, and can be transformed into rigid, strong materials after crosslinking with other multi-functional monomers. The incorporation of fillers, especially fibers, to resins leads to a composite material that shows enhanced properties.[4] Currently, the polymer-fiber composite materials rule a wide range of applications including automobile, aerospace, civil structures, electronic components and sports equipment. Additionally, coatings and inks are pigmented polymeric composite materials that are abundantly utilized in a variety of applications. The final state of most of the polymers in all of the above-mentioned applications is usually highly-crosslinked. Due to this reason and with increasing necessity for highly-crosslinkable, multi-functional polymers, the market for thermoset resins is expected to

increase at a rapid rate. In Table 1.2, the chemistry and applications of commonly used thermosets are listed.

Table 1.2: Thermoset polymers: Chemistry and applications

Thermoset Polymer	Typical monomers, oligomers and crosslinkers	Molecular Structures/ Reactions/ Crosslinks	Properties	Applications	Cost (USD/lb)	Ref
Phenol-Formaldehyde	Phenol, Formaldehyde, hexamethylene-tetramine (crosslinker)		Excellent chemical resistance, high mechanical strength, flame retardancy, heat stability	Wood composites, laminates, adhesives, photoresists	0.75-0.85	[5-9]
Epoxy	Diglycidylether of bisphenol-A (DGEBA), polyamine (crosslinker)		Excellent mechanical, thermal and electrical properties, high adhesion	Coatings, composites, adhesives, electronics	1-1.12	[9-11]
Unsaturated polyester	Maleic anhydride, ethylene glycol, phthalic anhydride, styrene (reactive diluent)		High crosslink density, chemical and corrosion resistance	Composites, electronics, sports equipment, automotive components	1.74-1.95	[9, 12-14]
Vinyl ester	Bis-glycidylmethacrylate, styrene (reactive diluent)		Excellent corrosion resistance, elevated temperature resistance, good adhesion, flexibility	Fiber-reinforced composites, marine construction and coatings	2.04-2.23	[9, 14]

Thermoset Polymer	Typical monomers, oligomers and crosslinkers	Molecular Structures/ Reactions/ Crosslinks	Properties	Applications	Cost (USD/lb)	Ref
Polyurethane	Polyol, diisocyanate		Good flexibility, biocompatibility, chemical resistance, versatility	Foams, elastomers, coatings, adhesives	1.05-1.15	[9, 15, 16]
Cyanate ester	2,2'-Bis-(4-cyanatophenyl)propane		Superior glass transition temperature, high mechanical strength, low dielectric constant	Aerospace components, radiation-resistant composites, radomes, photonics	Around 300	[17-22]
Benzoxazine	Bisphenol-A, formaldehyde, aniline		Near-zero volume change, low water absorption, high glass transition temperature	High performance composites	Around 300	[8, 22]
Amino resin	Urea/melamine, formaldehyde		Good adhesion, light colored and odorless, good resistance to electrical tracking	Domestic plugs, switches, wood adhesives, coatings, molding powders	0.95-1 (Urea) 1.35-1.75 (Melamine)	[9, 23, 24]

The development of thermoset networks depends on the monomer functionality and type. Organic compounds with multifunctional groups of alcohols, carboxylic acids, isocyanates, amines are often used for synthesis of crosslinked polymers. Aromatic compounds substituted with electron-donating groups (for example, phenol) also provide multifunctionality for successful development of polymers such as phenol-formaldehyde discussed in Table 1.2. Phenol is also used for synthesis of other monomers including cresol, resorcinol, bisphenol-A, bisphenol-F and their halogenated derivatives.[25, 26] All of the bisphenols offer bifunctionality of phenolic hydroxyl groups which lead to development of polymers such as epoxy resins, cyanate esters and polycarbonates. Many of the important monomers, including phenol, bisphenol-A, formaldehyde, styrene, are obtained through a series of processes starting from petroleum products. The future of crosslinked polymers depends on the uninterrupted supply of multifunctional monomers. As a result, it seeks the continuous supply of petrochemicals for the generation of monomers unless alternative resources are developed for their availability. A detailed discussion about effects of perpetual consumption of petroleum is outlined in the next section.

1.2. Petroleum: Recent problems and future consequences

Although the total global amount of fossil fuel seems to be enormous, the sources and quantity of petroleum are limited. With greatly increasing demand for energy and fuels, there are concerns over adequate supply of non-renewable fuels and petroleum products. The estimated global proved reserves of oil (1696.6 billion barrels), natural gas (193.5 trillion m³) and coal (1035 billion tones) at the end of 2017 indicate a caution considering the rapidly increasing growth rate of global consumption of all the fossil fuels.[27] Nearly 5 % of petroleum derivatives find applications in the production of chemicals whereas most of the remaining is currently used as transportation fuel.[28] Exponential growth in the global population,

enhanced industrialization and improved technologies have kept raising the petroleum consumption.[29] Coming years are expected to observe higher consumption of fossil fuels due to increased demand of energy and materials. Often, it is agreed that the proved reserves are subject to show an increase due to developing technologies of petroleum recovery and refining with time. Though this is true, it would be inappropriate to only depend on the unproven reserves converting to proved-reserves. Heavy dependence on the limited resources affects the economy when the gap between supply and demand is high. Since the naturally occurring deposits are geographically limited, the production of petroleum derivatives involves political aspects too. Though exports and imports might help to balance the international oil requirements, continuous depletion of fossil fuels deposits might lead to the world energy crisis.

It is also worthwhile to consider the ramifications of petroleum consumption on the environment. Burning of petroleum products such as natural gas or coal is fundamentally an oxidation reaction, which eventually yields carbon dioxide (CO₂) as a by-product. Human activities, such as the utilization of fuels to obtain energy lead to CO₂ emissions, are generally termed as anthropogenic CO₂ emissions.[30] The emitted carbon dioxide absorbs solar radiations and increases the overall temperature of the atmosphere. The effect is known as greenhouse effect and the gases that cause it are called greenhouse gases. Increasing amount of CO₂ emissions is a considerable impact on climate change. In brief, global warming can be directly related to ever increasing consumption of petroleum resources and energy generation. In last 10 years, net CO₂ emissions have raised by 1.6 % globally with China, United States of America and India cumulatively contributing to 50 % of global CO₂ emissions in 2016.[31] As per the Paris agreement, United Nations have aimed to restrict the rise in global temperature well below 2 °C in this century.[32]

1.3. Biomass: A potential alternative and an optimistic solution

Considering the mentioned limitations and environmental concerns, it is essential to shift the focus from petroleum to the renewable and environmentally benign resources. Biomass appearing in the form of plants, trees, crops, grass etc., can be grown periodically in a wide range of geographic conditions. In other words, the very characteristics of renewability renders biomass as a potential source of chemicals. Since the biomass is renewable unlike fossil fuels, it offers a sustainable path for indefinite period of time. Moreover, plants absorb CO₂ in presence of sunlight to produce energy via photosynthesis. Biomass growth is beneficial, as the plants would absorb more amount of CO₂ in the atmosphere thereby offsetting the CO₂ emissions. The amount of CO₂ emitted from the energy generation or combustion of biomass is lower than total amount of CO₂ absorbed in process of producing that biomass and hence carbon dioxide balance is always positive.[33] This clearly indicates that biomass and biofuels are necessary not only for fulfilling energy demands of humans but also for good environmental equilibrium.

1.4. Chemical transformation of biomass for crosslinked polymers: Overview and challenges

Biomass constituents can be chemically transformed to obtain desired compounds for polymer synthesis. Corma et al. have extensively reviewed biomass transformation methods for producing chemicals.[34] Plant oil triglycerides are often used for resin synthesis.[35] Depending on the species of the plant, varying triglycerides and fatty acids can be exploited for polymer network build-up.[36] Natural bio-resources can be utilized to yield functional compounds, which can lead to thermosetting polymers. Famous examples include the compounds cardanol, cardol, anacardic acid and 2-methylcardol from cashew nut shell liquid (CNSL) that is obtained from cashews.[37, 38] Many CNSL-based developments in resins,

crosslinked networks and composites have been documented in literature.[39-46] Abietic acid and its isomers found in rosin have been used for successful resin developments in various attempts.[47-52] Crosslinked polymers have been developed from bio-based phenolic monomers: vanillin,[53, 54] eugenol,[55, 56] and phenolic, natural macromolecules: tannins[57] and lignin.[58-60]

All the above-mentioned developments are based on a wide range of biomass species. Moreover, the monomers, oligomers and resins obtained through such bio-based resources go through a series of chemical reactions and purification processes that can be energy intensive and economically cumbersome. With every additional step, the yield of subsequent product decreases resulting into higher process costs. Further, utilization of edible biomass such as edible oils, vanilla extract, soy-based products, corn, sugars etc for materials development may bring food scarcity if used excessively. It is beneficial to enlighten more uniform and efficient processes for biomass transformation which can be less dependent on the biomass species and free from tedious process complexity.

1.5. Thermochemical transformation of biomass

Thermochemical transformation processes cause the biomass components to undergo chemical changes with the driving force of thermal energy. The products of thermochemical decomposition of biomass not only provide chemicals for polymer synthesis but also the fuels.[61] Woody biomass is complex assembly of biomacromolecules, viz., lignin, cellulose and hemicelluloses, which are oxygenated hydrocarbons.[62] and it has been found that virgin biomass has several limitations. For a long time, wood has been used by combustion process to yield heat energy, but it has lower energy density as compared to conventional fuels. To enhance the energy density, it is needed to reduce the oxygen and water content of virgin biomass and produce hydrocarbons similar to the ones found in petroleum derivatives. The

energy density is intensified in the case of thermochemical decomposition products. Depending on the thermochemical transformation used, the products can be chemically rich with particular category of compounds, for example, gasification yields syngas; while pyrolysis and liquefaction yield liquid bio-oil.[63]

1.5.1. Pyrolysis of biomass

Pyrolysis is a process in which biomass is heated at elevated temperatures in the absence of oxygen. Biomass pyrolysis carries out thermal decomposition of the lignocellulosic macromolecules and produces non-condensable gases (CO, H₂ etc.), solid char and condensable vapors which after condensation, yield liquid product termed as biomass pyrolysis oil or bio-oil.[64] Bio-oil is a crude mixture of nearly 200 organic compounds or more, most of which are oxygenated hydrocarbons with molecular weights relatively smaller than macromolecular components found in biomass.[65] Low molecular weight compounds offer benefits such as liquid fuels and chemicals. Depending on the process parameters, pyrolysis can be classified into slow, fast or flash pyrolysis. Slow pyrolysis generally yields solid bio-char as the major product while flash pyrolysis produces gases predominantly. Fast pyrolysis process is efficient for producing liquid bio-oil since it yields around 60-75 % of liquid bio-oil yield.[62] It is carried out at around 500 °C and short vapor residence time (0.5 - 2 s).[66] Several types of reactors can be used for biomass pyrolysis; bubbling fluidized bed reactor being the most commonly used on a large scale. Amongst others, transported bed, rotating cone, entrained flow and ablative pyrolyzers are used. Bubbling fluid bed and circulating fluid bed reactors are known for high heat transfer rate whereas entrained flow reactor employs lower heating rates. Circulating fluid bed produces more char than the bubbling fluid bed. Rotating cone pyrolyzer is a modification of circulated fluid bed with the difference being a rotating, heated cone designed for pyrolyzing the biomass. Ablative reactors are equipped with high

shearing heated plates that melt the wood and hence do not require any heat transfer gas.[67] Ground (less than 2 mm) and dried (less than 10 % water) biomass is fed to the pyrolyzer and is heated at a rapid rate while ensuring a good heat transfer to biomass particles. The biomass particles, after pyrolysis reactions, generally yield char and gases which are separated by cyclones. Of the generated gases, condensable vapors produce liquid bio-oil.[68] Recent advances have emphasized the use of Auger-type reactor, also considered as alternative reactor that can be used on lab-scale too.[69, 70] A schematic of pyrolysis using Auger-type reactor, and series of condensers is shown in Figure 1.2

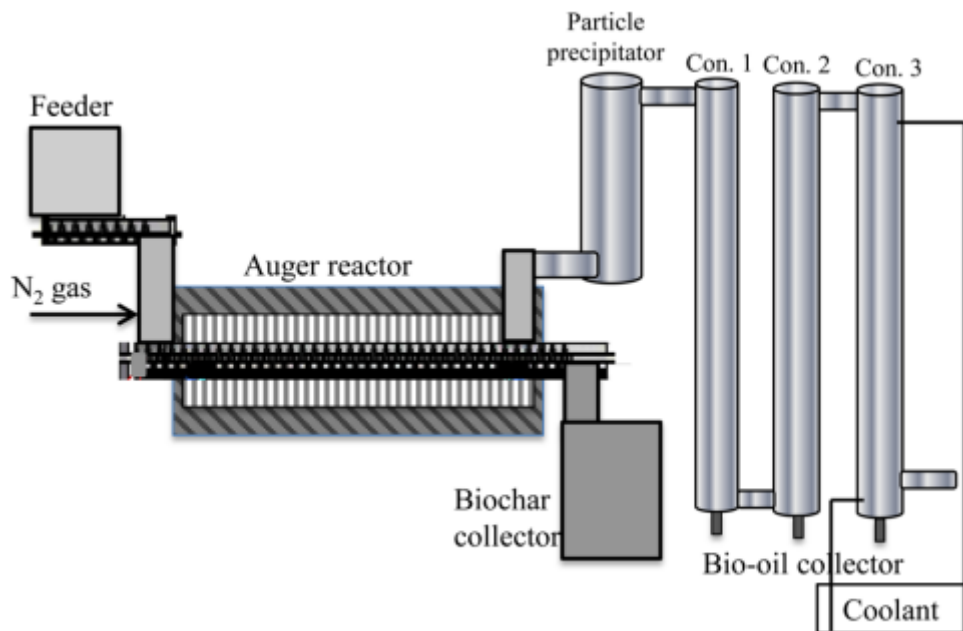


Figure 1.2: Auger-type pyrolysis reactor equipped with condensers [70]

[Reprinted with permission from Energy Fuels 28, 11, 6966-6973. Copyright 2014 American Chemical Society]

Pyrolysis process presents several advantages. Production efficiency of thermal conversion processes is generally higher than typical biochemical conversion processes due to controllable parameters such as flow rate, heating rate, residence time etc. Nearly any kind of biomass can

be fed to pyrolyzer, including waste from forests or agricultural residues. Thus, varying complicated structures and mixtures of natural polymers are susceptible to thermal breakdown due to pyrolysis and hence can be successfully converted to a homogeneous mixture of smaller organic compounds.

1.5.2. Biomass liquefaction

Liquefaction is another important thermochemical transformation process that can be used to derive liquid bio-oil from biomass. The main process parameters that differentiate liquefaction from pyrolysis are use of catalyst, solvent and low operating temperature.[71, 72] A brief comparison between pyrolysis and liquefaction is presented in Table 1.3

Table 1.3: Differentiation between liquefaction and pyrolysis [72]

Process	Solvent	Temperature (°C)	Pressure (bar)	Product
Direct Liquefaction	Yes	150 – 420	< 1 – 240	Organic Liquid
Flash/ Fast Pyrolysis	No	< 500	< 1 – 5	

[Adapted with permission from Chem. Eng. Technol. 31, 5, 667-677. Copyright 2008 John Wiley and Sons.]

Mechanistic studies have reflected that the organic molecules produced after the decomposition of biomass re-polymerize in different ways in liquefaction and pyrolysis. The decomposition during liquefaction is catalyzed and follows reactions of organic compounds in liquid media; whereas pyrolysis process is characterized by uncatalyzed, vapor-phase reactions of organic molecules.[71] The direct liquefaction process can be beneficial in some cases because drying

and grinding of biomass may not be necessary. However, the final liquid product from liquefaction generally has higher moisture content as compared to pyrolysis bio-oil.[73]

1.6. Bio-oil: Properties and characterization

The components in the bio-oil show variation depending on the nature of biomass feed. It is found that wood biomass yield highest organic yields while the agricultural residues tend to relatively lower yields due to higher ash content.[74, 75] Lignocellulosic biomass produces different pyrolysis products from lignin, cellulose and hemicelluloses.[76] Typical degradation components are shown in Figure 1.3, 1.4 and 1.5.

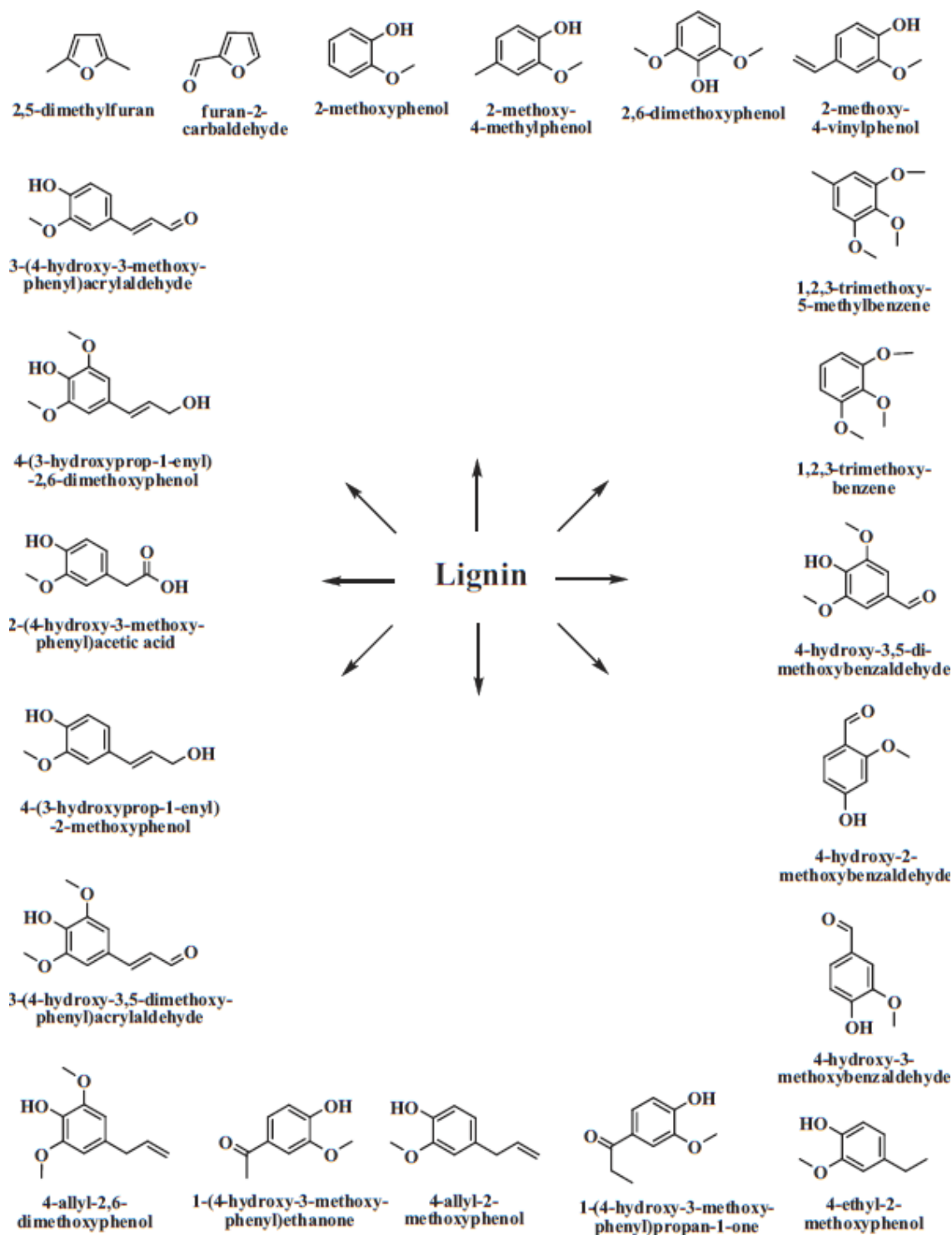


Figure 1.3: Pyrolysis products of lignin [76]

[Reprinted with permission from J. Anal. Appl. Pyrol. 105, 55-74. Copyright 2014 Elsevier]

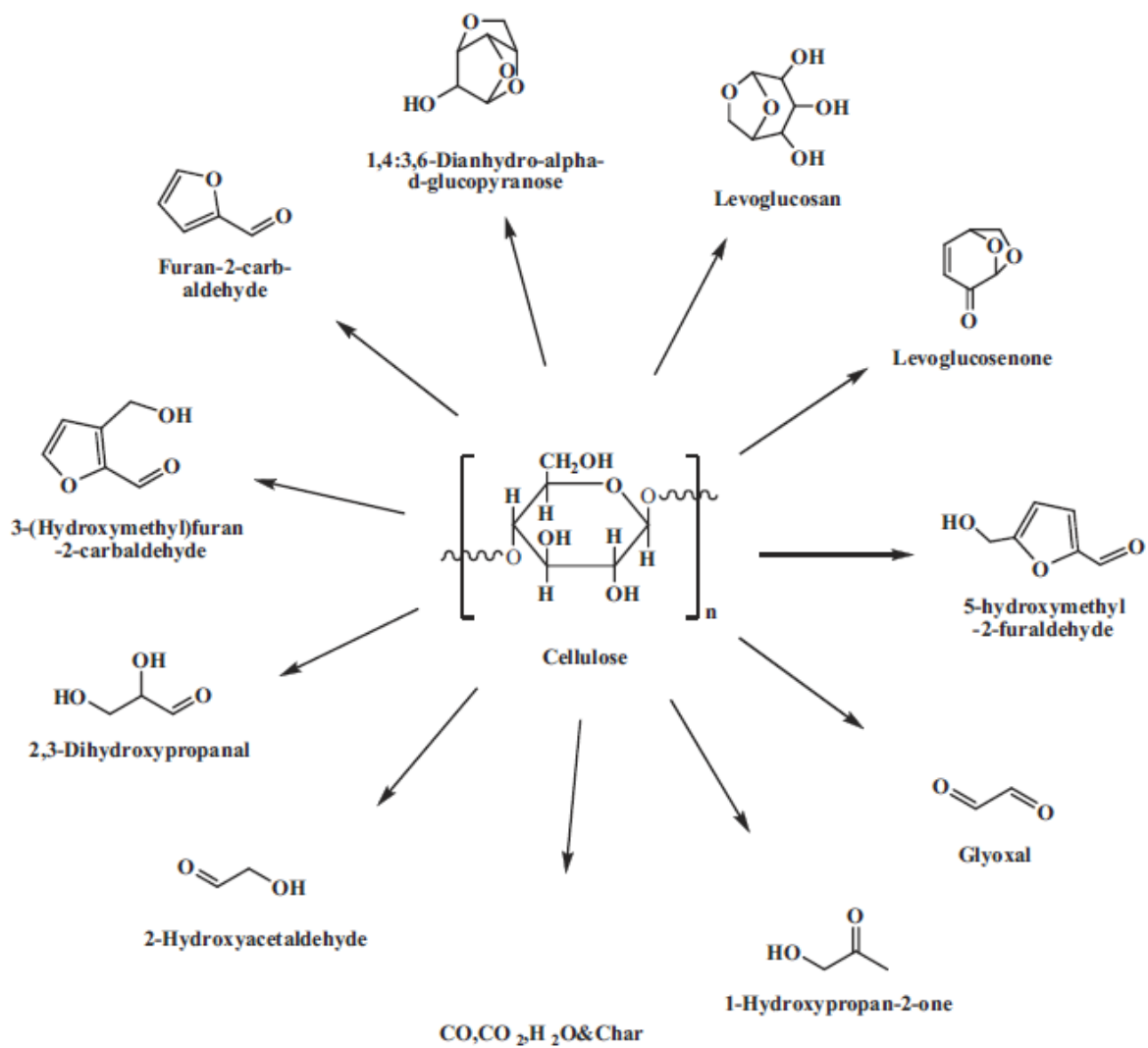


Figure 1.4: Pyrolysis products of cellulose [76]

[Reprinted with permission from J. Anal. Appl. Pyrol. 105, 55-74. Copyright 2014 Elsevier]

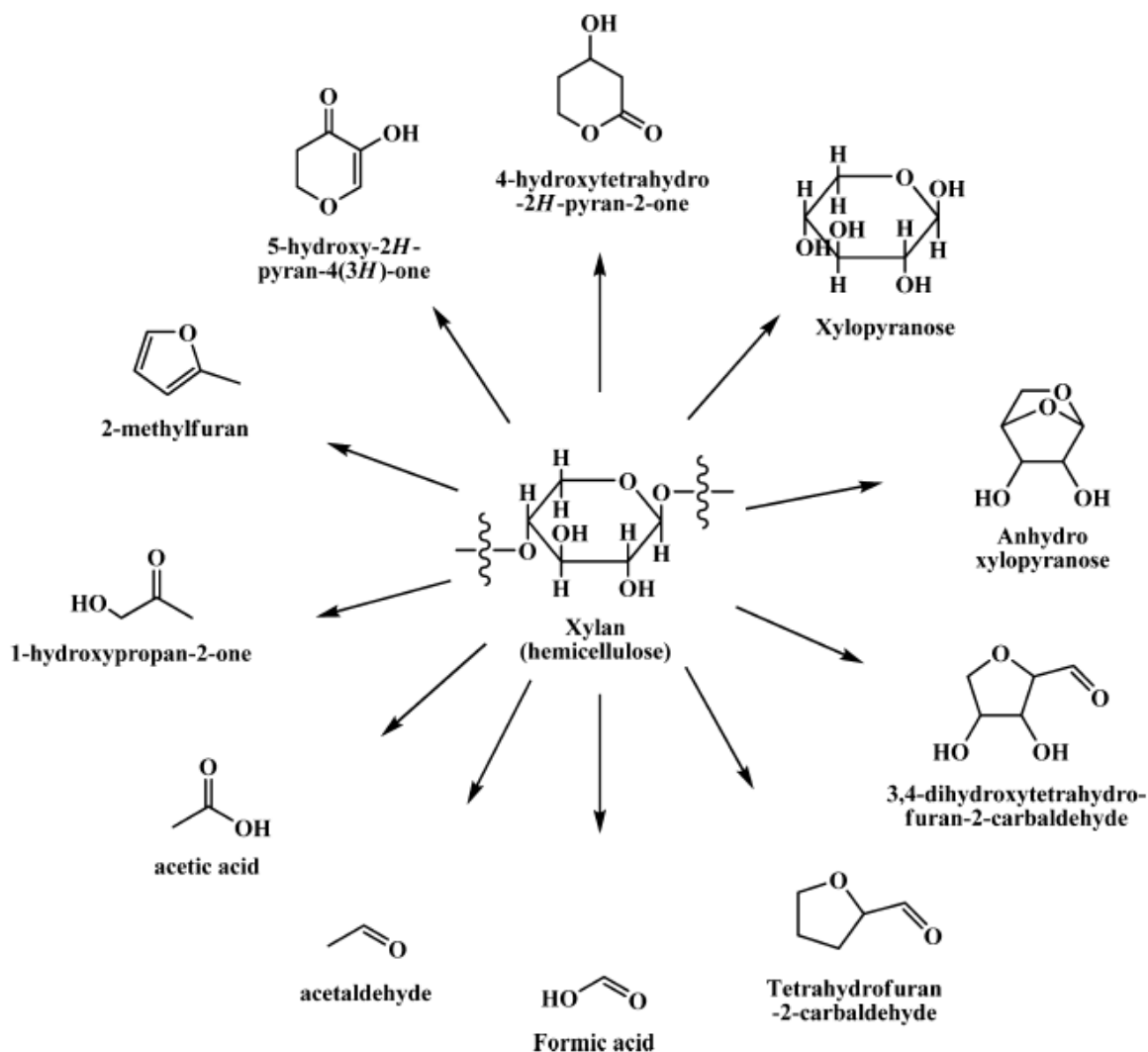


Figure 1.5: Pyrolysis products of hemicelluloses [76]

[Reprinted with permission from J. Anal. Appl. Pyrol. 105, 55-74. Copyright 2014 Elsevier]

Although the crude bio-oil proves to be more efficient than virgin biomass for energy generation, its applications are limited to boilers and turbines.[77, 78] For making it more usable, it has to be upgraded in specific ways so that either the calorific value can be enhanced or the particular fraction can be used as a rich source of chemicals. Enhancement of energy density is usually achieved by removal of oxygen from the oxygenated hydrocarbons using metal catalysts through catalytic cracking or hydrotreating.[79, 80] Zeolites have been intensively studied and used with good results to upgrade bio-oil compounds to

hydrocarbons.[81-83] Nevertheless, there are many challenges associated with using bio-oil as fuels. Crude bio-oil has a low heating value as compared to conventional fuels. Upgrading improves the heating value but increases the cost due to additional process and catalysts involved. Catalysts are expensive as well as vulnerable to poisoning and thus, great care needs to be taken for recovery of catalysts. The bio-oil offers additional challenges in storage and handling due to acidic character, viscosity and instability. It also does not blend with conventional fuels, thereby eliminating the possibilities of partial replacements. However, bio-oil is a potential source of multiple chemicals as it has a wider range of organic compounds than petroleum. Liquid-liquid extractions with addition of solvent to the crude bio-oil can concentrate the bio-oil with specific chemical categories.[84, 85] Diethyl ether and dichloromethane are commonly used for extraction of compounds but different solvents can be used.[86] This leads bio-oil to be a candidate for reservoir of chemicals. Organic compounds are necessary raw materials in many important applications such as medical, pharmaceuticals and especially, polymers. Most of the objects are made up of polymeric materials. Synthetic polymers make up domestic vessels, packaging films, building structures, adhesives, paints, furniture, medical devices, electronics, automotive and aerospace parts, protective clothing, shields, armors and many more. The molecular structures of polymers can be designed as per the desired properties and these molecular chains can be built from the components available in bio-oil.

Bio-oil contains many oxygenated compounds such as alcohol, acid, phenols and hence can be used to build polymeric structures. Moreover, some structures found in bio-oil are macromolecular fractions of lignin and resemble polyphenolic resins. As far as bio-oil is concerned, monomer separation or purification is more of a challenge than monomer synthesis is. Several researchers have attempted to build polymeric structures from bio-oil components.

Sibaja et al. have reviewed sustainable polymers from pyrolysis bio-oil.[87] With the help of hydroxyl functionality, several types of polymers can be developed from single bio-oil source.

1.7. Advances in Polymers from Bio-Oil

1.7.1. Phenol-Formaldehyde polymers

Phenol-formaldehyde resins are categorized into resol and novolac depending on the molar ratio and reaction conditions. Resols are prepared in basic condition with molar excess of formaldehyde over phenol whereas novolacs are synthesized in acidic condition with molar excess of phenol. Resols can be heat cured due to the general presence terminal, self-condensable methylol groups. Novolac resins are crosslinked by crosslinking agents such as hexamethylenetetramine at ortho-, para- positions on aromatic rings. Bio-oil contains substituted monomeric phenols and macromolecular phenolic fractions. With substituent groups on aromatic rings, derived phenols can show different reactivity towards formaldehyde. However, the phenolic-rich fraction after separation from whole bio-oil is expected to have considerably lower price than pure phenol derived from petroleum. This gives a cost-effective opportunity for producing phenol-formaldehyde resins. Immense research has been done on phenol-formaldehyde type resins from biomass pyrolysis oil[88], lignin[89-91] and other types of bio-derivatives such as cashew nut shell liquid[92-95], vanillin[96] etc. Phenol was partially replaced by phenolic-rich fraction of the bio-oil to synthesize resol-type phenol-formaldehyde resins.[97] Resol resins were also attempted by modifying the bark autoclave extractives.[98] Formate-assisted fast pyrolysis was used to obtain bio-oil, which was reacted with formaldehyde in acidic medium for preparing novolac-type resins.[99] Most of these bio-oil derived phenolic resins find application in wood adhesives.

1.7.2. Epoxy resins

Many researchers have crosslinked epoxy resins with bio-oil obtained from varying sources and processes. Pyrolysis of loblolly pine was carried out and the subsequent bio-oil was substituted in conventional epoxy resin formulations before catalyzing with triphenylphosphine. It was found that the bio-oil had good compatibility with epoxy resin and was able to process thermoset materials with high glass transition temperature and crosslinking density.[100] In another attempt of successful replacement, acetone treated blend of bio-oil and epoxy resin was reacted with diethylenetriamine hardener.[101] The bio-derived substituent component was obtained from liquefaction process by changing several parameters.[102] Wood liquefied with polyethylene glycol/glycerol and H_2SO_4 [103, 104], ozone-pretreated wood liquefied with polyethylene glycol/glycerol and H_2SO_4 [105], bagasse liquefied with ethylene carbonate[106] were blended with epoxy resins and were cured to yield crosslinked epoxies. Sibaja[107] and Celikbag et al.[108] carried out direct glycidylation of biomass pyrolysis oil and biomass liquefaction oil, respectively. It was found that the acidic and phenolic hydroxyl functionalities can be epoxidized with a two-step glycidylation reaction with epichlorohydrin under basic conditions.

1.7.3. Polyurethanes

Polyurethane foams with a potential application in car-cushion, have been prepared from fast pyrolysis oil of wheat straw.[109] Organic extract of bio-oil from ethyl acetate was used along with polyethylene glycol to react with blend of polymethylene polyphenylene isocyanate and polymeric diphenylmethane diisocyanate. The resulting foams had a comparable resilience, tensile strength and tear strength. In a similar study, biomass liquefaction heavy oil was blended with polyethylene glycol and reacted with diphenylmethane diisocyanate to yield polyurethane

foams.[110] Foams were also developed by reacting polymeric diphenylmethane diisocyanate with bio-polyol derived from liquefaction of soybean straw with crude glycerol.[111] Lignin has been used as direct or indirect reactant in the polyurethane synthesis.[112-115] Microwave-assisted pyrolysis oil also has been used to prepare polyurethane foams.[116]

1.8. Research objectives

Pyrolyzed lignocellulosic biomass produces liquid bio-oil, composition of which mainly depends on the presence of lignin, cellulose and hemicellulose in the biomass. The decomposed organic compounds dominate their presence in organic phase or aqueous phase depending on the hydrophilicity and hydrophobicity. A crude bio-oil consists of hundreds of organic compounds. It is challenging to selectively transform the bio-oil compounds to functional monomers. The current research is dedicated to produce categories of chemically similar monomers and polymers using specific organic transformation of the bio-oil. Following research objectives have been designed in such a way that maximum utilization of bio-oil components can be made for polymer synthesis. Both phases of bio-oil have been considered for development of monomers, resins and resulting crosslinked polymers. Bio-oil based monomers can be a new class of bio-refined monomers for development of thermosetting networks. Figure 1.6 shows the overview of present research.

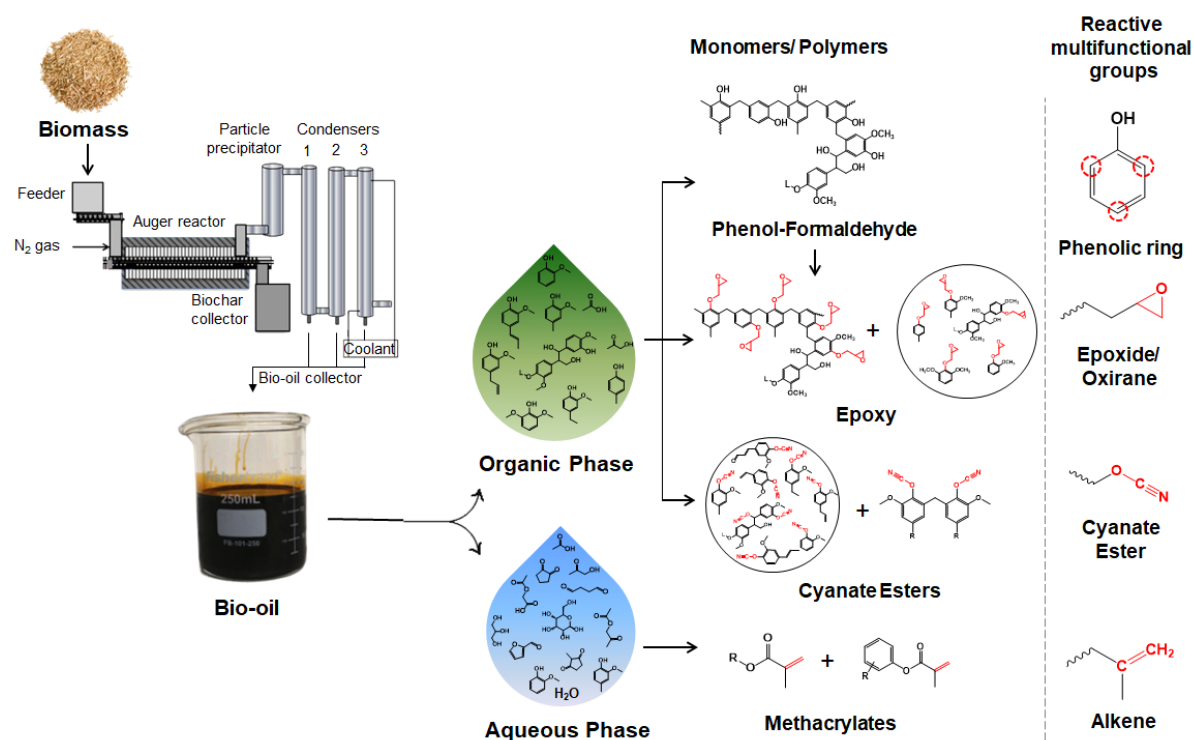


Figure 1.6: Research overview

Chapter 2: Semi-interpenetrating bio-novolac/epoxy thermoset polymer networks

In the second chapter, bio-oil was used as replacement of phenol in the production of phenol-formaldehyde novolac resins. Phenolic resins have been an important class of thermoset polymers over last 100 years and are synthesized from phenol, a petroleum-based expensive chemical. Attempts have been made to synthesize bio-oil based phenol-formaldehyde resin (bio-novolac). Semi-interpenetrating polymer networks from bio-novolac and an epoxy resin from α -resorcylic acid were developed. Polymerization of epoxy resin from α -resorcylic acid was initiated by 4-(dimethylamino)pyridine in the immediate presence of prepolymeric bio-novolac to build the networks. These networks were less dependent on petroleum resources because of reduced use of phenol as well as no utilization of traditional, petroleum-based amine/anhydride hardeners for crosslinking epoxies.

Chapter 3: Crosslinked networks of epoxidized bio-novolac and epoxy resins from fast pyrolysis bio-oil

In the third chapter of this dissertation, bio-novolac and bio-oil were epoxidized to produce epoxy resins that can compete with conventional epoxidized novolac and bisphenol-A based epoxy resins. Emphasis was given on epoxidation reactions of several phenolic substrates and the resulting epoxy resins were crosslinked with conventional amine hardeners. Chemical characterization and mechanical tests were performed to compare the bio-oil and bio-novolac based epoxides to petroleum-based analogues. Direct glycidylation of bio-oil and bio-novolac was aimed to replace bisphenol-A which has health hazards to humans. Additionally, these systems consume less amount of petrochemicals as compared to commercially available epoxide systems. Epoxy-amine two component systems are famous and prevalent in many applications such as surface coatings, adhesives, composites and hence, the systems presented in this objective attempt to satisfy the epoxy market requirements.

Chapter 4: High performance cyanate ester resins from biomass pyrolysis oil

In chapter 4, the bio-oil organic phase was derivetized to cyanate ester functionality to obtain high performance polycyanate ester thermosets. Cyanate esters have proved to possess extraordinary thermal and thermo-mechanical properties. The cyanation approach gives an opportunity to produce similar high performance, high-valued materials from a low value bio-oil. Synthesis of biphenolic compounds from monophenolic compounds is also emphasized for subsequent cyanation to produce bifunctional cyanate ester monomers. The bifunctionality is expected to improve the performance of crosslinked cyanate ester networks.

Chapter 5: Crosslinked acrylic polymers from aqueous phase of biomass pyrolysis oil and acrylated epoxidized soybean oil

Previous objectives have mainly exploited phenolic functionalities present in the organic phase of bio-oil. In the final chapter, the aqueous phase of bio-oil is considered as the raw material for monomer synthesis. Bio-oil aqueous phase has significant amount of water (around 50 wt%) and is often treated as a waste stream. Apart from water, it contains aliphatic hydroxy and phenolic compounds which can be functionalized by reacting with specific reagents. Methacrylation of hydroxyl groups with methacryloyl chloride offers an opportunity to incorporate polymerizable C=C groups. Crosslinking of the methacrylated bio-oil with acrylated epoxidized soybean oil is also considered for tuning the properties while maintaining the sustainability.

References

- [1] R. Geyer, J.R. Jambeck, K.L. Law, Production, use, and fate of all plastics ever made, *Science Advances* 3(7) (2017) 5.
- [2] H. Dodiuk, S.H. Goodman, Introduction, in: H. Dodiuk, S.H. Goodman (Eds.), *Handbook of Thermoset Plastics*, Elsevier, San Diego, 2014, pp. 1-12.
- [3] M. Biron, The plastics industry: economic overview, in: M. Biron (Ed.), *Thermosets and Composites: Technical information for plastic users*, Elsevier Science & Technology Books 2003, pp. 31-144.
- [4] B.Z. Jang, Part I: Materials-Dominated Issues for Composites, in: B.Z. Jang (Ed.), *Advanced Polymer Composites: Principles and Applications*, ASM International, Materials Park, Ohio, 1994, pp. 1-83.
- [5] A. Knop, L.A. Pilato, *Phenolic Resins: Chemistry, Applications and Performance*, Springer-Verlag Berlin Heidelberg, New York and Tokyo, 1985.
- [6] J.A. Brydson, Phenolic Resins, in: J.A. Brydson (Ed.), *Plastic Materials*, Butterworth-Heinemann, Oxford, 1999, pp. 635-666.
- [7] K.J. Saunders, Phenol-Formaldehyde Polymers, in: K.J. Saunders (Ed.), *Organic Polymer Chemistry*, Chapman and Hall, New York, 1988, pp. 316-340.
- [8] S.K.S.N. Kumar, Reghunadhan C.P., Polybenzoxazines and State-of-the-Art High-Temperature Polymers, in: S.K.S. Kumar, R.C.P. Nair (Eds.), *Polybenzoxazines: Chemistry and Properties*, iSmithers, Shawbury, UK, 2010, pp. 1-50.
- [9] Current Resin Pricing. <http://www.plasticsnews.com/resin/thermosets/current-pricing>. (Accessed 25th July 2018).

- [10] B. Ellis, Introduction to the chemistry, synthesis, manufacture and characterization of epoxy resins, in: B. Ellis (Ed.), *Chemistry and Technology of Epoxy Resins* Chapman & Hall, United Kingdom, 1993, pp. 1-35.
- [11] M. Ogata, N. Kinjo, T. Kawata, Effects of crosslinking on physical properties of phenol-formaldehyde novolac cured epoxy resins, 48(4) (1993) 601.
- [12] D. Ratna, Chemistry, Properties and Applications of Thermoset Resins, in: D. Ratna (Ed.), *Handbook of Thermoset Resins*, iSmithers, Shawbury, UK, 2009, pp. 83-99.
- [13] C.F. Jasso-Gastine, O. Laguna, Unsaturated Polyester Resins (Polyester Composites), in: J.C. Salamone (Ed.) *Polymeric Materials Encyclopedia*, CRC Press, Boca Raton, FL, 1996, pp. 8476-8485.
- [14] C.E. Browning, Introduction: New Applications from New Materials, in: J.M. Margolis (Ed.), *Advanced Thermoset Composites: Industrial and Commercial Applications*, Van Nostrand Reinhold Company, New York, 1986, pp. 7-13.
- [15] I.R. Clemitson, Castable Polyurethane Elastomers, Taylor & Francis Group, United States of America, 2008, pp. 1-2.
- [16] M. Szycher, in: M. Szycher (Ed.), *Szycher's Handbook of Polyurethanes*, CRC Press, Boca Raton, FL, 1999, pp. 3:31-3:34.
- [17] C.P.R. Nair, D. Mathew, K.N. Ninan, Cyanate ester resins, recent developments, *New Polymerization Techniques and Synthetic Methodologies* 155 (2001) 1-99.
- [18] M.R. Kessler, Cyanate Ester Resins, in: L. Nicolais, A. Borzacchiello (Eds.) *Wiley Encyclopedia of Composites*, John Wiley & Sons, Inc., 2012, pp. 658-672.
- [19] T. Fang, D.A. Shimp, Polycyanate esters - Science and applications, *Progress in Polymer Science* 20(1) (1995) 61-118.

- [20] G. Wang, G. Fu, T.L. Gao, H. Kuang, R.G. Wang, F. Yang, W.C. Jiao, L.F. Hao, W.B. Liu, Preparation and characterization of novel film adhesives based on cyanate ester resin for bonding advanced radome, *International Journal of Adhesion and Adhesives* 68 (2016) 80-86.
- [21] A. Inamdar, J. Cherukattu, A. Anand, B. Kandasubramanian, Thermoplastic-Toughened High-Temperature Cyanate Esters and Their Application in Advanced Composites, *Industrial & Engineering Chemistry Research* 57(13) (2018) 4479-4504.
- [22] Commercial Sources.
<https://scifinder.cas.org/scifinder/view/scifinder/scifinderExplore.jsf>. (Accessed 29th July 2018).
- [23] A. Pizzi, C.C. Ibeh, Amines, in: H. Dodiuk, S.H. Goodman (Eds.), *Handbook of Thermoset Plastics*, Elsevier, San Diego, CA, 2014, pp. 75-92.
- [24] B. Meyer, in: B. Meyer (Ed.), *Urea-Formaldehyde Polymers*, Addison-Wesley Publishing Company, Massachusetts, 1979, pp. 156-214.
- [25] J. Wallace, Phenol, *Kirk-Othmer Encyclopedia of Chemical Technology*, John Wiley & Sons, Inc., 2005, pp. 1-11.
- [26] H. Fiege, H.-W. Voges, T. Hamamoto, S. Umemura, T. Iwata, H. Miki, Y. Fujita, H.-J. Buysch, D. Garbe, W. Paulus, Phenol Derivatives, *Ullmann's Encyclopedia of Industrial Chemistry*, Wiley-VCH Verlag GmbH & Co. KGaA, Weinheim, 2000, pp. 521-576.
- [27] BP Statistical Review of World Energy 2018, BP, London, UK, 2018, pp. 1-53.
- [28] A.J. Ragauskas, C.K. Williams, B.H. Davison, G. Britovsek, J. Cairney, C.A. Eckert, W.J. Frederick, J.P. Hallett, D.J. Leak, C.L. Liotta, J.R. Mielenz, R. Murphy, R. Templer, T. Tschaplinski, The path forward for biofuels and biomaterials, *Science* 311(5760) (2006) 484-489.
- [29] L. Suganthi, A.A. Samuel, Energy models for demand forecasting-A review, *Renewable & Sustainable Energy Reviews* 16(2) (2012) 1223-1240.

- [30] G.A. Folberth, T.M. Butler, W.J. Collins, S.T. Rumbold, Megacities and climate change - A brief overview, *Environmental Pollution* 203 (2015) 235-242.
- [31] BP Statistical Review of World Energy 2017, London, UK, 2017, pp. 1-49.
- [32] The Paris Agreement, 2015. <https://unfccc.int/process-and-meetings/the-paris-agreement/the-paris-agreement>. (Accessed 17th August 2018).
- [33] S. Capareda, Biomass as Energy Source, in: S. Capareda (Ed.), *Introduction to Biomass Energy Conversions*, CRC Press, Florida, USA, 2014, p. 8.
- [34] A. Corma, S. Iborra, A. Velty, Chemical routes for the transformation of biomass into chemicals, *Chemical Reviews* 107(6) (2007) 2411-2502.
- [35] F. Seniha Güner, Y. Yağcı, A. Tuncer Erciyes, Polymers from triglyceride oils, *Progress in Polymer Science* 31(7) (2006) 633-670.
- [36] J.R. Kim, S. Sharma, The development and comparison of bio-thermoset plastics from epoxidized plant oils, *Industrial Crops and Products* 36(1) (2012) 485-499.
- [37] J.M. Raquez, M. Deleglise, M.F. Lacrampe, P. Krawczak, Thermosetting (bio)materials derived from renewable resources: A critical review, *Progress in Polymer Science* 35(4) (2010) 487-509.
- [38] M. Yuliana, T.N.T. Bich, S. Faika, L.H. Huynh, F.E. Soetaredjo, Y.H. Ju, Separation and purification of cardol, cardanol and anacardic acid from cashew (*Anacardium occidentale* L.) nut-shell liquid using a simple two-step column chromatography, *Journal of the Taiwan Institute of Chemical Engineers* 45(5) (2014) 2187-2193.
- [39] S. Kanehashi, S. Tamura, K. Kato, T. Honda, K. Ogino, T. Miyakoshi, Photopolymerization of Bio-Based Epoxy Prepolymers Derived from Cashew Nut Shell Liquid (CNSL), *Journal of Fiber Science and Technology* 73(9) (2017) 210-221.

- [40] F. Jaillet, H. Nouailhas, B. Boutevin, S. Caillol, Synthesis of novel bio-based vinyl ester from dicyclopentadiene prepolymer, cashew nut shell liquid, and soybean oil, *European Journal of Lipid Science and Technology* 118(9) (2016) 1336-1349.
- [41] A. Maiorana, L.Y. Ren, G. Lo Re, S. Spinella, C.Y. Ryu, P. Dubois, R.A. Gross, Bio-based epoxy resin toughening with cashew nut shell liquid-derived resin, *Green Materials* 3(3) (2015) 80-92.
- [42] A.E. Costa, A.C.H. Barreto, D.S. Rosa, F.J.N. Maia, D. Lomonaco, S.E. Mazzetto, Thermal and mechanical properties of biocomposites based on a cashew nut shell liquid matrix reinforced with bamboo fibers, *Journal of Composite Materials* 49(18) (2015) 2203-2215.
- [43] T.S. Gandhi, M.R. Patel, B.Z. Dholakiya, Mechanical, thermal and fire properties of sustainable rigid polyurethane foam derived from cashew nut shell liquid, *International Journal of Plastics Technology* 19(1) (2015) 30-46.
- [44] P. Kasemsiri, A. Neramittagapong, P. Chindaprasirt, Curing kinetic, thermal and adhesive properties of epoxy resin cured with cashew nut shell liquid, *Thermochimica Acta* 600 (2015) 20-27.
- [45] M. Telascreea, A.L. Leao, M.Z. Ferreira, H.F.F. Pupo, B.M. Cherian, S. Narine, Use of a Cashew Nut Shell Liquid Resin as a Potential Replacement for Phenolic Resins in the Preparation of Panels - A Review, *Molecular Crystals and Liquid Crystals* 604(1) (2014) 222-232.
- [46] T.S. Gandhi, M.R. Patel, B.Z. Dholakiya, Synthesis and characterization of different types of epoxide-based Mannich polyols from low-cost cashew nut shell liquid, *Research on Chemical Intermediates* 40(3) (2014) 1223-1232.
- [47] L.L. Deng, C.Y. Ha, C.N. Sun, B.W. Zhou, J. Yu, M.M. Shen, J.Q. Mo, Properties of Bio-based Epoxy Resins from Rosin with Different Flexible Chains, *Industrial & Engineering Chemistry Research* 52(37) (2013) 13233-13240.

- [48] Y.P. Yang, M.G. Shen, X. Huang, H.B. Zhang, S.B. Shang, J. Song, Synthesis and performance of a thermosetting resin: Acrylated epoxidized soybean oil curing with a rosin-based acrylamide, *Journal of Applied Polymer Science* 134(9) (2017) 7.
- [49] T.T. Li, X.Q. Liu, Y.H. Jiang, S.Q. Ma, J. Zhu, Bio-based shape memory epoxy resin synthesized from rosin acid, *Iranian Polymer Journal* 25(11) (2016) 957-965.
- [50] G.G. Sacripante, K. Zhou, M. Farooque, Sustainable Polyester Resins Derived from Rosins, *Macromolecules* 48(19) (2015) 6876-6881.
- [51] C. Mantzaridis, A.L. Brocas, A. Llevot, G. Cendejas, R. Auvergne, S. Caillol, S. Carlotti, H. Cramail, Rosin acid oligomers as precursors of DGEBA-free epoxy resins, *Green Chemistry* 15(11) (2013) 3091-3098.
- [52] L.L. Deng, M.M. Shen, J. Yu, K. Wu, C.Y. Ha, Preparation, Characterization, and Flame Retardancy of Novel Rosin-Based Siloxane Epoxy Resins, *Industrial & Engineering Chemistry Research* 51(24) (2012) 8178-8184.
- [53] M. Fache, B. Boutevin, S. Caillol, Vanillin, a key-intermediate of biobased polymers, *European Polymer Journal* 68 (2015) 488-502.
- [54] B.G. Harvey, A.J. Guenther, H.A. Meylemans, S.R.L. Haines, K.R. Lamison, T.J. Groshens, L.R. Cambrea, M.C. Davis, W.W. Lai, Renewable thermosetting resins and thermoplastics from vanillin, *Green Chemistry* 17(2) (2015) 1249-1258.
- [55] D. Guzman, X. Ramis, X. Fernandez-Francos, S. De la Flor, A. Serra, Preparation of new biobased coatings from a triglycidyl eugenol derivative through thiol-epoxy click reaction, *Progress in Organic Coatings* 114 (2018) 259-267.
- [56] B.G. Harvey, A.J. Guenther, G.R. Yandek, L.R. Cambrea, H.A. Meylemans, L.C. Baldwin, J.T. Reams, Synthesis and characterization of a renewable cyanate ester/polycarbonate network derived from eugenol, *Polymer* 55(20) (2014) 5073-5079.

- [57] C. Aouf, S. Benyahya, A. Esnouf, S. Caillol, B. Boutevin, H. Fulcrand, Tara tannins as phenolic precursors of thermosetting epoxy resins, *European Polymer Journal* 55 (2014) 186-198.
- [58] L.B. Tavares, C.V. Boas, G.R. Schleder, A.M. Nacas, D.S. Rosa, D.J. Santos, Bio-based polyurethane prepared from Kraft lignin and modified castor oil, *Express Polymer Letters* 10(11) (2016) 927-940.
- [59] S. Zhao, M.M. Abu-Omar, Synthesis of Renewable Thermoset Polymers through Successive Lignin Modification Using Lignin-Derived Phenols, *Acs Sustainable Chemistry & Engineering* 5(6) (2017) 5059-5066.
- [60] Y. Jiang, D.C. Ding, S. Zhao, H.Y. Zhu, H.I. Kenttamaa, M.M. Abu-Omar, Renewable thermoset polymers based on lignin and carbohydrate derived monomers, *Green Chemistry* 20(5) (2018) 1131-1138.
- [61] B. Kamm, M. Gerhardt, S. Leiß, The Biorefinery Concept - Thermochemical Production of Building Blocks and Syngas, in: M. Crocker (Ed.), *Thermochemical Conversion of Biomass to Liquid Fuels and Chemicals*, Royal Society of Chemistry, Cambridge, UK, 2010, pp. 46-62.
- [62] D. Mohan, C.U. Pittman, P.H. Steele, Pyrolysis of wood/biomass for bio-oil: A critical review, *Energy & Fuels* 20(3) (2006) 848-889.
- [63] S.C. Capareda, Biomass Conversion Processes, in: S.C. Capareda (Ed.), *Introduction to Biomass Energy Conversions*, CRC Press, Boca Raton, FL, 2014, pp. 43-82.
- [64] T. Kan, V. Strezov, T.J. Evans, Lignocellulosic biomass pyrolysis: A review of product properties and effects of pyrolysis parameters, *Renewable & Sustainable Energy Reviews* 57 (2016) 1126-1140.
- [65] K. Jacobson, K.C. Maheria, A.K. Dalai, Bio-oil valorization: A review, *Renewable & Sustainable Energy Reviews* 23 (2013) 91-106.

- [66] A.A. Peterson, F. Vogel, R.P. Lachance, M. Froling, M.J. Antal, J.W. Tester, Thermochemical biofuel production in hydrothermal media: A review of sub- and supercritical water technologies, *Energy & Environmental Science* 1(1) (2008) 32-65.
- [67] A.V. Bridgwater, Principles and practice of biomass fast pyrolysis processes for liquids, *Journal of Analytical and Applied Pyrolysis* 51(1-2) (1999) 3-22.
- [68] A.V. Bridgwater, Fast Pyrolysis of Biomass for Energy and Fuels, in: M. Crocker (Ed.), *Thermochemical Conversion of Biomass to Liquid Fuels and Chemicals*, Royal Society of Chemistry, Cambridge, 2010, pp. 151-156.
- [69] J.N. Brown, Development of a lab-scale auger reactor for biomass fast pyrolysis and process optimization using response surface methodology, *Mechanical Engineering*, Iowa State University, Ames, Iowa, 2009, p. 249.
- [70] P. Kim, S. Weaver, K. Noh, N. Labbe, Characteristics of Bio-Oils Produced by an Intermediate Semipilot Scale Pyrolysis Auger Reactor Equipped with Multistage Condensers, *Energy & Fuels* 28(11) (2014) 6966-6973.
- [71] A. Demirbaş, Mechanisms of liquefaction and pyrolysis reactions of biomass, *Energy Conversion and Management* 41(6) (2000) 633-646.
- [72] F. Behrendt, Y. Neubauer, M. Oevermann, B. Wilmes, N. Zobel, Direct liquefaction of biomass, *Chemical Engineering & Technology* 31(5) (2008) 667-677.
- [73] S.C. Capareda, Biomass Liquefaction, in: S.C. Capareda (Ed.), *Introduction to Biomass Energy Conversions*, CRC Press, Boca Raton, 2014, pp. 439-470.
- [74] Y. Solantausta, A. Oasmaa, K. Sipila, C. Lindfors, J. Lehto, J. Autio, P. Jokela, J. Alin, J. Heiskanen, Bio-oil Production from Biomass: Steps toward Demonstration, *Energy & Fuels* 26(1) (2012) 233-240.
- [75] A. Oasmaa, Y. Solantausta, V. Arpiainen, E. Kuoppala, K. Sipila, Fast Pyrolysis Bio-Oils from Wood and Agricultural Residues, *Energy & Fuels* 24 (2010) 1380-1388.

- [76] P.K. Kanaujia, Y.K. Sharma, M.O. Garg, D. Tripathi, R. Singh, Review of analytical strategies in the production and upgrading of bio-oils derived from lignocellulosic biomass, *Journal of Analytical and Applied Pyrolysis* 105 (2014) 55-74.
- [77] D. Chiamonti, A. Oasmaa, Y. Solantausta, Power generation using fast pyrolysis liquids from biomass, *Renewable & Sustainable Energy Reviews* 11(6) (2007) 1056-1086.
- [78] D.C. Elliott, Historical developments in hydroprocessing bio-oils, *Energy & Fuels* 21(3) (2007) 1792-1815.
- [79] S.C. Capareda, Pyrolysis, in: S.C. Capareda (Ed.), *Introduction to Biomass Energy Conversions*, CRC Press, Boca Raton, 2014, p. 346.
- [80] C. Briens, J. Piskorz, F. Berruti, - Biomass Valorization for Fuel and Chemicals Production -- A Review, *International Journal of Chemical Reactor Engineering* - 6(1) (2008).
- [81] Y.C. Shi, E.H. Xing, K.J. Wu, J.L. Wang, M.D. Yang, Y.L. Wu, Recent progress on upgrading of bio-oil to hydrocarbons over metal/zeolite bifunctional catalysts, *Catalysis Science & Technology* 7(12) (2017) 2385-2415.
- [82] M. Shemfe, S. Gu, B. Fidalgo, Techno-economic analysis of biofuel production via bio-oil zeolite upgrading: An evaluation of two catalyst regeneration systems, *Biomass & Bioenergy* 98 (2017) 182-193.
- [83] A. Veses, B. Puertolas, M.S. Callen, T. Garcia, Catalytic upgrading of biomass derived pyrolysis vapors over metal-loaded ZSM-5 zeolites: Effect of different metal cations on the bio-oil final properties, *Microporous and Mesoporous Materials* 209 (2015) 189-196.
- [84] A. Oasmaa, E. Kuoppala, J.F. Selin, S. Gust, Y. Solantausta, Fast pyrolysis of forestry residue and pine. 4. Improvement of the product quality by solvent addition, *Energy & Fuels* 18(5) (2004) 1578-1583.
- [85] K. Sipila, E. Kuoppala, L. Fagernas, A. Oasmaa, Characterization of biomass-based flash pyrolysis oils, *Biomass & Bioenergy* 14(2) (1998) 103-113.

- [86] H.W. Chen, Q.H. Song, B. Liao, Q.X. Guo, Further Separation, Characterization, and Upgrading for Upper and Bottom Layers from Phase Separation of Biomass Pyrolysis Oils, *Energy & Fuels* 25(10) (2011) 4655-4661.
- [87] B.S. Hernandez, M. Barde, B. Via, M.L. Auad, Sustainable products from bio-oils, *Mrs Bulletin* 42(5) (2017) 365-370.
- [88] A. Effendi, H. Gerhauser, A.V. Bridgwater, Production of renewable phenolic resins by thermochemical conversion of biomass: A review, *Renewable & Sustainable Energy Reviews* 12(8) (2008) 2092-2116.
- [89] A. Tejado, G. Kortaberria, C. Pena, J. Labidi, J.M. Echeverria, I. Mondragon, Lignins for phenol replacement in novolac-type phenolic formulations, part I: Lignophenolic resins synthesis and characterization, *Journal of Applied Polymer Science* 106(4) (2007) 2313-2319.
- [90] A. Tejado, G. Kortaberria, C. Pena, J. Labidi, J.M. Echeverria, I. Mondragon, Isocyanate curing of novolac-type ligno-phenol-formaldehyde resins, *Industrial Crops and Products* 27(2) (2008) 208-213.
- [91] L. Kouisni, Y.L. Fang, M. Paleologou, B. Ahvazi, J. Hawari, Y.L. Zhang, X.M. Wang, Kraft lignin recovery and its use in the preparation of lignin-based phenol formaldehyde resins for plywood, *Cellulose Chemistry and Technology* 45(7-8) (2011) 515-520.
- [92] A. Devi, D. Srivastava, Cardanol-based novolac-type phenolic resins. I. A kinetic approach, *Journal of Applied Polymer Science* 102(3) (2006) 2730-2737.
- [93] R. Yadav, D. Srivastava, Kinetics of the acid-catalyzed cardanol-formaldehyde reactions, *Materials Chemistry and Physics* 106(1) (2007) 74-81.
- [94] N.L. Huong, N.H. Nieu, T.T.M. Tan, U.J. Griesser, Cardanol-phenol-formaldehyde resins. Thermal analysis and characterization, *Die Angewandte Makromolekulare Chemie* 243(1) (1996) 77-85.

- [95] R. da Silva Santos, A.A. de Souza, M.-A. De Paoli, C.M.L. de Souza, Cardanol–formaldehyde thermoset composites reinforced with buriti fibers: Preparation and characterization, *Composites Part A: Applied Science and Manufacturing* 41(9) (2010) 1123-1129.
- [96] N.P.S. Chauhan, Facile synthesis of environmental friendly halogen-free microporous terpolymer from renewable source with enhanced physical properties, *Designed Monomers and Polymers* 15(6) (2012) 587-600.
- [97] S.S. Kelley, X.-M. Wang, M.D. Myers, D.K. Johnson, J.W. Scahill, Use of biomass pyrolysis oils for preparation of modified phenol formaldehyde resins, in: B. A.V., B. D.G.B. (Eds.) *Developments in Thermochemical Biomass Conversion*, Springer·Science+Business Media, B. V., United Kingdom, 1997, pp. 557-574.
- [98] Y. Zhao, N. Yan, M. Feng, Synthesis and Characterization of Bio-Based Phenol-Formaldehyde Resol Resins from Bark Autoclave Extractives, *Forest Products Journal* 66(1-2) (2016) 18-28.
- [99] A.E. Vithanage, E. Chowdhury, L.D. Alejo, P.C. Pomeroy, W.J. DeSisto, B.G. Frederick, W.M. Gramlich, Renewably sourced phenolic resins from lignin bio-oil, *Journal of Applied Polymer Science* 134(19) (2017) 10.
- [100] Y. Celikbag, T.J. Robinson, B.K. Via, S. Adhikari, M.L. Auad, Pyrolysis oil substituted epoxy resin: Improved ratio optimization and crosslinking efficiency, *Journal of Applied Polymer Science* 132(28) (2015) 9.
- [101] Y. Liu, B.K. Via, Y.F. Pan, Q.Z. Cheng, H.W. Guo, M.L. Auad, S. Taylor, Preparation and Characterization of Epoxy Resin Cross-Linked with High Wood Pyrolysis Bio-Oil Substitution by Acetone Pretreatment, *Polymers* 9(3) (2017) 14.
- [102] H. Pan, Synthesis of polymers from organic solvent liquefied biomass: A review, *Renewable & Sustainable Energy Reviews* 15(7) (2011) 3454-3463.

- [103] M. Kobayashi, K. Tukamoto, B. Tomita, Application of liquefied wood to a new resin system-synthesis and properties of liquefied wood/epoxy resins, *Holzforschung* 54(1) (2000) 93-97.
- [104] M. Kobayashi, Y. Hatano, B. Tomita, Viscoelastic properties of liquefied wood/epoxy resin and its bond strength, *Holzforschung* 55(6) (2001) 667-671.
- [105] T. Asano, M. Kobayashi, B. Tomita, M. Kajiyama, Syntheses and properties of liquefied products of ozone treated wood/epoxy resins having high wood contents, *Holzforschung* 61(1) (2007) 14-18.
- [106] T. Xie, F.G. Chen, Fast liquefaction of bagasse in ethylene carbonate and preparation of epoxy resin from the liquefied product, *Journal of Applied Polymer Science* 98(5) (2005) 1961-1968.
- [107] B.H. Sibaja, *Thermosetting Polymers from Renewable Resources*, Polymer and Fiber Engineering, Auburn University, Auburn, Alabama, 2016, p. 213.
- [108] Y. Celikbag, S. Meadows, M. Barde, S. Adhikari, G. Buschle-Diller, M.L. Auad, B.K. Via, Synthesis and Characterization of Bio-oil-Based Self-Curing Epoxy Resin, *Industrial & Engineering Chemistry Research* 56(33) (2017) 9389-9400.
- [109] H.W. Li, N. Mahmood, Z. Ma, M.Q. Zhu, J.Q. Wang, J.L. Zheng, Z.S. Yuan, Q. Wei, C. Xu, Preparation and characterization of bio-polyol and bio-based flexible polyurethane foams from fast pyrolysis of wheat straw, *Industrial Crops and Products* 103 (2017) 64-72.
- [110] X. Zou, T. Qin, Y. Wang, L. Huang, Y. Han, Y. Li, Synthesis and properties of polyurethane foams prepared from heavy oil modified by polyols with 4,4'-methylene-diphenylene isocyanate (MDI), *Bioresource Technology* 114 (2012) 654-657.
- [111] S.J. Hu, C.X. Wan, Y.B. Li, Production and characterization of biopolyols and polyurethane foams from crude glycerol based liquefaction of soybean straw, *Bioresource Technology* 103(1) (2012) 227-233.

- [112] Y. Li, A.J. Ragauskas, Kraft Lignin-Based Rigid Polyurethane Foam, *Journal of Wood Chemistry and Technology* 32(3) (2012) 210-224.
- [113] P. Cinelli, I. Anguillesi, A. Lazzeri, Green synthesis of flexible polyurethane foams from liquefied lignin, *European Polymer Journal* 49(6) (2013) 1174-1184.
- [114] J. Bernardini, P. Cinelli, I. Anguillesi, M.B. Coltelli, A. Lazzeri, Flexible polyurethane foams green production employing lignin or oxypropylated lignin, *European Polymer Journal* 64 (2015) 147-156.
- [115] X.G. Luo, A. Mohanty, M. Misra, Lignin as a reactive reinforcing filler for water-blown rigid biofoam composites from soy oil-based polyurethane, *Industrial Crops and Products* 47 (2013) 13-19.
- [116] Y.H. Wang, J.P. Wu, F. Yu, P. Chen, R. Ruan, I&EC 62-Preparation of polyurethane foam from microwave pyrolytic bio-oils, *Abstracts of Papers of the American Chemical Society* 234 (2007).

Chapter 2

Bio-novolac/epoxy semi-interpenetrating polymer networks (semi-IPN)

2.1. Introduction

Increased scientific attention to the use of biomass is due to an increased demand for alternate resources for energy and materials. In anticipation of an increasing gap between supply and demand of petroleum, the market has been inclined to perform more research on the better utilization of biomass. Biomass is advantageous because it is abundant, renewable and carbon-neutral. There are opportunities to modify the biomass components for the production of the fuels, chemicals and materials.[1] In order to reduce the complexity of the biomass and to make it more efficiently usable for fuels and chemicals, various thermochemical and bio-chemical conversion processes have been developed. Pyrolysis, a thermochemical conversion process carried out in the absence of oxygen and at high temperature (around 500 °C), is beneficial in terms of producing high yields of the liquid fraction, i.e. bio-oil.[2] When a high heating rate and short vapor residence time is used, the pyrolysis process is termed fast pyrolysis.[2-4] Bio-oil contains different classes of organic compounds such as sugars, phenolic oligomers and monomers, aldehydes, carboxylic acids, alcohols, ketones and furans [5] which can be utilized as monomers for polymer synthesis. In particular, crosslinked thermosetting polymers offer versatility by providing a wide range of properties such as high chemical resistance, heat resistance, high tensile strength and modulus, high glass transition temperature etc, due to the crosslinked structure.[6] Traditionally, crosslinked

structures are built by grafting polymeric chains by crosslinking agent to form a continuous network. In case of traditional phenol-formaldehyde systems, oligomeric phenol-formaldehyde resin is synthesized by reaction of phenol and formaldehyde. The oligomeric resin is further crosslinked either by heating or by reacting with crosslinking agents such as hexamethylenetetramine. Epoxy systems are another famous example of crosslinkable polymers in which oligomeric/prepolymeric epoxide is reacted with amine, anhydride hardeners to yield a crosslinked material. Depending on crosslinking conditions, the grafts joining polymer chains can arise from crosslinking agents (amine, anhydrides for epoxides; and hexamethylenetetramine for phenol-formaldehyde) or from the polymer itself (unreacted functional groups of the oligomeric phenol-formaldehyde resin). An interpenetrating polymer network (IPN) can be formed with two or more polymer networks of which at least one of the networks is crosslinked in the presence of the other either simultaneously or sequentially.[7, 8] In such cases, networks are not grafted to each other at all crosslinking sites; rather their chains are entangled at the molecular level. Similarly, a semi-interpenetrating polymer network (semi-IPN) is a result of one polymer network crosslinked in the presence of a linear or branched, non-crosslinked polymer. IPNs offer benefits in terms of synergism of the properties of two individual polymer networks.[9, 10]

Phenol-formaldehyde and epoxy have been very important thermosetting resins due to their high market share and diverse applications such as adhesives, coatings, industrial laminates, abrasive materials.[11] Phenol is the precursor of phenol-formaldehyde resins and it is derived from petroleum. Phenol can be replaced by naturally occurring compounds and thus, modified phenol-formaldehyde resins can be developed. An example of naturally occurring substituted phenol is cardanol which can be extracted from cashew nut shell liquid. Synthesis and characterization of cardanol-based phenolic resins were studied by several researchers.[12-15] Vanillin, another

naturally occurring substituted phenol, was co-reacted with furfural and 4-methylacetophenone in acidic medium to yield a bio-based phenol-formaldehyde resin.[16] Varying types of lignin were reacted, without further modifications, with phenol and formaldehyde to produce lignin-phenol-formaldehyde novolac resins.[17] Lignin is a natural polymer found in plant biomass and forms hemicellulose-lignin modules which bind the cellulose microfibrils bundles, thereby providing strength to the plant cell walls.[18] Lignin is composed of polyphenolic, macromolecular, complex structure[19, 20] capable of breaking down to oligophenolic molecular structures that can be re-polymerized to a more specific phenol-formaldehyde type skeleton. Bio-based phenolic foams were prepared by using hydrolysis lignin depolymerized by a low temperature and low pressure method.[21] Since pyrolysis and liquefaction can be often used to break down lignin along with cellulose and hemi-cellulose, mono-phenols or oligophenolic structures can be found in the liquid bio-oil. Phenol was partially replaced by phenolic-rich fraction of the bio-oil to synthesize resol-type phenol-formaldehyde resins.[22] In addition, resol resins were also attempted by modifying the bark autoclave extractives.[23] In another study, formate-assisted fast pyrolysis was used to obtain bio-oil which was reacted with formaldehyde in acidic medium for preparing novolac-type resins.[24] Effendi et al. have critically reviewed the phenolic resins produced by thermochemical conversion of plant biomass.[25]

Epoxy resins are polymeric materials utilized in many applications; and have competed with phenolic resins for a long period. Tremendous amount of research has been carried out on epoxy resins and their applications. There is a versatility to design molecular structures of prepolymeric epoxides and curing agents; and hence, the properties can be altered accordingly. Epoxy resins most commonly appear as diglycidyl ether of bisphenol-A (DGEBA) and its oligomers, all of which are synthesized from bisphenol-A (BPA) and epichlorohydrin.[26, 27] Bisphenol-A is not

only a petroleum-derived compound but also can affect human health.[28] In an attempt to avoid the use of bisphenol-A, epoxy resins have been successfully derived from fatty acid triglycerides present in vegetable plant oil. Fatty acid chains of several oils such as soybean oil, linseed oil, tung oil, dehydrated castor oil contain unsaturation and can be derivatized to oxirane functionality.[29, 30] These resin structures are mainly composed of aliphatic chains due to the involvement of aliphatic acids. Absence of aromaticity can result in reduced mechanical performance.[6] Aromatic moieties from bio-based resources have been successfully introduced in epoxy resins by epoxidizing phenolic hydroxyl groups appearing in bark extractives[31, 32], tannins[33], biomass pyrolysis oil[34] and hydrothermal liquefaction oil.[35] Our previous work focused on the synthesis and evaluation of thermoset networks of epoxy resin derived from 3,5-dihydroxybenzoic acid.[36, 37] With a more commonly accepted name, α -resorcylic acid, it is a monocyclic aromatic monomer naturally occurring in red sandalwood, hill raspberry, chickpeas and peanuts.[38] In comparison with bisphenol-A that has two aromatic rings per molecule, the reduction of hydrophobic content per molecule due to the single aromatic ring may decrease the binding tendency of α -resorcylic acid to estrogen receptor.[28] Decreased interaction with the receptor and natural occurrence of α -resorcylic acid can potentially make it to be a replacement of bisphenol-A. The resulting epoxy resin, with three epoxide rings per molecule, offers the advantage of having a low epoxy equivalent weight (hence, a high epoxy content) and low viscosity.[36, 37] The present work is mainly focused on developing interpenetrating networks of bio-oil based novolac polymers and epoxy resins derived from α -resorcylic acid.

2.2. Experimental section

2.2.1. Materials

Fast pyrolysis bio-oil derived from hardwood was obtained from Red Arrow, USA. Phenol (detached crystals, 99%), formalin solution (37% w/w), acetone, methanol, sodium hydroxide, (±)-epichlorohydrin (99%), 3,5-dihydroxybenzoic acid, chromium(III)acetyl acetonate, N-hydroxy-5-norbornene-2,3-dicarboximide (NHND), deuterated chloroform were purchased from VWR International. 2-Chloro-4,4,5,5-tetramethyl-1,3,2-dioxaphospholane (TMDP) was ordered from Sigma Aldrich. Oxalic acid, anhydrous, was supplied by Spectrum Chemical Mfg. Corp. Benzyltriethylammonium chloride was obtained from TCI. 4-(Dimethylamino)pyridine (DMAP) (prilled, 99%) was obtained from Beantown Chemical.

2.2.2. Methods

2.2.2.1. Characterization of fast pyrolysis bio-oil

Fast pyrolysis bio-oil contained water which was removed by using rotary evaporator. After removal of water, the chemical composition of bio-oil was qualitatively analyzed by Gas Chromatography-Mass Spectroscopy (GC-MS) according to procedure reported.[39] Around 0.5 g of bio-oil was diluted with 12 mL of methanol and mixed well. A split ratio of 20:1 was set for injecting 1 μ L of diluted bio-oil into a DB-1701 column equipped to an Agilent 7890 GC/5975MS. The hydroxyl (OH) content of bio-oil was quantitatively measured by ^{31}P -NMR spectroscopy as per the procedure mentioned.[40] The stock solution was prepared by dissolving 40 mg of NHND and 40 mg of chromium(III)acetyl acetonate in the mixture of 6 mL pyridine and 4 mL deuterated chloroform. Approximately 20 mg of bio-oil was dissolved in 500 μ L of stock solution. 150 μ L of TMDP was added to the mixture to phosphitylate the hydroxyl groups in bio-oil. The sample was

then transferred to the NMR spectroscopy tube and the spectrum was acquired with a Bruker Avance II 250 MHz spectrometer using inverse gated decoupling pulse sequence, 90-degree pulse angle, 25 s pulse delay and 128 scans.

2.2.2.2. Synthesis of novolac and BioNovolac resins

Novolac resin (phenol-formaldehyde resin synthesized with molar excess of phenol over formaldehyde in acidic medium) was synthesized as per the procedure described in the literature. [41] The molar ratio of phenol to formaldehyde was kept constant at 1:0.8 for all resin formulations. Oxalic acid (0.0522 per mol of phenol) was added to the reaction flask and the temperature was raised to 90 °C. The calculated amount of formaldehyde aqueous solution (formalin, 37 %) was added dropwise to the constantly agitated reaction mixture and the reaction was continued at 90 °C for next three hours. BioNovolac resins were synthesized by the same procedure, replacing phenol with bio-oil in varying proportions. A specific amount of phenol was replaced by bio-oil on weight basis (10 %, 50 %), and the oxalic acid was added to the physical blend of fast pyrolysis bio-oil and phenol. The progress of reaction was monitored by Fourier Transform Infrared (FTIR) spectroscopy. The synthesis routes and the structures of Novolac and BioNovolac resins are shown in Figure 2.1.

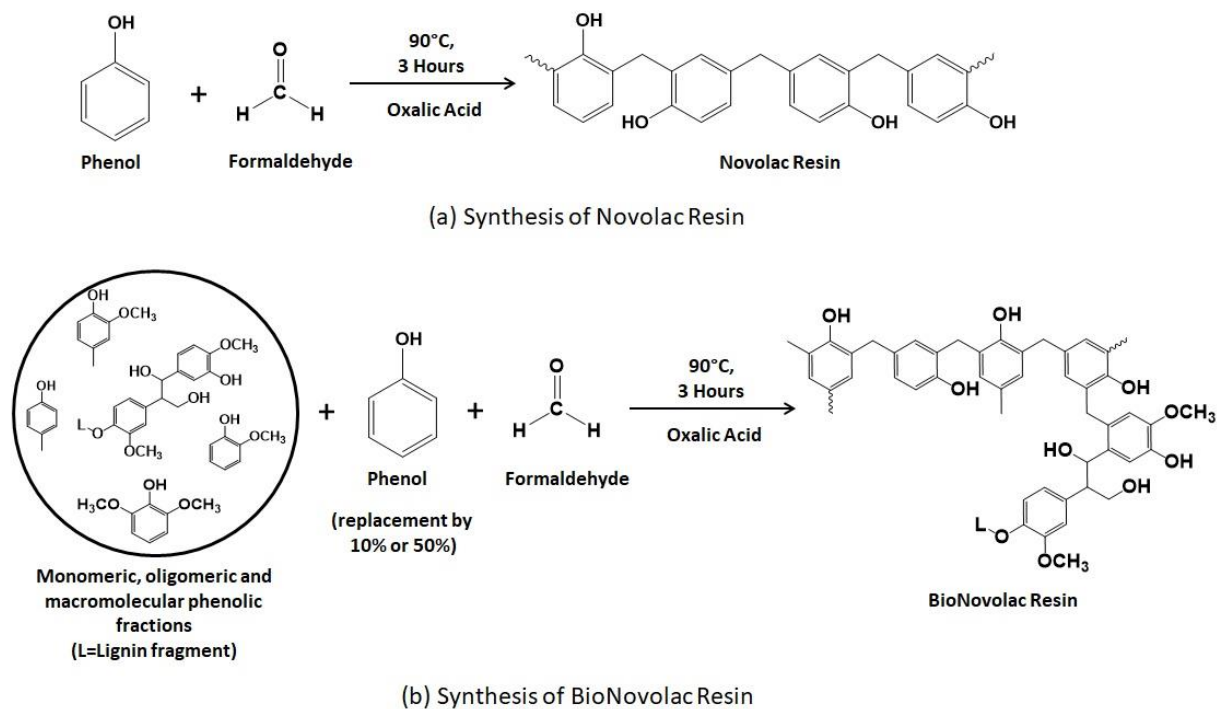


Figure 2.1: Synthesis of (a) Novolac resin, (b) BioNovolac resin.

2.2.2.3. Synthesis of glycidyl 3,5-diglycidoxybenzoate (GDGB)

In order to carry out glycidylation of α -resorcylic acid, the procedure was used as per the literature. [33, 42] Epichlorohydrin (4 M eq/OH) was added to RA and the temperature was raised to 100 °C. Benzyltriethylammonium chloride (0.012 M eq/OH) was added as the phase transfer catalyst. The reaction was carried out for 1 hour to produce chlorohydrin intermediate and the reaction mixture was cooled down to 30 °C. An aqueous solution of sodium hydroxide (2 M eq/OH) was added along with the same previous amount of benzyltriethylammonium chloride and the reaction was continued for 90 minutes. The organic layer was separated and washed with water to remove the salt. The product was further purified by removing unreacted epichlorohydrin at 90 °C under reduced pressure by rotary evaporation. A stepwise synthesis of GDGB is depicted in Figure 2.2.

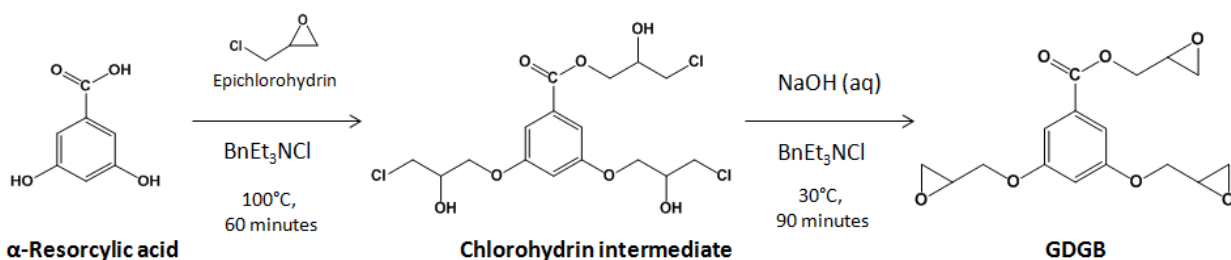


Figure 2.2: Glycidylation of α -resorcylic acid.

2.2.2.4. Determination of epoxy equivalent weight (EEW)

The epoxy equivalent weight was measured by the hydrogen bromide-glacial acetic acid solution method. Around 0.3-0.4 g of sample was taken in a 50 mL Erlenmeyer flask and 10 mL acetone was added to it. The contents of the flask were stirred well so as to dissolve GDGB sample in acetone. Just before the titration, a drop of crystal violet indicator solution (1 g/L, in glacial acetic acid) was added and the contents were titrated with 0.1 N HBr-glacial acetic acid solution until the end point “blue-green color” persisted for 30 seconds. The epoxy equivalent weight (EEW) was calculated as per the following equation:

$$\text{EEW} = \frac{1000 \times (\text{wt. of sample})}{N \times V}$$

where, N= Normality of HBr-glacial acetic acid solution

V=Volume of HBr-glacial acetic acid solution required to titrate the sample

2.2.2.5. Crosslinking of thermoset polymer networks

GDGB was crosslinked in the physical presence of BioNovolac polymers. Varying amounts of 10% BioNovolac and 50% BioNovolac were separately blended with GDGB before curing. All

thermoset systems were prepared by crosslinking with 0.08 mol of 4-(dimethylamino)pyridine (DMAP) per epoxide. Anionic addition polymerization of epoxides by DMAP is reported elsewhere.[43] The initiator quantities required are considerably less as compared to that of amine hardeners traditionally used for curing epoxides and help to reduce the overall consumption of petroleum-derived compounds. The curing procedure consisted of heating the samples in aluminum molds in a conventional oven at 60 °C for 2 hours followed by 80, 90, 100, 120, 140 °C for 1 hour each and finally at 165 °C for 15 minutes.

2.2.2.6. FTIR spectroscopy

Novolac, BioNovolac and GDGB were analyzed by Fourier transform infrared (FTIR) spectroscopy which was performed with attenuated total reflection (ATR) method using Thermo Scientific Nicolet 6700 FT-IR spectrophotometer and OMNIC 7.3 software. The spectra were collected in the wavenumber range 400 cm^{-1} to 4000 cm^{-1} at a resolution of 4 cm^{-1} and 40 scans. Cured thermosets were also analyzed by FTIR spectroscopy to confirm several phenomena such as ring opening of epoxides, grafting of polymeric chains and semi-IPN formation.

2.2.2.7. Evaluation of thermo-mechanical performance

Dynamic mechanical analysis is generally used to observe the viscoelastic region of the polymeric system. A cyclical strain is applied while increasing the temperature and the dynamic mechanical moduli are measured. The storage modulus is indicative of the energy stored elastically while the loss modulus is the characteristic energy lost via heat.[44] The tangent of the phase angle between cyclic strain and cyclic stress, or in other terms, the ratio of loss modulus to the storage modulus is termed as $\tan \delta$, the maximum of which appears generally at the glass transition temperature of

the polymeric system. Therefore, this technique can be used to measure the glass transition temperature of the crosslinked systems. In the current study, a three-point bending geometry was used with a TA Instruments RSAIII Dynamic Mechanical Analyzer, on the samples with approximate dimensions of 25 × 10 × 3 mm. A constant strain of 0.1 % and cyclic frequency of 1 Hz was applied while increasing the temperature from 25 °C to 200 °C at 10 °C/min. The storage modulus and tanδ were plotted against temperature and the glass transition temperature was measured at the maximum tanδ. The active chains density was calculated by the following equation

$$n = \frac{E'}{3RT}$$

where E' is storage modulus (Pa) at the temperature T

T is (glass transition temperature +50) expressed in Kelvin, and

R is the universal gas constant, 8.314 Jmol⁻¹K⁻¹

Differential scanning calorimetry was used to observe the glass transition temperature of the crosslinked polymer networks. The temperature was increased from 20 °C to 200 °C by the heating rate 10 °C/min, reduced from 200 °C to 20 °C by the cooling rate 20 °C/min and was again increased to 200 °C by the heating rate 10 °C/min

For all crosslinked thermoset systems, Soxhlet extraction was carried out with a refluxing action of 200 mL dichloromethane for 24 hours. After extraction, the residual solids were dried and weighed. Then mass retained was calculated by the following equation:

$$\text{Mass retained (\%)} = \frac{\text{Weight of dried solids after extraction}}{\text{Initial weight of solids}} \times 100$$

Table 2.1: Hydroxyl content determined by ³¹P-NMR spectroscopy

Hydroxyl Type			Range (ppm)	Hydroxyl Content (mmol/g)	
Aliphatic OH			150.00-145.50	3.58	3.58
Phenolic OH	C-5 substituted condensed phenolic OH	β-5	144.70-142.80	0.38	1.71
		4-O-5	142.80-141.70	0.33	
		5-5	141.70-140.20	0.26	
	Guaiacyl phenolic OH		140.20-139.00	0.31	
	Catechol type OH		139.00-138.20	0.33	
	p-hydroxy-phenyl OH		138.20-137.30	0.10	
Acidic OH			136.60-133.60	0.51	0.51
Total					5.80

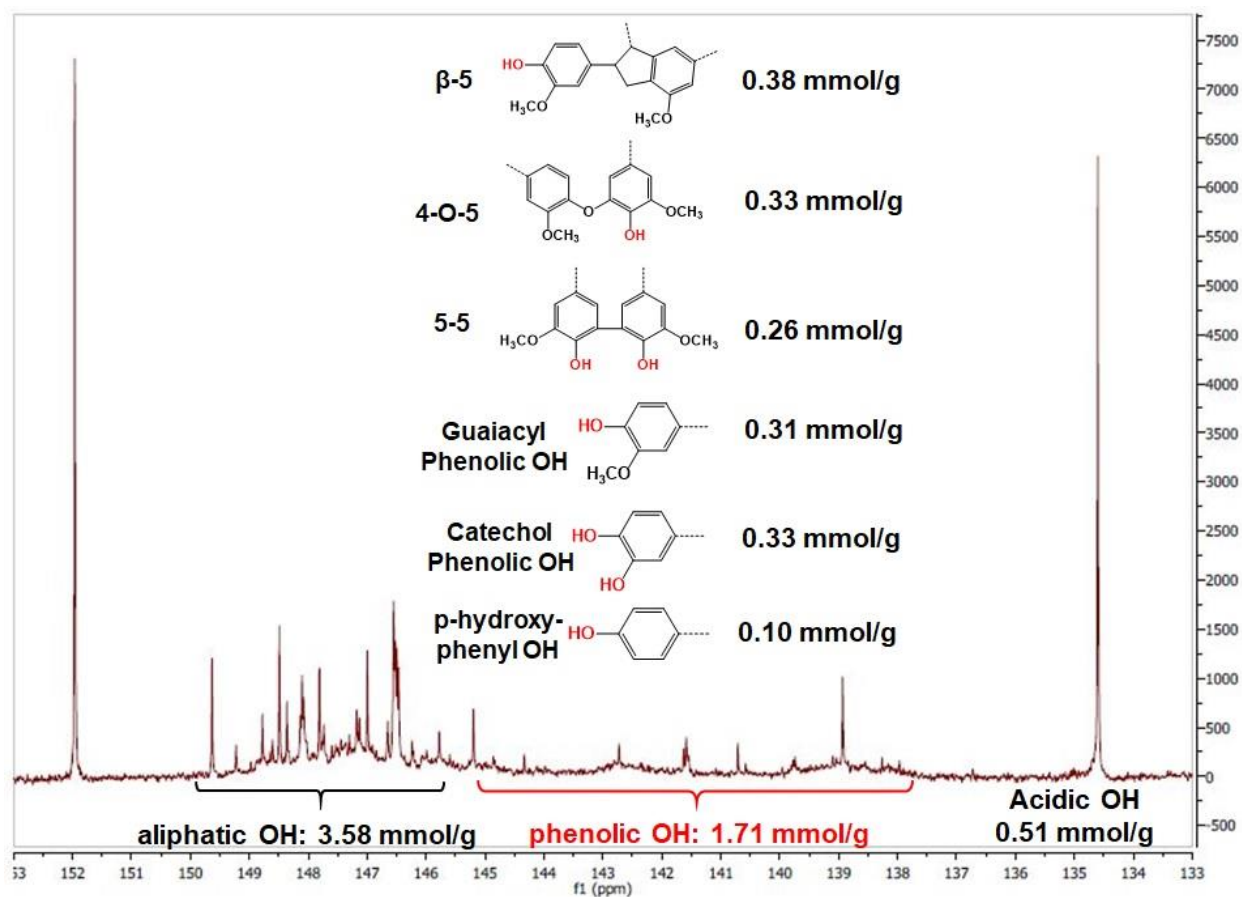


Figure 2.4: ^{31}P -NMR spectrum of bio-oil

With the help of GC-MS and ^{31}P -NMR spectroscopy, monocyclic phenolic compounds and phenolic hydroxyl groups were observed which led to a confirmation of presence of substituted phenols that might have formed after depolymerization of lignin during pyrolysis. Aliphatic alcohols, aldehydes, ketones, carboxylic acids and levoglucosan were also identified using GC-MS. Further, ^{31}P -NMR spectroscopy showed the presence of aliphatic hydroxyl and acidic hydroxyl groups, indicating that compounds other than substituted aromatics were present due to the decomposition of cellulose and hemicelluloses during pyrolysis.

2.2.3.2. Characterization of BioNovolac resins

Figure 2.5 shows the FTIR spectra of BioNovolac and Novolac resins. The same peaks with varying intensities were observed in all the spectra, which confirmed that the synthesis of BioNovolac resin followed a similar reaction pathway than the novolac resin.

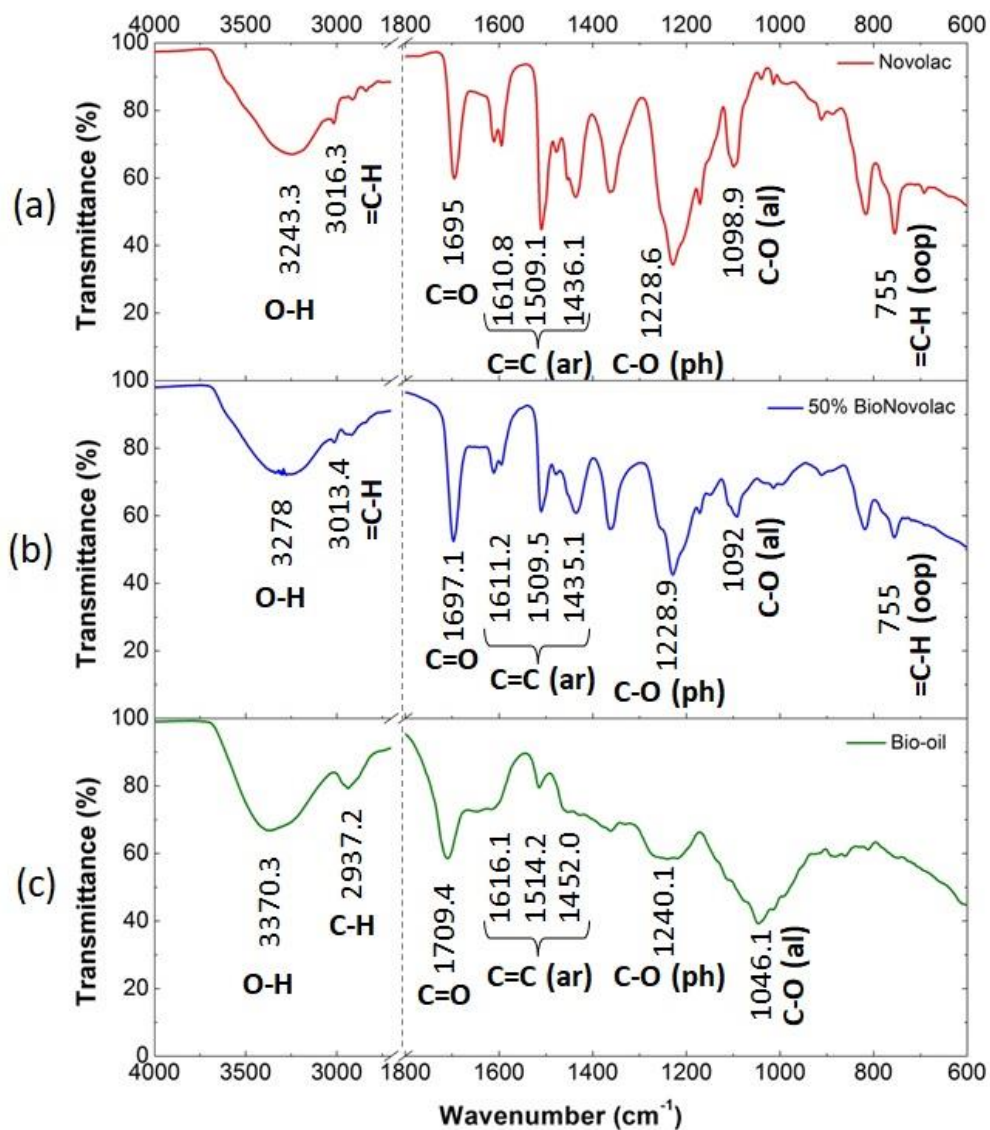


Figure 2.5: FTIR spectra of (a) novolac (b) 50% BioNovolac and (c) bio-oil. Notes: ar – aromatic, ph – phenolic, oop – out of plane bending, al – aliphatic

The decreasing intensity of the peaks corresponding to the bonds C=C (ar), C-O (ph) and =C-H (oop), with increasing bio-oil content is attributable to the reduction in total phenolic content of bio-oil/phenol blend. The bio-oil is not only comprised of substituted phenols but also contains many other organic compounds observed in GC-MS results. (Refer Figure 2.3). Formation of phenol-formaldehyde network is carried out by the selective reaction of formaldehyde at ortho and para sites of phenol and substituted phenols.

The progress of reaction of Novolac, 10% BioNovolac and 50% BioNovolac was observed using a peak at 755 cm^{-1} that reflects the aromatic C-H out of plane vibration band. The intensity of the peak reduced with time due to the formation of C-C bond at ortho/para positions. The extent of conversion of phenolic monomers, x_t , is calculated by the equation reported in the literature.[45]

$$x_t = \left(1 - \frac{\text{peak height at time } t}{\text{initial peak height}} \right) \times 100$$

Figure 2.6 contains the plot of the extent of conversion of phenolic monomers with time. The extent of conversion of phenolic monomers in all three reactions had a similar trend.

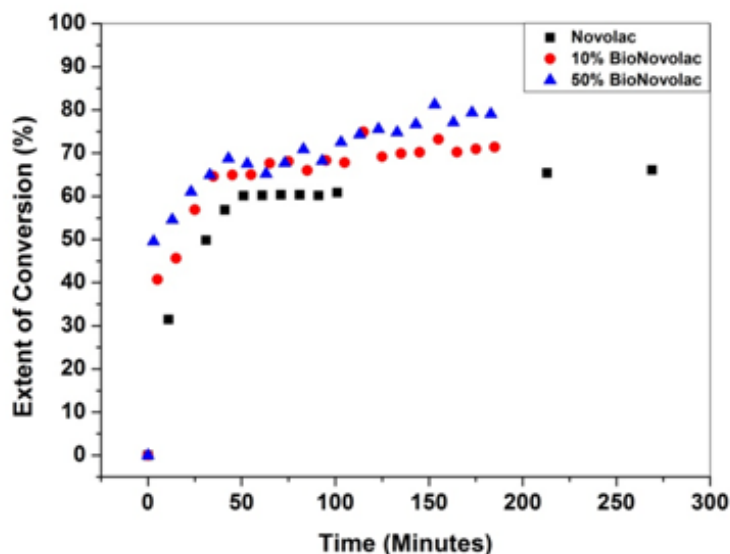


Figure 2.6: BioNovolac extent of conversion

2.2.3.3. Characterization of glycidyl 3,5-diglycidoxybenzoate (GDGB)

FTIR spectroscopy of GDGB has been carried out extensively and led to the detection of several important peaks. Figure 2.7 displays FTIR spectra of α -resorcylic acid and GDGB.

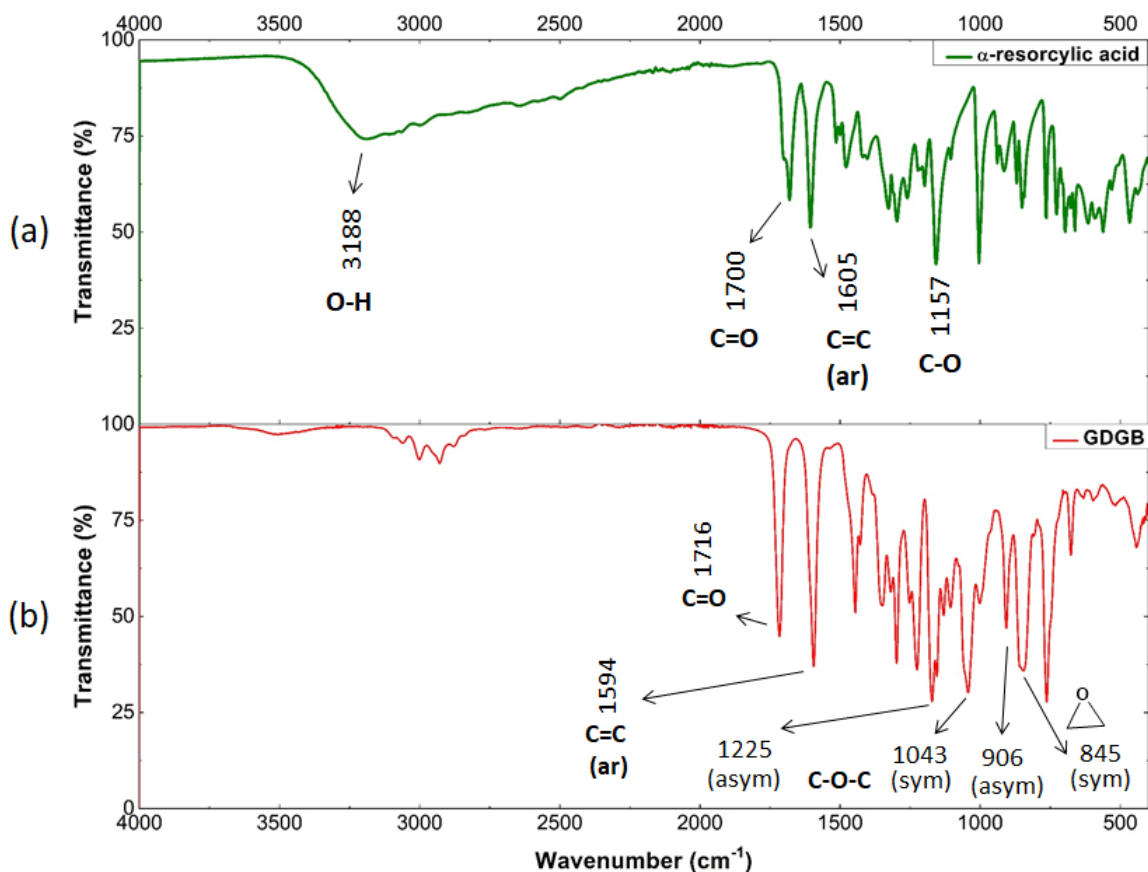


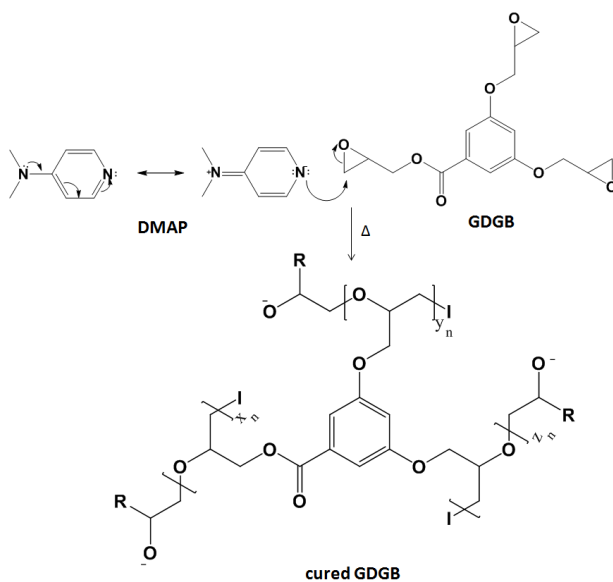
Figure 2.7: FTIR spectra of (a) α -resorcylic acid, (b) GDGB

A broad peak at 3188 cm^{-1} present in α -resorcylic acid, corresponding to O-H stretching vibrations disappeared in the spectrum of GDGB due to the conversion of one carboxyl and two hydroxyl groups into glycidyl functionality. Epoxide ring formation was confirmed by the epoxide ring deformation bands at 906 cm^{-1} (asymmetric) and 845 cm^{-1} (symmetric). Two bands that appeared due to C-O-C stretch were also observed at 1225 cm^{-1} (asymmetric) and 1043 cm^{-1} (symmetric).

GDGB showed peaks responsible for C=C bonds in aromatic ring and C=O bond. The EEW for GDGB was experimentally found to be 106.83 ± 3.02 g/eq which was comparable to the value reported earlier by Sibaja et al.[36]

2.2.3.4. Network Formation

The epoxy ring can be opened via nucleophilic attack by electron-rich nitrogen atom of DMAP as shown in Figure 2.8.



where,

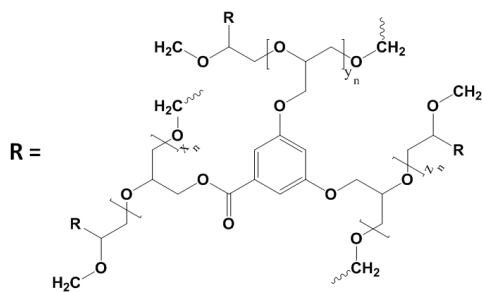
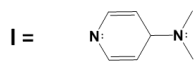


Figure 2.8: Crosslinking of GDGB by DMAP

Opening of the ring is followed by formation of an alkoxide anion, which attacks another epoxy ring, thereby creating a new alkoxide ion. In addition, the successive epoxy monomers lead to a chain reaction – anionic polymerization of epoxides. In the case of GDGB that has three epoxy rings, a three-dimensional network is formed by anionic polymerization. Figure 2.8 also depicts the structure of cured GDGB network in which R is itself a macromolecular repeating unit and “I” is the DMAP initiator fragment.

When BioNovolac is present along with GDGB, additional reaction can occur in which the DMAP initiator abstracts phenolic proton resulting in the formation of phenoxide anion which can open the epoxy rings. (Refer Figure 2.9) The BioNovolac chains can be grafted to GDGB network. These reactions were observed with FTIR and are discussed in the next section.

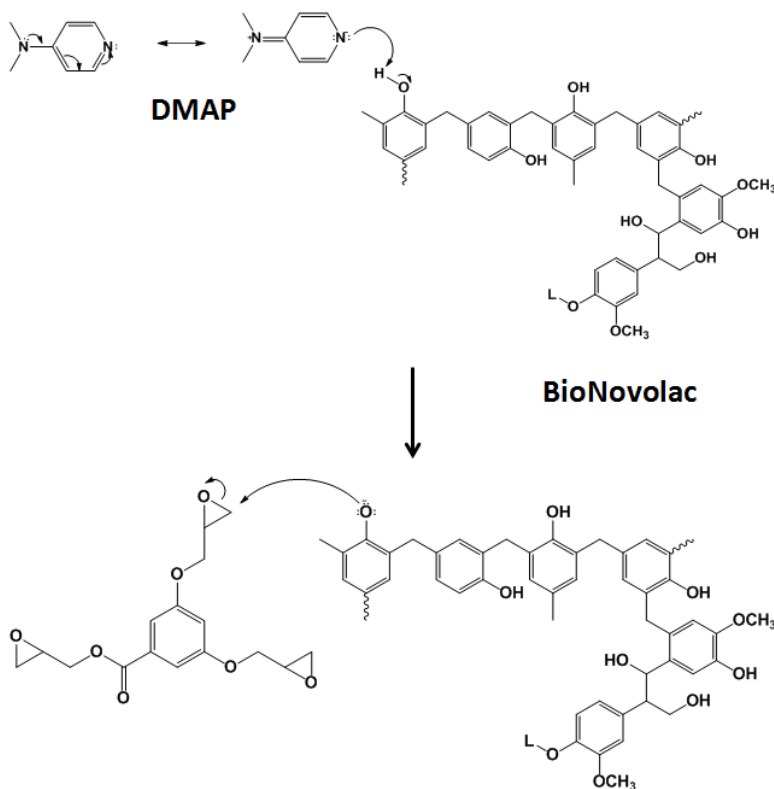


Figure 2.9: Grafting of BioNovolac and GDGB networks

In the cured GDGB-50%BioNovolac (50:50), opening of epoxy rings was confirmed by the disappearance of the epoxide ring deformation bands at 906 cm^{-1} (asymmetric) and 845 cm^{-1} (symmetric) as shown in Figure 2.10. It also depicts a peak corresponding to 1652 cm^{-1} due to overlap of vinylidene groups formed by chain transfer and iminium group resulted from DMAP.

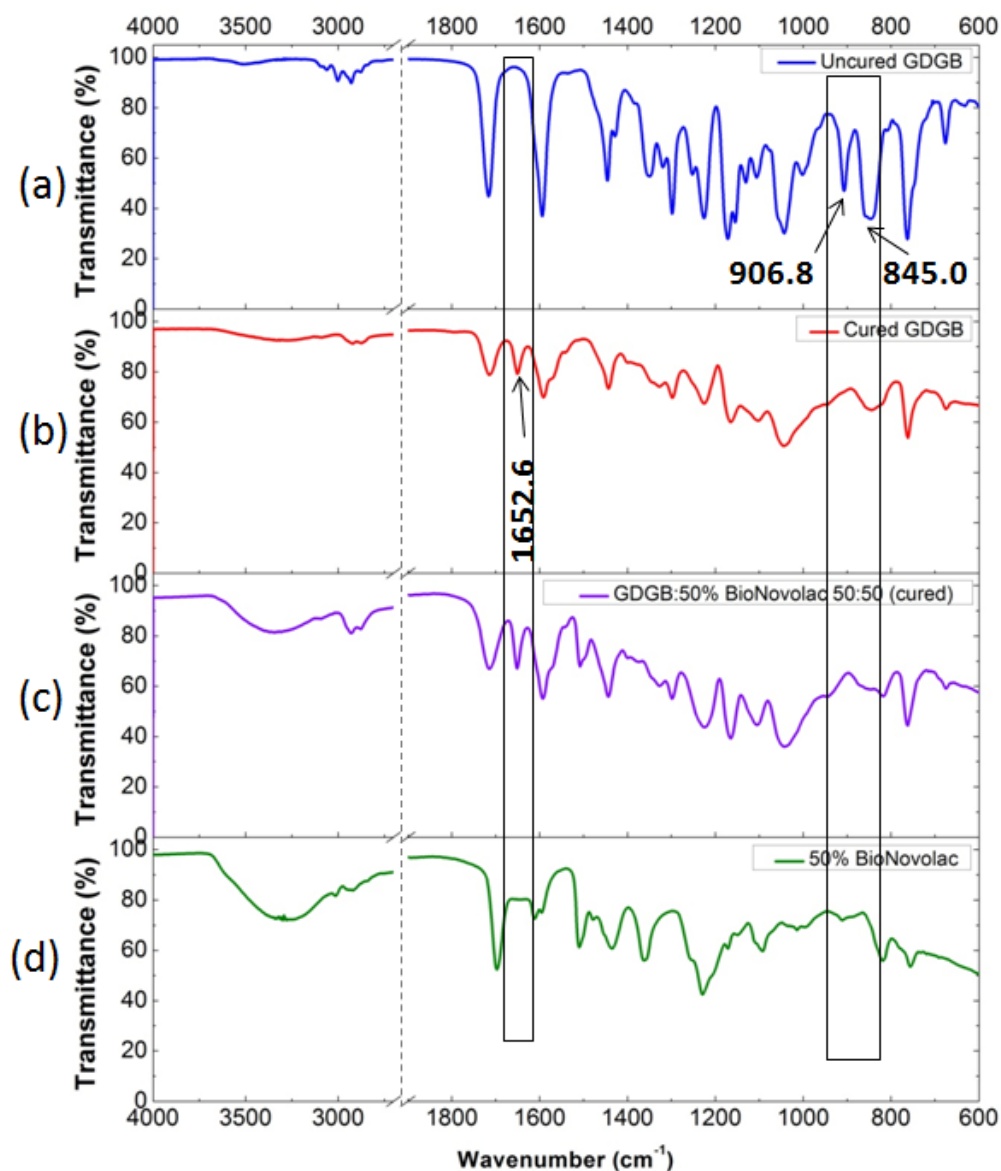


Figure 2.10: FTIR spectra of (a) uncured GDGB (b) cured GDGB (c) cured GDGB: 50% BioNovolac 50:50 and (d) 50% BioNovolac

Figure 2.11 explains a general mechanism of intramolecular chain transfer. During chain transfer reactions, an initiator fragment can be detached to form an anion which can lead to further ring opening and a vinylidene group can be formed on the dead chain.

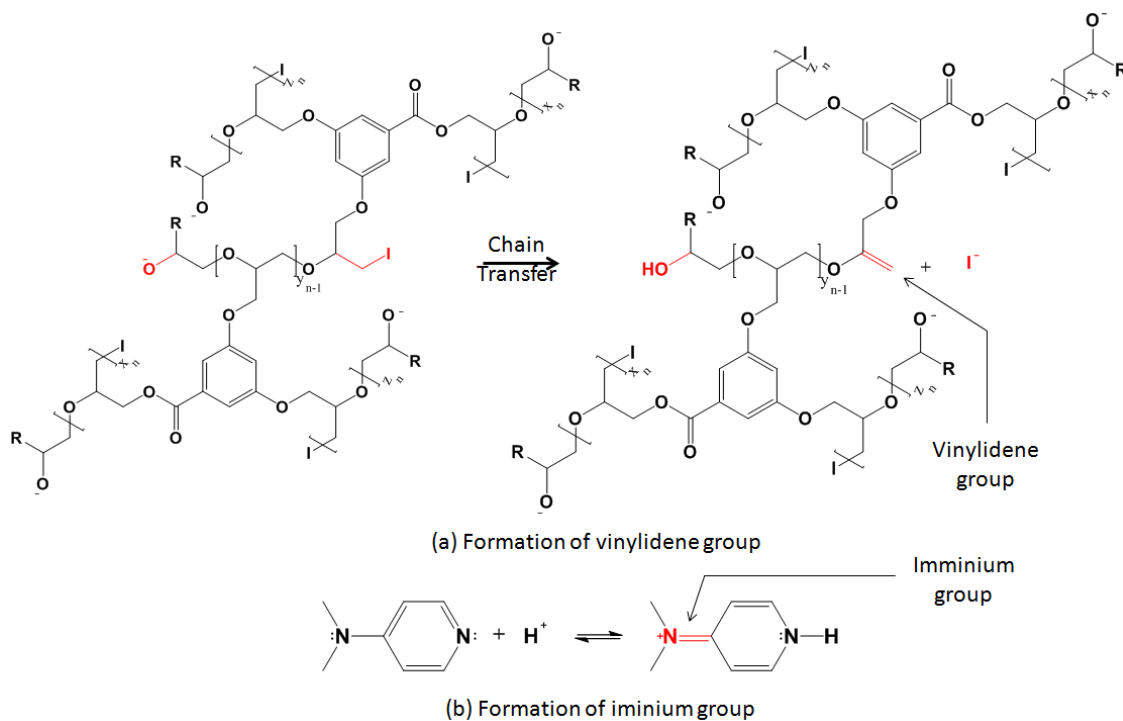


Figure 2.11: Species responsible for IR peak at 1652 cm^{-1} in cured networks

FTIR spectroscopy was used to observe the effect of DMAP on curing BioNovolac. Spectra of uncured BioNovolac were compared to the spectra of heated BioNovolac with and without addition of DMAP. In Figure 2.12, the peak near 1647.7 cm^{-1} can be attributed to formation of iminium ion discussed in previous section, while the peak corresponding to 1562.4 cm^{-1} is due to amine N-H of DMAP. The peak observed at 1362.7 cm^{-1} was contributed by in-plane bending of phenolic C-O-H groups and disappeared only in case of BioNovolac + DMAP combination since phenolic protons were abstracted by excess DMAP.

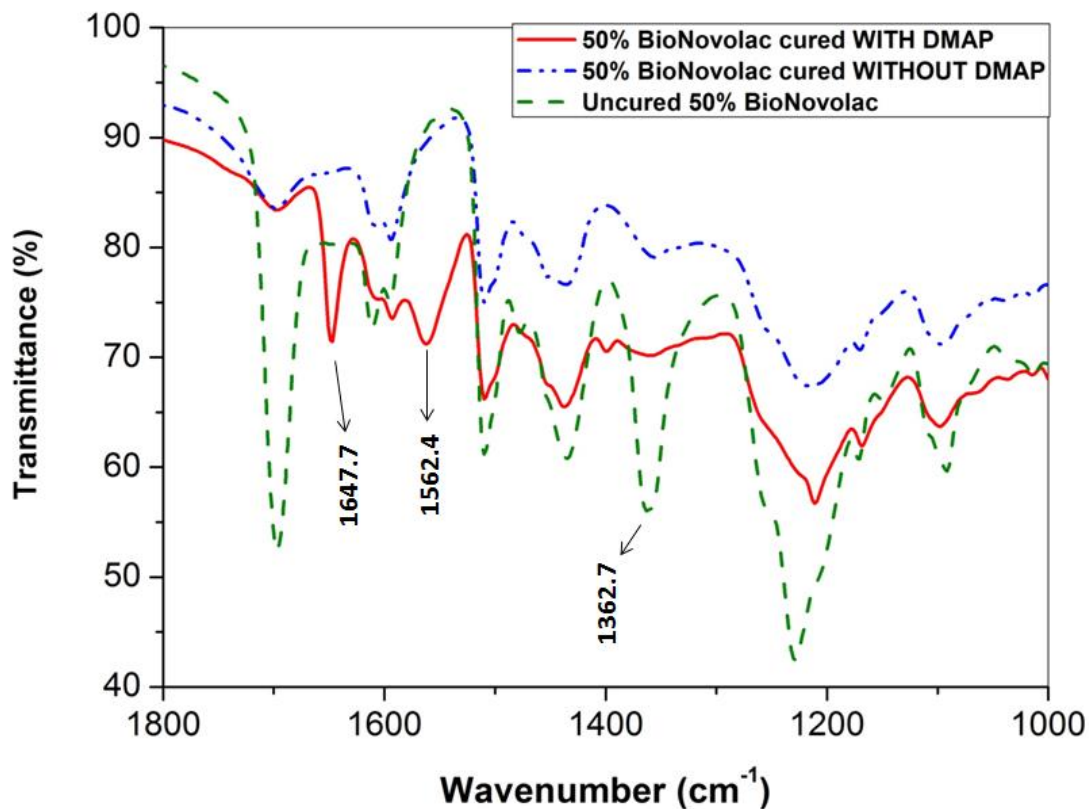


Figure 2.12: Curing of 50% BioNovolac, with and without DMAP

However, in presence of GDGB, all phenolic hydroxyl groups are generally not converted to phenoxide anions due to competing reaction of initiator and epoxy. Such a combination of competing reactions leads to the formation of a semi-interpenetrating polymer network in which BioNovolac polymer chains are grafted only at several points to the densely cured GDGB network.

2.2.3.5. Evaluation of thermo-mechanical performance

With increasing amount of GDGB, storage moduli and glass transition temperatures of the cured systems enhanced. GDGB content was increased from 0 to 100 wt% by an interval of 25 wt%. It was observed that the GDGB-10% BioNovolac samples with 10% BioNovolac content more than

50 wt%, were brittle enough to be unable to be tested with DMA. Similar brittleness was observed for GDGB-50% BioNovolac samples with 50% BioNovolac content more than 75 wt%. The glass transition temperatures measured by DSC showed an increase with increasing the GDGB content, and followed the same trend indicated by the glass transition temperatures measured by DMA. Fox equation was used to predict the glass transition temperature profile and the experimental values were found to be in agreement with the predicted values. (Refer Figure 2.13)

$$\frac{1}{T_{g, \text{ predicted}}} = \frac{f_{\text{GDGB}}}{T_{g, \text{ GDGB}}} + \frac{f_{\text{BioNovolac}}}{T_{g, \text{ BioNovolac}}}$$

where, f = weight fraction

T_g = glass transition temperature, K

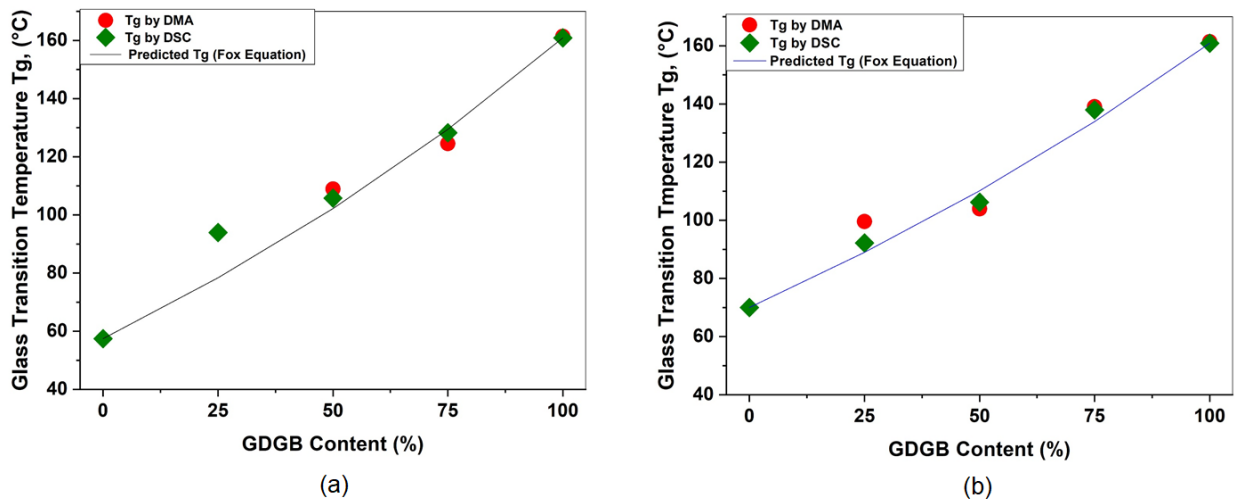


Figure 2.13: Glass transition temperature of semi-IPNs with (a) 10% BioNovolac (b) 50%

BioNovolac

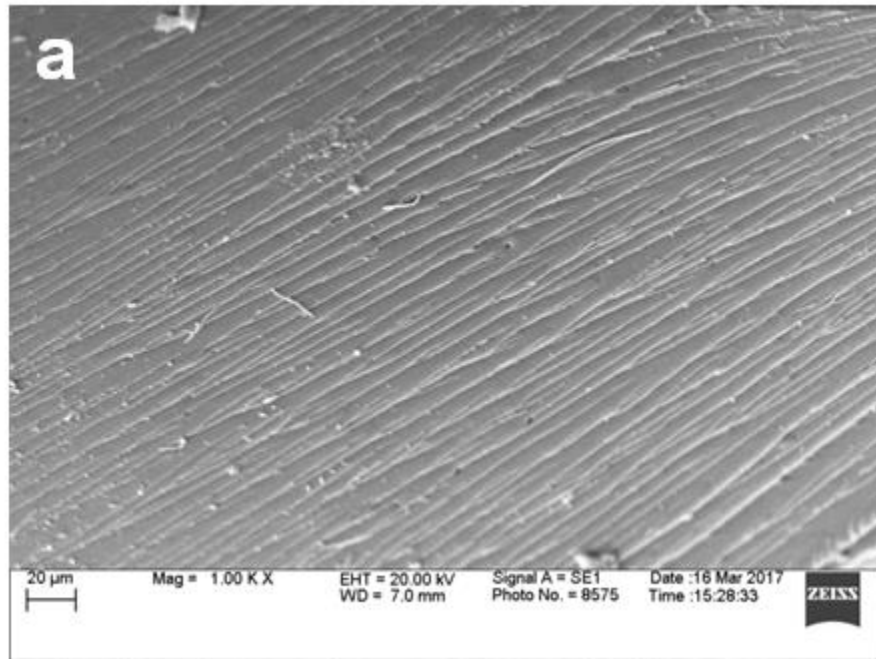
Table 2.2 lists the values of glass transition temperature, storage modulus, active chains density and mass retained for the thermoset networks. The glass transition temperature was measured by DMA ($\tan \delta$ peak) as well as DSC (change in the slope of heat flow). It was observed that the active chains density decreased with decreasing GDGB content. Increasing bio-content of BioNovolac improved active chain density. This is probably due to the impact of the polymeric structure of lignin fragments present in the bio-oil on the BioNovolac properties. The mass retained was more than 75 % for all the systems with most being in the range 88-99 %, after 24 hours of extraction with dichloromethane.

Table 2.2: Thermo-mechanical properties of thermosets (* = too brittle to be tested with DMA)

System	T_g (°C), DMA	T_g (°C), DSC	E' (GPa) at room temperature	Active Chains Density, n (mol/m³)	Mass (%) Retained
GDGB	161	161	1.78	13721	94
GDGB:10% BioNovolac					
75:25	125	128	1.88	2759	89
50:50	109	106	1.15	1119	93
25:75	*	94	*	*	79
10% BioNovolac	*	58	*	*	80
GDGB:50% BioNovolac					
75:25	139	138	2.59	6355	99
50:50	104	106	2.65	1793	98
25:75	100	92	0.30	31	96
50% BioNovolac	*	70	*	*	78

2.2.3.7. Morphology

Figure 2.14 includes the comparison of morphology of three systems (GDGB-50%BioNovolac) with varying ratios. The samples show similar fracture lines at the cross-sections, with negligible phase separation observed. Maximum brittle lines were observed in case of cured GDGB. The brittle lines decreased with increasing amount of 50%BioNovolac. In other words, brittleness reduced with increasing 50%BioNovolac content due to reduction in the active chains density. This phenomenon was in agreement with the observed thermo-mechanical results too.



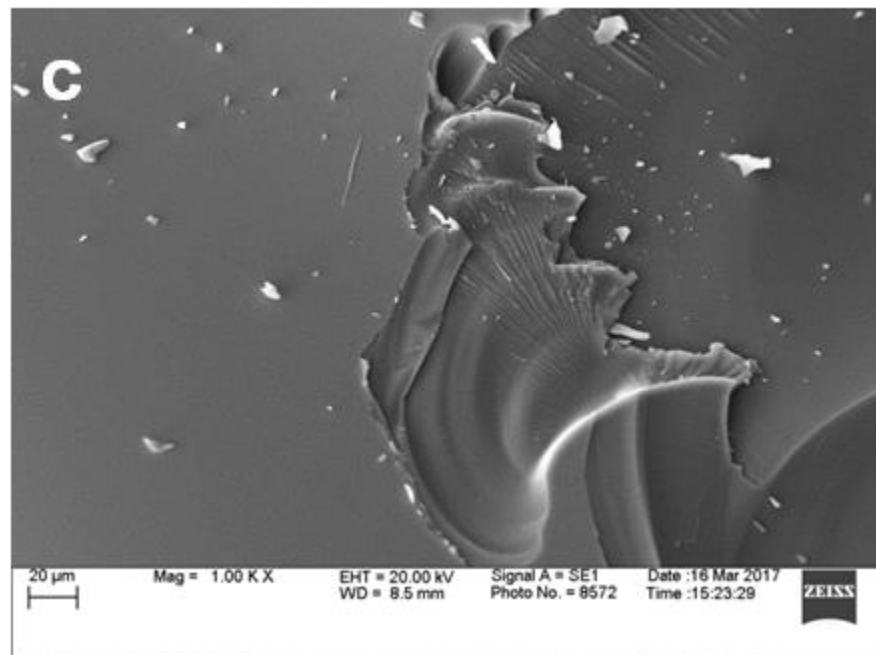
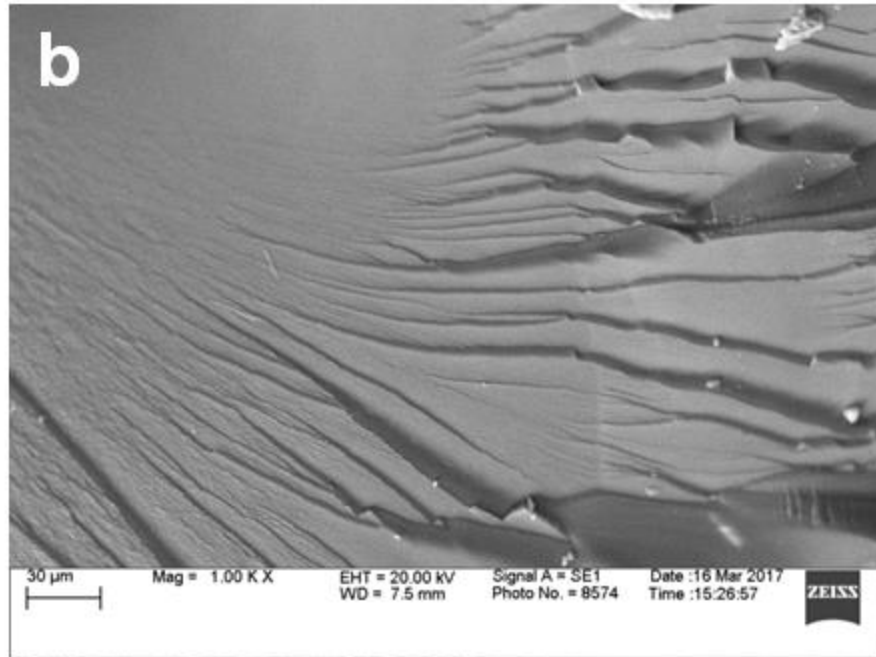


Figure 2.14: SEM Photographs (a) cured GDGB (b) cured GDGB:50%BioNovolac (50:50) (c) uncured 50%BioNovolac

2.3. Conclusions

It can be concluded that the compounds present in the fast pyrolysis bio-oil can be selectively polymerized to phenol-formaldehyde polymers - BioNovolac resins. BioNovolac can be blended homogeneously with GDGB, a resin that is not derived from bio-oil, and hence proves the compatibility of complex structured, high molecular weight BioNovolac with a simple, low molecular weight GDGB. GDGB can be densely crosslinked via anionic polymerization route; however, BioNovolac polymers cannot be homo-linked by DMAP. Nevertheless, the graft points between BioNovolac and GDGB networks prove that it is a semi-interpenetrating polymer network in which long chains of BioNovolac are interpenetrated in the presence of GDGB polymer network. The crosslinked networks show high thermo-mechanical performance and high glass transition temperatures. It is also important to note that the utilization of fast pyrolysis bio-oil, α -resorcylic acid and anionic polymerization initiator reduced the amount of petroleum-derived compounds. Since phenol was partially replaced in the synthesis of BioNovolac and bisphenol-A was not used at all, the thermoset networks are expected to have reduced toxicity concerns.

References

- [1] A.J. Ragauskas, C.K. Williams, B.H. Davison, G. Britovsek, J. Cairney, C.A. Eckert, W.J. Frederick, J.P. Hallett, D.J. Leak, C.L. Liotta, J.R. Mielenz, R. Murphy, R. Templer, T. Tschaplinski, The path forward for biofuels and biomaterials, *Science* 311(5760) (2006) 484-489.
- [2] A.V. Bridgwater, D. Meier, D. Radlein, An overview of fast pyrolysis of biomass, *Organic Geochemistry* 30(12) (1999) 1479-1493.
- [3] D. Mohan, C.U. Pittman, P.H. Steele, Pyrolysis of wood/biomass for bio-oil: A critical review, *Energy & Fuels* 20(3) (2006) 848-889.
- [4] A.V. Bridgwater, Review of fast pyrolysis of biomass and product upgrading, *Biomass & Bioenergy* 38 (2012) 68-94.
- [5] M. Stas, D. Kubicka, J. Chudoba, M. Pospisil, Overview of Analytical Methods Used for Chemical Characterization of Pyrolysis Bio-oil, *Energy & Fuels* 28(1) (2014) 385-402.
- [6] J.M. Raquez, M. Deleglise, M.F. Lacrampe, P. Krawczak, Thermosetting (bio)materials derived from renewable resources: A critical review, *Progress in Polymer Science* 35(4) (2010) 487-509.
- [7] L. Sperling, H., V. Mishra, The Current Status of Interpenetrating Polvrner Networks *Polymers for Advanced Technologies* 7(4) (1996) 197-208.
- [8] N. Gupta, A.K. Srivastava, Interpenetrating polymer networks - a review on synthesis and properties, *Polymer International* 35(2) (1994) 109-118.

- [9] L. Maleki, U. Edlund, A.C. Albertsson, Synthesis of full interpenetrating hemicellulose hydrogel networks, *Carbohydrate Polymers* 170 (2017) 254-263.
- [10] R. Ballesterro, B.M. Sundaram, H.V. Tippur, M.L. Auad, Sequential graft-interpenetrating polymer networks based on polyurethane and acrylic/ester copolymers, *Express Polymer Letters* 10(3) (2016) 204-215.
- [11] A. Knop, L.A. Pilato, *Phenolic Resins: Chemistry, Applications and Performance*, Springer-Verlag Berlin Heidelberg, New York and Tokyo, 1985.
- [12] A. Devi, D. Srivastava, Cardanol-based novolac-type phenolic resins. I. A kinetic approach, *Journal of Applied Polymer Science* 102(3) (2006) 2730-2737.
- [13] R. Yadav, D. Srivastava, Kinetics of the acid-catalyzed cardanol-formaldehyde reactions, *Materials Chemistry and Physics* 106(1) (2007) 74-81.
- [14] N.L. Huong, N.H. Nieu, T.T.M. Tan, U.J. Griesser, Cardanol-phenol-formaldehyde resins. Thermal analysis and characterization, *Die Angewandte Makromolekulare Chemie* 243(1) (1996) 77-85.
- [15] R. da Silva Santos, A.A. de Souza, M.-A. De Paoli, C.M.L. de Souza, Cardanol-formaldehyde thermoset composites reinforced with buriti fibers: Preparation and characterization, *Composites Part A: Applied Science and Manufacturing* 41(9) (2010) 1123-1129.
- [16] N.P.S. Chauhan, Facile synthesis of environmental friendly halogen-free microporous terpolymer from renewable source with enhanced physical properties, *Designed Monomers and Polymers* 15(6) (2012) 587-600.
- [17] A. Tejado, G. Kortaberria, C. Pena, J. Labidi, J.M. Echeverria, I. Mondragon, Lignins for phenol replacement in novolac-type phenolic formulations, part I: Lignophenolic resins synthesis and characterization, *Journal of Applied Polymer Science* 106(4) (2007) 2313-2319.

- [18] N. Terashima, K. Kitano, M. Kojima, M. Yoshida, H. Yamamoto, U. Westermark, Nanostructural assembly of cellulose, hemicellulose, and lignin in the middle layer of secondary wall of ginkgo tracheid, *Journal of Wood Science* 55(6) (2009) 409-416.
- [19] S. Sen, S. Patil, D.S. Argyropoulos, Thermal properties of lignin in copolymers, blends, and composites: a review, *Green Chemistry* 17(11) (2015) 4862-4887.
- [20] A. Gandini, T.M. Lacerda, From monomers to polymers from renewable resources: Recent advances, *Progress in Polymer Science* 48 (2015) 1-39.
- [21] B. Li, Y. Wang, N. Mahmood, Z. Yuan, J. Schmidt, C. Xu, Preparation of bio-based phenol formaldehyde foams using depolymerized hydrolysis lignin, *Industrial Crops and Products* 97 (2017) 409-416.
- [22] S.S. Kelley, X.-M. Wang, M.D. Myers, D.K. Johnson, J.W. Scahill, Use of biomass pyrolysis oils for preparation of modified phenol formaldehyde resins, in: B. A.V., B. D.G.B. (Eds.) *Developments in Thermochemical Biomass Conversion*, Springer·Science+Business Media, B. V., United Kingdom, 1997, pp. 557-574.
- [23] Y. Zhao, N. Yan, M. Feng, Synthesis and Characterization of Bio-Based Phenol-Formaldehyde Resol Resins from Bark Autoclave Extractives, *Forest Products Journal* 66(1-2) (2016) 18-28.
- [24] A.E. Vithanage, E. Chowdhury, L.D. Alejo, P.C. Pomeroy, W.J. DeSisto, B.G. Frederick, W.M. Gramlich, Renewably sourced phenolic resins from lignin bio-oil, *Journal of Applied Polymer Science* 134(19) (2017) 10.
- [25] A. Effendi, H. Gerhauser, A.V. Bridgwater, Production of renewable phenolic resins by thermochemical conversion of biomass: A review, *Renewable & Sustainable Energy Reviews* 12(8) (2008) 2092-2116.

- [26] B. Ellis, Introduction to the chemistry, synthesis, manufacture and characterization of epoxy resins, in: B. Ellis (Ed.), *Chemistry and Technology of Epoxy Resins* Chapman & Hall, United Kingdom, 1993, pp. 1-35.
- [27] W. Brostow, S.H. Goodman, J. Wahrmund, Epoxies, in: H. Dodiuk, S.H. Goodman (Eds.), *Handbook of Thermoset Plastics*, Elsevier, USA, 2014, pp. 191-252.
- [28] F.F. Ng, G. Couture, C. Philippe, B. Boutevin, S. Caillol, Bio-Based Aromatic Epoxy Monomers for Thermoset Materials, *Molecules* 22(1) (2017) 48.
- [29] F. Seniha Güner, Y. Yağcı, A. Tuncer Erciyes, Polymers from triglyceride oils, *Progress in Polymer Science* 31(7) (2006) 633-670.
- [30] J.R. Kim, S. Sharma, The development and comparison of bio-thermoset plastics from epoxidized plant oils, *Industrial Crops and Products* 36(1) (2012) 485-499.
- [31] P.Y. Kuo, M. Sain, N. Yan, Synthesis and characterization of an extractive-based bio-epoxy resin from beetle infested *Pinus contorta* bark, *Green Chemistry* 16(7) (2014) 3483-3493.
- [32] P.Y. Kuo, L.D. Barros, M. Sain, J.S.Y. Tjong, N. Yan, Effects of Reaction Parameters on the Glycidyl Etherification of Bark Extractives during Bioepoxy Resin Synthesis, *Acs Sustainable Chemistry & Engineering* 4(3) (2016) 1016-1024.
- [33] C. Aouf, S. Benyahya, A. Esnouf, S. Caillol, B. Boutevin, H. Fulcrand, Tara tannins as phenolic precursors of thermosetting epoxy resins, *European Polymer Journal* 55 (2014) 186-198.
- [34] Y. Celikbag, T.J. Robinson, B.K. Via, S. Adhikari, M.L. Auad, Pyrolysis oil substituted epoxy resin: Improved ratio optimization and crosslinking efficiency, *Journal of Applied Polymer Science* 132(28) (2015) 9.

[35] Y. Celikbag, S. Meadows, M. Barde, S. Adhikari, G. Buschle-Diller, M.L. Auad, B. Via, Synthesis and Characterization of Bio-oil-based Self-curing Epoxy Resin, 253rd American Chemical

Society (ACS) National Meeting and Exposition, San Francisco, 2017.

[36] B. Sibaja, C.P. Matheus, R.B. Mendez, J. Vega-Baudrit, M.L. Auad, Synthesis and Characterization of Interpenetrating Polymer Networks (IPNs) from Acrylated Soybean Oil and a-Resorcylic Acid: Part 1. Kinetics of Network Formation, Journal of Renewable Materials (2017).

[37] B. Sibaja, C.P. Matheus, R.B. Mendez, R. Farag, J. Vega Baudrit, M.L. Auad, Synthesis and Characterization of Interpenetrating Polymer Networks (IPNs) from Acrylated Soybean Oil a-Resorcylic Acid: Part 2. Thermo-Mechanical Properties and Linear Fracture Mechanics, Journal of Renewable Materials (2017).

[38] S. Khadem, R.J. Marles, Monocyclic Phenolic Acids; Hydroxy- and Polyhydroxybenzoic Acids: Occurrence and Recent Bioactivity Studies, Molecules 15(11) (2010) 7985-8005.

[39] R. Shakya, J. Whelen, S. Adhikari, R. Mahadevan, S. Neupane, Effect of temperature and Na₂CO₃ catalyst on hydrothermal liquefaction of algae, Algal Research 12 (2015) 80-90.

[40] H.X. Ben, A.J. Ragauskas, NMR Characterization of Pyrolysis Oils from Kraft Lignin, Energy & Fuels 25(5) (2011) 2322-2332.

[41] G. Zhang, W. Choi, A low-cost sensitizer based on a phenolic resin for charge-transfer type photocatalysts working under visible light, Chemical Communications 48(86) (2012) 10621-10623.

[42] C. Aouf, C. Le Guerneve, S. Caillol, H. Fulcrand, Study of the O-glycidylation of natural phenolic compounds. The relationship between the phenolic structure and the reaction mechanism, Tetrahedron 69(4) (2013) 1345-1353.

- [43] I.E. Dell'Erba, R.J.J. Williams, Homopolymerization of epoxy monomers initiated by 4-(dimethylamino)pyridine, *Polymer Engineering and Science* 46(3) (2006) 351-359.
- [44] L.H. Sperling, *Introduction to Physical Polymer Science*, John Wiley & Sons, Inc, New Jersey, 2006, pp. 355-365.
- [45] I. Poljansek, M. Krajnc, Characterization of phenol-formaldehyde prepolymer resins by in line FT-IR spectroscopy, *Acta Chimica Slovenica* 52(3) (2005) 238-244.

Chapter 3

Crosslinked networks from epoxidized bio-novolac and epoxidized bio-oil

3.1. Introduction

Epoxy resins are important thermosetting polymers due to their versatile applications in coatings, adhesives, composites and electronics industry.[1] General characteristics such as aromatic structures and macromolecular network formation after crosslinking offer excellent chemical, mechanical and electrical properties to epoxy systems.[2] Using novolac resin as a precursor of epoxy resins has been a great choice as it improves the thermo-mechanical performance of epoxies due to higher hydroxyl functionality and additional properties of novolac polymers.[3] Novolac resins are traditionally made by reacting phenol and formaldehyde with a molar excess of phenol over formaldehyde in acidic medium. With a strong aromatic backbone, they offer high solvent, heat and water resistance. They possess enhanced thermal properties, mechanical performance and good dimensional stability.[4, 5] Nevertheless, all epoxy and epoxidized novolac resins commercially utilized are derived from petrochemicals. Concerns over petroleum resources have caused a greater need for technological advances in biomass conversion. Specific types of biomass-derived compounds such as plant oils have been used for synthesizing epoxy monomers and polymers.[6-8] Historically, the plant biomass was often used to deliver energy by direct combustion processes, but this method provided limited energy due to its lower heating value than other petroleum based fuels.[9] Over a long period of time, plant and animal biomass had been

converted to fossil fuels by natural processes. Although there are several challenges to bio-refining of plant biomass in an efficient manner,[10] thermo-chemical transformations such as fast pyrolysis have been successful in producing a mixture of diverse functional organic compounds.[9, 11, 12] This mixture is termed as bio-oil and generally contains oxygenated aliphatic and aromatic hydrocarbons.[13] Reactive functional groups of organic compounds can be derivetized to produce monomers or oligomers, which further can be polymerized to yield polymers. Since pyrolysis and liquefaction can be often used to break down lignin along with cellulose and hemi-cellulose, mono-phenols or oligophenolic structures can be found in the liquid bio-oil. Phenol derivatives from bio-oil have been used in several ways to produce phenol-formaldehyde polymeric materials.[14-16] Biomass-based phenolic foams were prepared by using hydrolysis lignin depolymerized by a low temperature and low pressure method by Li et al.[17] Pan synthesized novolac and resol-type phenol-formaldehyde polymers from organic solvent liquefied biomass.[18] Similar approaches on the production of epoxides from bio-oil and biomass have been well documented, and have been discussed in chapter 1. In the current study, the resins were also blended with a previously studied, epoxy oligomer produced from α -resorcylic acid to observe the effect of low viscosity and molecular weight epoxide on the final properties. The resulting resins can be aimed for replacing traditional epoxy matrices in composite applications and as binders in coatings and adhesives. These resins can be crosslinked with hardeners to build high performance thermosetting networks. Crosslinked bio-thermosets in this study were also compared to crosslinked traditional thermosets.

3.2. Experimental section

3.2.1. Materials

Fast pyrolysis bio-oil derived from hardwood was obtained from Red Arrow, USA. Phenol (detached crystals, 99%), formalin solution (37% w/w), acetone, methanol, sodium hydroxide, (\pm)-epichlorohydrin (99%), 3,5-dihydroxybenzoic acid (α -resorcylic acid), chromium(III)acetyl acetonate, N-hydroxy-5-norbornene-2,3-dicarboximide (NHND), deuterated chloroform were purchased from VWR International, USA. 2-Chloro-4,4,5,5-tetramethyl-1,3,2-dioxaphospholane (TMDP) was ordered from Sigma Aldrich. Oxalic acid, anhydrous, was supplied by Spectrum Chemical Mfg. Corp. Benzyltriethylammonium chloride was obtained from TCI. EPON 828, an epoxy resin based on bisphenol-A, was provided by Momentive, USA. Jeffamine T-403, a polyetheramine-based epoxy hardener, was ordered from Huntsman, USA.

3.2.2. Methods

3.2.2.1. Characterization of fast pyrolysis bio-oil

Water from fast pyrolysis bio-oil was removed by a rotary evaporator at 60 °C under reduced pressure. The bio-oil was qualitatively analyzed by Gas Chromatography-Mass Spectroscopy (GC-MS) as per the procedure described in chapter 2. Around 0.5 g of bio-oil was diluted with 12 mL of methanol and mixed well. A split ratio of 20:1 was set for injecting 1 μ L of diluted bio-oil into a DB-1701 column equipped to an Agilent 7890 GC/5975MS.

^{31}P -nuclear magnetic resonance (^{31}P -NMR) spectroscopy was used to measure the hydroxyl number and quantify different categories of hydroxyl groups present in the bio-oil using phosphorylation procedure described in chapter 2. The stock solution was prepared by dissolving 20 mg of NHND and 20 mg of chromium(III)acetyl acetonate in the mixture of 3 mL pyridine and

2 mL deuterated chloroform. To the pre-weighed bio-oil amount (approximately, 20 mg), 550 μL of stock solution was added and the vial was stirred. TMDP (150 μL) was added to the mixture and the vial was stirred well to make sure no precipitates were formed. The sample was transferred to the NMR spectroscopy tube and the spectrum was acquired with a Bruker Avance II 250 MHz spectrometer using inverse gated decoupling pulse sequence, 90-degree pulse angle, 25 s pulse delay and 128 scans.

Fourier transform infrared (FTIR) spectroscopy was performed with attenuated total reflection (ATR) method using Thermo Scientific Nicolet 6700 FT-IR spectrophotometer and OMNIC 7.3 software. The spectra were collected in the wavenumber range 400 cm^{-1} to 4000 cm^{-1} at a resolution of 4 cm^{-1} and 40 scans. Same parameters were used for collecting FTIR spectra of all materials discussed henceforth.

3.2.2.2. Synthesis of novolac and bio-novolac resins

Novolac and bio-novolac resins was synthesized as per the procedure described in the chapter 2. For synthesizing bio-novolac resin, phenol was replaced by 50 wt% bio-oil and co-reacted with formaldehyde. The progress of reaction was monitored by FTIR spectroscopy. The hydroxyl number of the novolac and bio-novolac resins was measured by ^{31}P -NMR spectroscopy.

3.2.2.3. Synthesis of epoxy resins

Epoxy resins were synthesized from four different phenolic substrates, i.e., bio-oil, novolac, bio-novolac and α -resorcylic acid. A two-step glycidylation method reported in the literature was followed.[19, 20] Desired amount of phenolic monomer was taken in a glass reactor and epichlorohydrin equivalent to 4 M eq/OH was added to it. The temperature was raised to 100 $^{\circ}\text{C}$

while continuous stirring and benzyltriethylammonium chloride (BnEt₃NCl), a phase transfer catalyst, was added (0.012 M eq/OH). Reaction was carried out for 1 hour at 100 °C, and then the temperature was allowed to fall to 30 °C. In the second step, a mixture of BnEt₃NCl (0.012 M eq/OH) and 20 wt% aqueous solution of sodium hydroxide (2 M eq/OH) was added dropwise to the reaction mixture maintained at 30 °C while stirring. After the addition was completed, the reaction was continued for 90 minutes at 30 °C. The organic layer was washed several times with water to remove salt. Unreacted epichlorohydrin that might be present in the organic layer was distilled off by rotary evaporation under reduced pressure and at 90 °C. Epoxy resins were named as epoxidized bio-oil (EBO), epoxidized novolac (EN), epoxidized bio-novolac (EBN) and glycidyl 3,5-diglycidoxybenzoate (GDGB). ³¹P-NMR spectra of EBO, EN and EBN were collected as per the method described earlier in this study. Stepwise synthesis of epoxy resins is described in Figure 3.1. Epoxy resins were analyzed by FTIR spectroscopy and the epoxy equivalent weight (EEW) was measured by the hydrogen bromide-glacial acetic acid solution method described in chapter 2.

3.2.2.4. Crosslinking of epoxy resins

Epoxy resins and their physical blends were mixed with calculated amount of Jeffamine T-403.

The following equation was used while calculating the required amount of Jeffamine T-403, W_J

$$W_J = \frac{W_E}{EEW} \times AHEW$$

where,

W_E = amount of epoxy resin

AHEW = Amine hydrogen equivalent weight, is the weight of amine hardener containing one equivalent of amine hydrogen

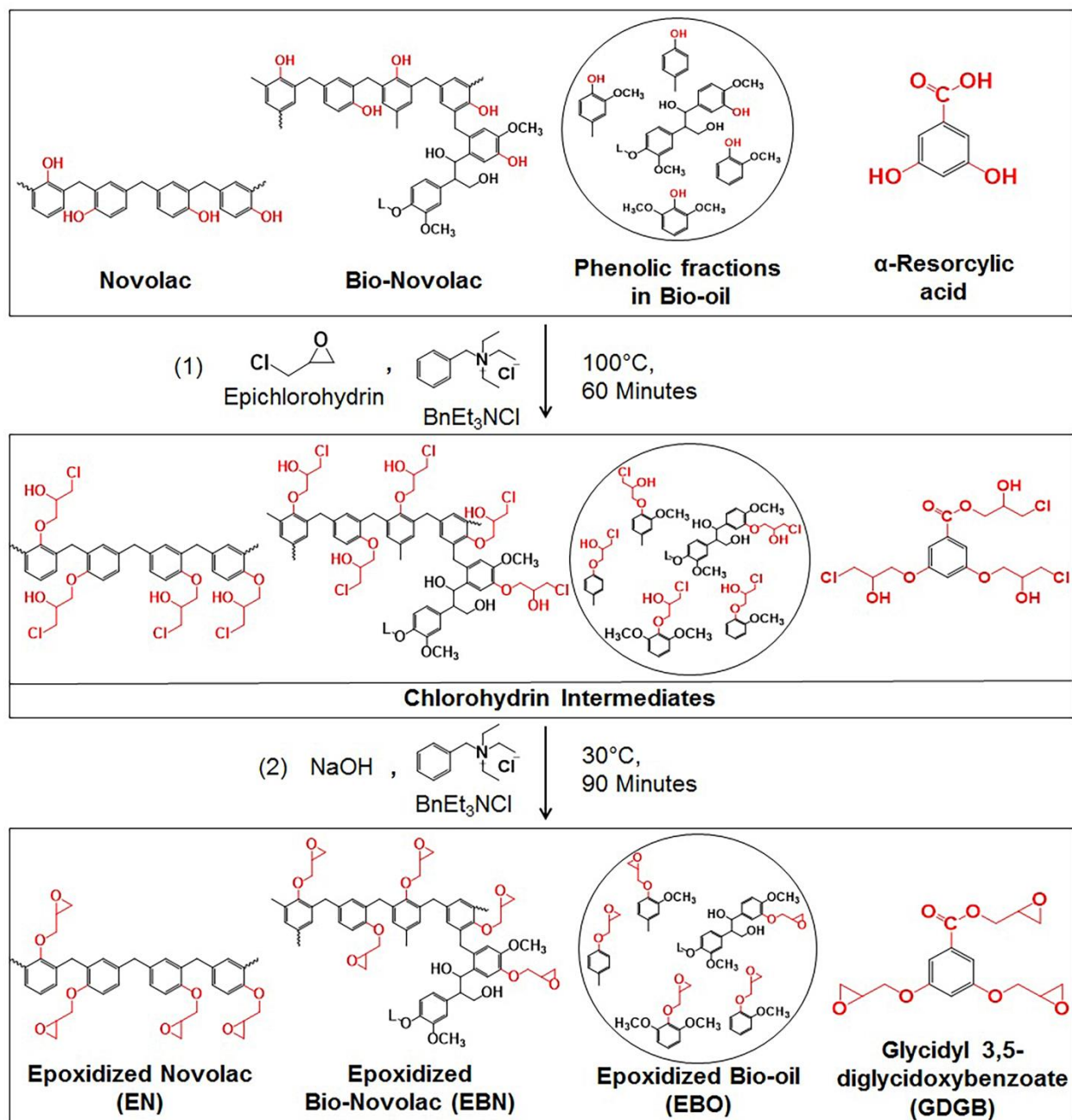


Figure 3.1: Glycidylation of phenolic substrates

All resin mixtures were added to Teflon molds and heated in conventional oven at 60°C for 2 hours followed by $80, 90, 100, 120, 140^\circ\text{C}$ for 1 hour each and finally at 165°C for 15 minutes.

3.2.2.5. Evaluation of thermo-mechanical performance

For assessing thermo-mechanical properties of crosslinked samples, three-point bending geometry was used using a TA Instruments RSAIII Dynamic Mechanical Analyzer, with approximate sample dimensions of $30 \times 10 \times 3$ mm. The constant strain of 0.1 % and oscillating frequency of 1 Hz was applied while increasing the temperature from 25 °C to 200 °C at 10 °C/min. Storage modulus and $\tan\delta$ were plotted against temperature and the glass transition temperature was measured at the maximum $\tan\delta$. The active chains density was calculated using the value of storage modulus in the rubbery plateau, at the temperature 50 °C higher than glass transition temperature of the sample.

3.2.2.6. Other techniques

Differential scanning calorimetry (DSC) was used to observe the glass transition temperature of the crosslinked polymer networks by using a heat-cool-heat temperature program.

Soxhlet extraction was carried out with 200 mL dichloromethane (continuously refluxed) for 24 hours. After extraction, the residual solids were dried and weighed. The mass retained after drying the samples was compared.

Crosslinked thermoset systems were analyzed under scanning electron microscope. The samples were immersed in liquid nitrogen and then cut to observe the cross-sections. All samples were sputter-coated with gold before SEM analysis.

3.2.3. Results and discussion

3.2.3.1. Characterization of fast pyrolysis bio-oil

Using GC-MS, it was observed that the bio-oil consisted of substituted phenols, carboxylic acids, hydroxyaldehydes, hydroxyketones, alcohols and monosaccharides. The total hydroxyl content of bio-oil measured by ^3P -NMR spectroscopy was 5.80 mmol OH/g.

3.2.3.2. Characterization of bio-novolac resins

FTIR spectroscopy of both novolac and bio-novolac resins confirmed the appearance of peaks at 3300 – 3200 cm^{-1} (O-H stretch), 3013 cm^{-1} (sp^2 C-H stretch), 1612 – 1435 cm^{-1} (aromatic C=C stretch), 1229 cm^{-1} (phenolic C-O stretch) and 755 cm^{-1} (aromatic C-H, out of plane bend). It indicated that bio-novolac resin was chemically similar to novolac resin.

3.2.3.3. Characterization of epoxy resins

Figure 3.2 – 3.4 show identifiable differences between epoxy resins and their phenolic precursors. The peaks observed in the range 906 cm^{-1} to 911 cm^{-1} appear due to asymmetric bending of the epoxide ring whereas the peaks ranging between 835 cm^{-1} and 845 cm^{-1} are due to symmetric bending. Similarly, deformation peaks were observed for C-O-C in the range 1225 cm^{-1} to 1250 cm^{-1} and in the range 1026 cm^{-1} to 1043 cm^{-1} for asymmetric and symmetric bending, respectively. A broad peak in the range 3100 – 3500 cm^{-1} corresponding to O-H stretching vibrations was observed to reduce in every case. This is due to the conversion of phenolic hydroxyl and carboxyl OH groups into glycidyl functionality. Aliphatic hydroxyl, however, tend to appear due to low reactivity during epoxidation.

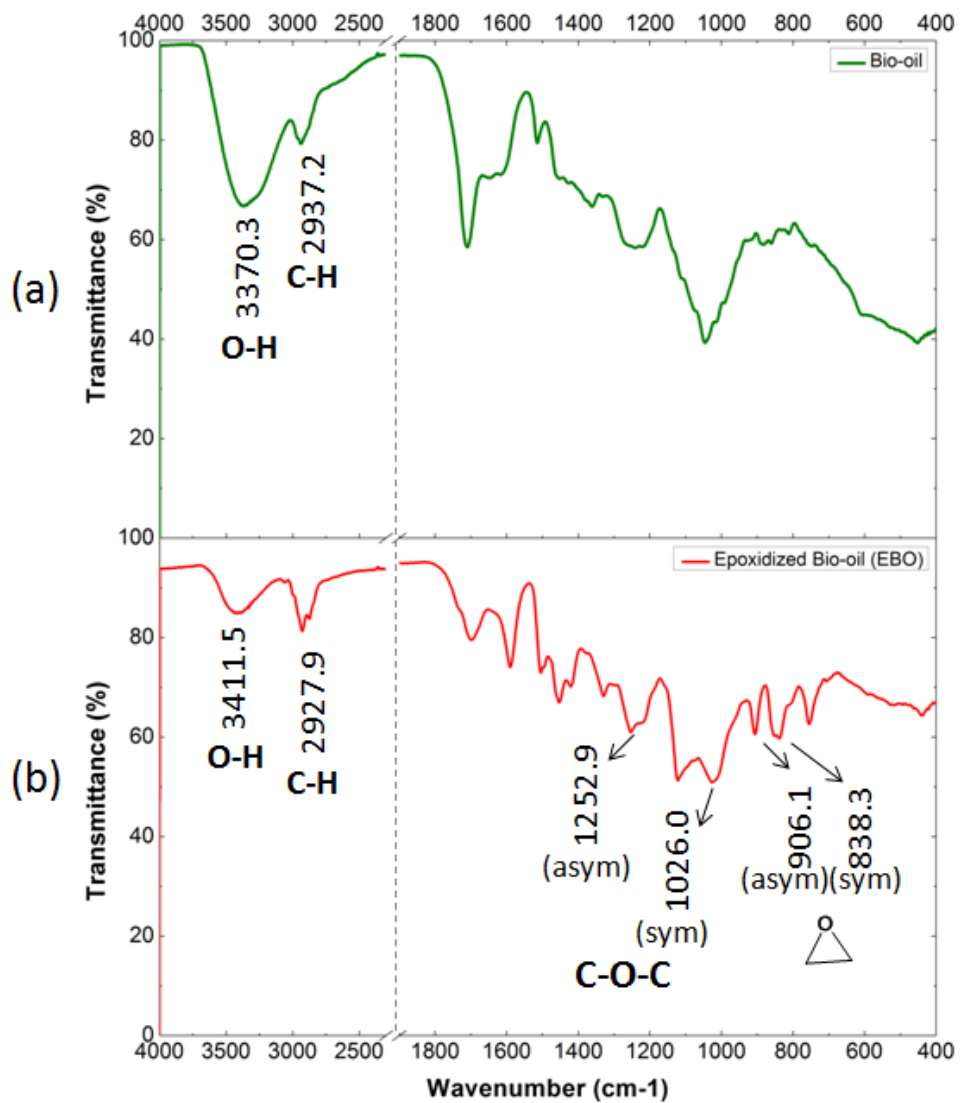


Figure 3.2: FTIR spectra of (a) bio-oil (b) epoxidized bio-oil

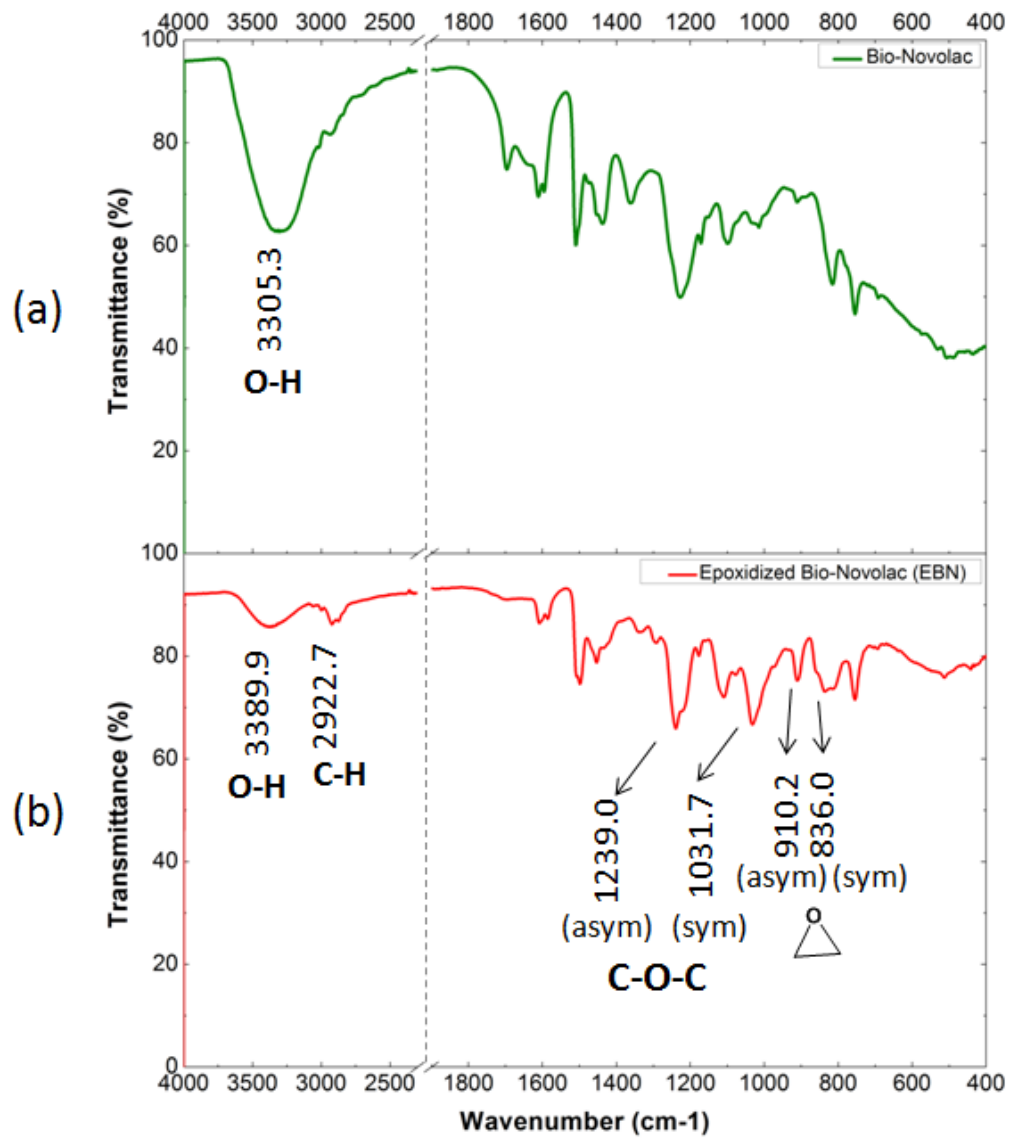


Figure 3.3: FTIR spectra of (a) bio-novolac (b) epoxidized bio-novolac

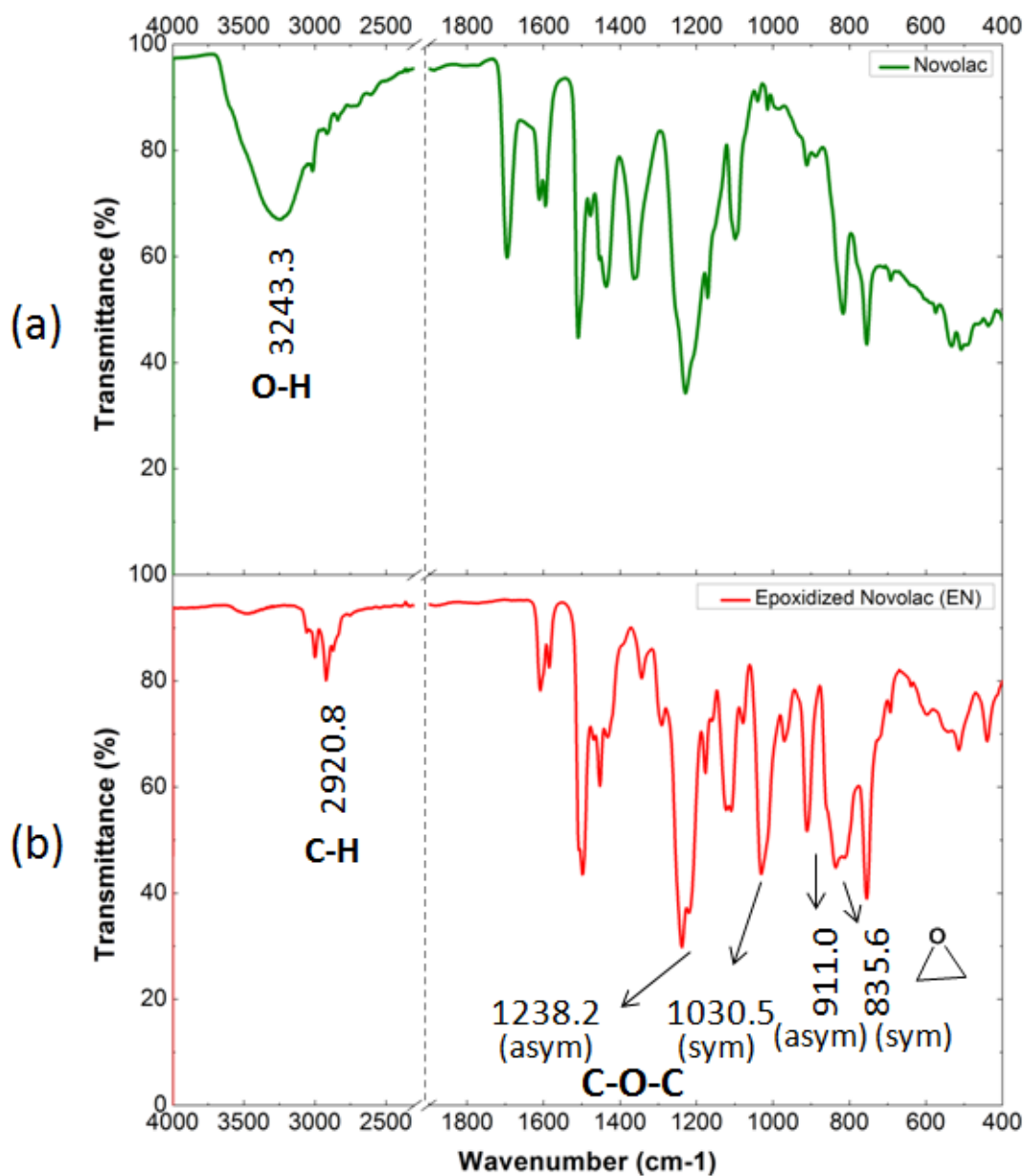


Figure 3.4: FTIR spectra of (a) novolac (b) epoxidized novolac

The conversion of phenolic OH groups was confirmed by ³¹P-NMR spectroscopy as depicted in Table 3.1. In all cases, different phenolic groups were successfully epoxidized although epoxidized bio-novolac shows residual phenolic OH content for β-5 and 4-O-5 type phenolic OH. The aliphatic OH content was observed to increase in each epoxy resin. This is due to ring opening of

epoxy groups to form secondary aliphatic hydroxyl groups. Acidic OH groups were absent in novolac and bio-novolac resins because of the purification performed before the epoxidation reaction. Bio-oil, however, was used as it was, and hence consisted of carboxylic acids which also took part in epoxidation. It can be proved from zero acidic OH content of epoxidized bio-oil.

Table 3.1: Hydroxyl number measured by ³¹P-NMR spectroscopy for (a) bio-oil and epoxidized bio-oil, (b) novolac and epoxidized novolac, (c) bio-novolac and epoxidized bio-novolac

OH Type		Range (ppm)	Bio-oil		Epoxidized Bio-oil		Novolac		Epoxidized Novolac		Bio-Novolac		Epoxidized Bio-Novolac			
Aliphatic OH		150.00-145.50	3.58		5.54		0		0.92		0.75		2.65			
Phenolic OH	C-5 substituted condensed phenolic OH	β-5	144.70-142.80	0.38	1.71	0	8.09	0	0	6.03	0.24	0.50	0.18	0.06		
		4-O-5	142.80-141.70	0.33								0			0.74	
		5-5	141.70-140.20	0.26								0			0.25	
	Guaiacyl phenolic OH	140.20-139.00	0.31	0								0			0.17	0
	Catechol type OH	139.00-138.20	0.33	0								0			0.45	0
	p-hydroxy-phenyl OH	138.20-137.30	0.10	0								0			3.92	0
	Acidic OH	136.60-133.60	0.51	0								0			0	
TOTAL			5.80		5.54		8.09		0.92		6.78		2.89			

The epoxy equivalent weights of epoxy resins are tabulated in Table 3.2. An epoxy resin derived from compound containing higher amount of phenolic and carboxyl OH groups, is more likely to have a higher number of epoxide after the epoxidation reaction. Thus, a higher amount of epoxides tends to show less EEW. Novolac and bio-novolac are prepolymers while bio-oil is a mixture of monomeric, oligomeric and macromolecular phenolic components. Due to high phenolic OH content, EN showed a lower EEW than EBN and EBO. EEW of EBN was higher than EBO since EBN is a prepolymer and probably has a high molecular weight. The reason GDGB displayed lowest EEW since its precursor, α-resorcylic acid, is a low molecular weight monomer bearing

three OH groups per molecule (one carboxyl and two phenolic hydroxyls) all of which have tendency to be converted into epoxides. EPON 828 is a commercially manufactured epoxy resin and is generally made to have desired EEW.

Table 3.2: Epoxy equivalent weights of epoxy resins

Epoxy Resin	Epoxy Equivalent Weight (EEW), g/eq
Epoxidized novolac (EN)	132 ± 2
Epoxidized bio-novolac (EBN)	326 ± 6
Epoxidized bio-oil (EBO)	314 ± 2
Epoxy resin from α -resorcylic acid (GDGB)	107 ± 3
EPON 828 (a commercial epoxy resin)	158 ± 3

3.2.3.4. Thermo-mechanical performance of epoxy resins and other techniques

In the case of DMA, the temperature at which $\tan \delta$ achieved maximum value was taken as glass transition temperature while for DSC, the temperature at maximum decline in slope of heat flow against temperature was considered. The measured values of glass transition temperature, storage modulus at room temperature, active chain density and mass retained (Soxhlet extraction) are listed in Table 3.3. Figure 3.5 depicts the plot of storage modulus of crosslinked epoxy resins against temperature.

Table 3.3: Thermo-mechanical properties of crosslinked epoxy resins

Epoxy Resin	Notes	T_g (°C), DMA	T_g (°C), DSC	E' (GPa) at room tempera ture	Active Chains Density, n (mol/m³)	Mass (%) Retained
Epoxidized novolac (EN)	not made from bio-oil	127	119	1.68	5321	99
Epoxidized bio-novolac (EBN)		91	89	2.00	1855	91
EBN:GDGB 50:50	50:50 (wt%) blend of epoxidized bio-novolac and GDGB, crosslinked by Jeffamine T-403	99	102	2.80	4665	97
EPON 828	a commercial epoxy resin based on bisphenol-A, cured by Jeffamine T-403	80	76	1.77	2599	99
Epoxidized bio-oil (EBO)		92	89	1.88	404	77

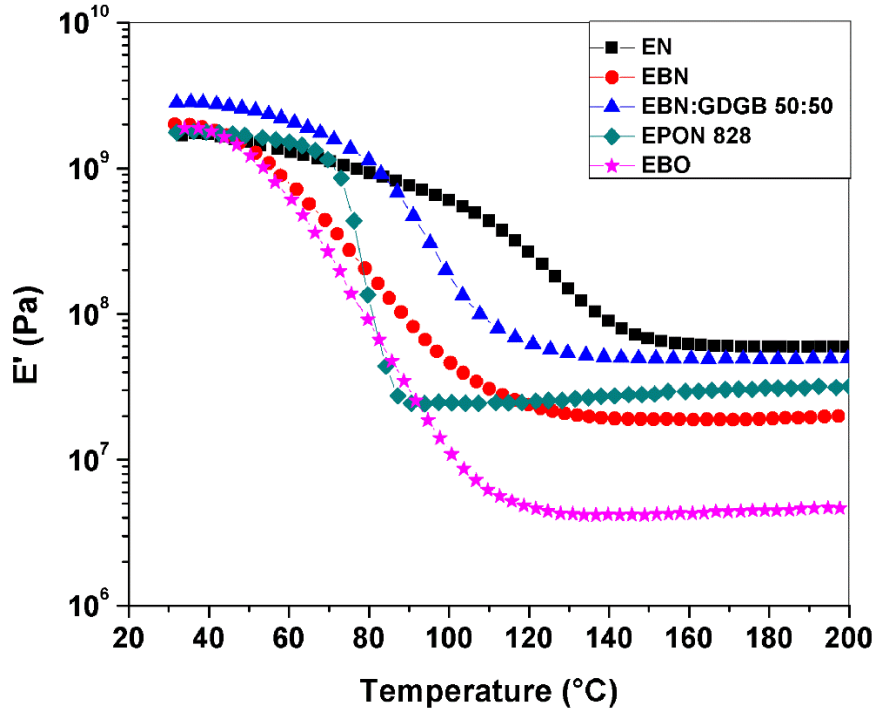
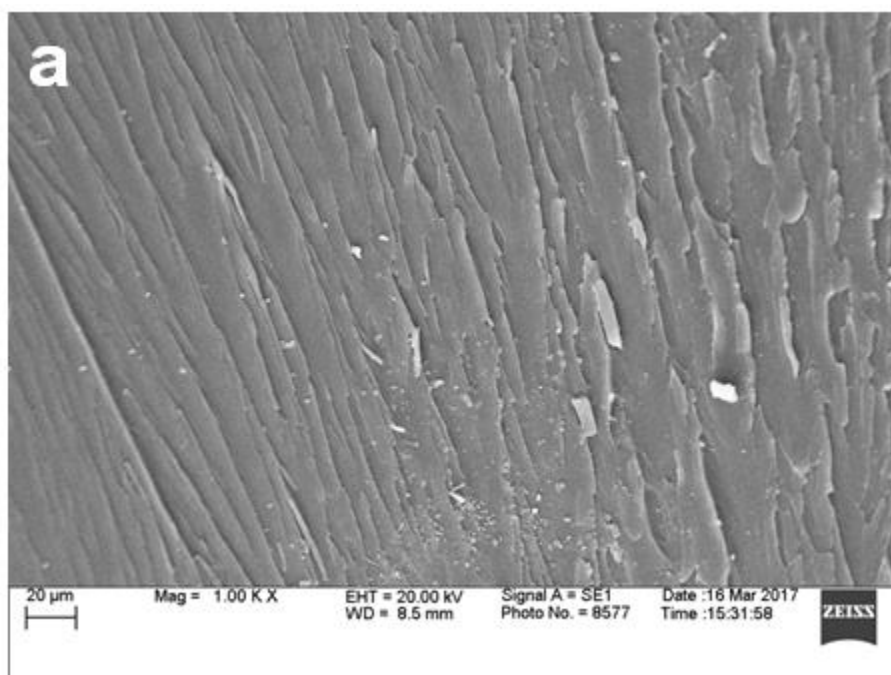
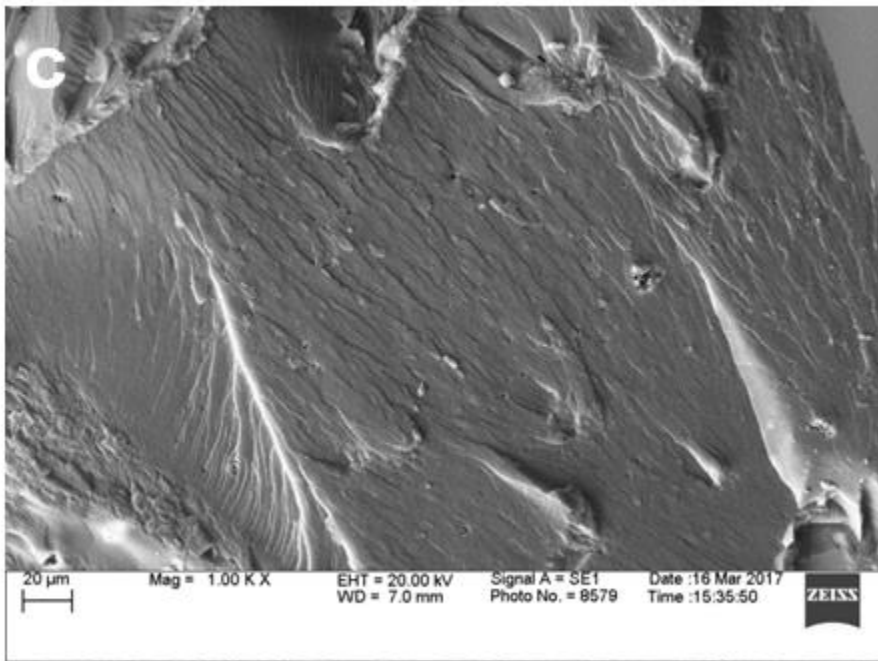
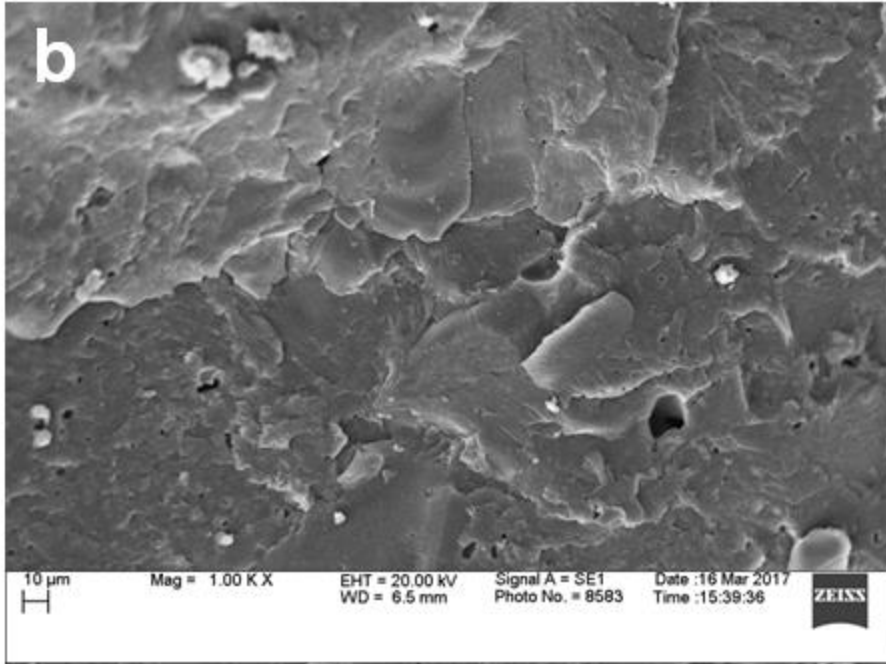


Figure 3.5: Storage modulus of crosslinked epoxy resins

It was observed that the epoxy resins derived from phenol-formaldehyde prepolymers (novolac and epoxidized bio-novolac) showed higher performance than epoxy resin based only on bio-oil. At the molecular level, novolac and bio-novolac resins consist of a continuous network of phenolic compounds bridged by methylene groups; whereas epoxidized bio-oil contains monomeric and oligomeric epoxide compounds with lignin fractions. Epoxidized phenol-formaldehyde resins retain the macromolecular aromatic network after epoxidation and hence display better properties than epoxidized bio-oil. Moreover, incorporation of GDGB helped to enhance the properties of epoxidized bio-novolac due to higher epoxide content of GDGB. All epoxy resins derived from bio-oil, directly or indirectly, showed a higher glass transition temperature than commercially used epoxy resin, EPON 828 despite its higher epoxide content. The lignin fractions available in bio-

oil form a part of molecular structure of the bio-oil derived epoxy resins and offer additional strength to the network. The active chain density was found to be lower in the case of bio-oil derived epoxy resins compared to their petroleum-derived counter parts. Lower value of active chains density is impacted by lower modulus at elevated temperature, which probably was due to poor thermal stability of lignin fractions at elevated temperature. Similar effect was reflected by mass (%) retained during Soxhlet extraction. Morphology of cured epoxy resins was found to be comparable as seen in Figure 3.6.





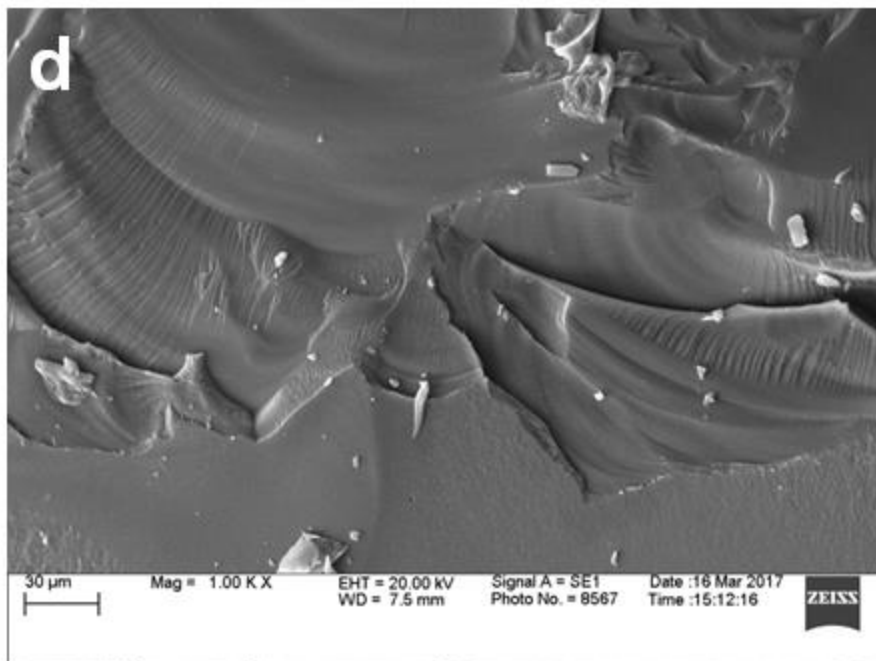


Figure 3.6: SEM photographs of crosslinked thermosets: (a) epoxidized novolac, (b) epoxidized bio-novolac (EBN), (c) EBN:GDGB 50:50, (d) epoxidized bio-oil

All cured samples indicated similar homogeneity. The fractured surface of EN suggested high brittleness; whereas EBO revealed low extent of brittleness. Moreover, the fractured surface of EBN is indicative of a more diverse system due to the possibility of formation of bio-novolac from several aromatic substituted compounds. Incorporation of GDGB to EBN had an effect on increasing the overall homogeneity of the system due to reduced complexity. It was found that resins derived from phenol-formaldehyde networks had higher brittle lines indicating more brittleness of the cured systems.

3.3. Conclusions

The phenolic hydroxyl and carboxylic functional groups in the bio-derived compounds can be functionalized to epoxides. Bio-oil proves to be a potential phenolic resource and can be epoxidized directly or by synthesizing its novolac-type prepolymer. Bio-oil based epoxy resins have structural and chemical similarity with petroleum-derived ones and can also be crosslinked by the existing amine hardeners. Synthesis of novolac-type pre-polymer followed by epoxidation helps to achieve properties of epoxy and novolac resins. The synthesized resin systems yielded thermoset materials with high glass transition temperatures and high moduli despite having higher bio-content and more uncontrolled, complex chemistry than traditional epoxy resins. Compatibility of bio-oil-based epoxy resin with non-bio-oil-based resin (GDGB) helped to achieve homogeneity of the final thermosets. This phenomenon was also confirmed by scanning electron microscopy which revealed the comparable morphologies of bio-oil based epoxies to their petrochemical-based analogues. As the bio-oil-based epoxy polymers performed on par with the phenol and bisphenol-A based epoxides, they can be a potential replacement in many applications such as matrices for composites, resins for coatings and adhesives etc. Further, the fact that the bio-oil can be sourced from any lignocellulosic biomass, can open a whole new category of raw materials including but not limited to the energy crops, forest waste, saw dust, agricultural waste etc. Utilization of such resources would help to reduce the consumption of petrochemicals and to achieve higher sustainability.

References

- [1] B. Ellis, Introduction to the chemistry, synthesis, manufacture and characterization of epoxy resins, in: B. Ellis (Ed.), *Chemistry and Technology of Epoxy Resins* Chapman & Hall, United Kingdom, 1993, pp. 1-35.
- [2] M. Ogata, N. Kinjo, T. Kawata, Effects of crosslinking on physical properties of phenol–formaldehyde novolac cured epoxy resins, *48(4)* (1993) 601.
- [3] R.S. Gour, K.G. Raut, M.V. Badiger, Flexible epoxy novolac coatings: Use of cardanol-based flexibilizers, *Journal of Applied Polymer Science* *134(23)* (2017) 12.
- [4] C.P.R. Nair, Advances in addition-cure phenolic resins, *Progress in Polymer Science* *29(5)* (2004) 401-498.
- [5] A. Knop, L.A. Pilato, *Phenolic Resins: Chemistry, Applications and Performance*, Springer-Verlag Berlin Heidelberg, New York and Tokyo, 1985.
- [6] G.Z. Yang, B.J. Rohde, M.L. Robertson, Hydrolytic degradation and thermal properties of epoxy resins derived from soybean oil, *Green Materials* *1(2)* (2013) 125-134.
- [7] A. Maiorana, L.Y. Ren, G. Lo Re, S. Spinella, C.Y. Ryu, P. Dubois, R.A. Gross, Bio-based epoxy resin toughening with cashew nut shell liquid-derived resin, *Green Materials* *3(3)* (2015) 80-92.
- [8] J.R. Kim, S. Sharma, The development and comparison of bio-thermoset plastics from epoxidized plant oils, *Industrial Crops and Products* *36(1)* (2012) 485-499.

- [9] A.V. Bridgwater, D. Meier, D. Radlein, An overview of fast pyrolysis of biomass, *Organic Geochemistry* 30(12) (1999) 1479-1493.
- [10] A.J. Ragauskas, C.K. Williams, B.H. Davison, G. Britovsek, J. Cairney, C.A. Eckert, W.J. Frederick, J.P. Hallett, D.J. Leak, C.L. Liotta, J.R. Mielenz, R. Murphy, R. Templer, T. Tschaplinski, The path forward for biofuels and biomaterials, *Science* 311(5760) (2006) 484-489.
- [11] A.V. Bridgwater, Review of fast pyrolysis of biomass and product upgrading, *Biomass & Bioenergy* 38 (2012) 68-94.
- [12] A.A. Peterson, F. Vogel, R.P. Lachance, M. Froling, M.J. Antal, J.W. Tester, Thermochemical biofuel production in hydrothermal media: A review of sub- and supercritical water technologies, *Energy & Environmental Science* 1(1) (2008) 32-65.
- [13] M. Stas, D. Kubicka, J. Chudoba, M. Pospisil, Overview of Analytical Methods Used for Chemical Characterization of Pyrolysis Bio-oil, *Energy & Fuels* 28(1) (2014) 385-402.
- [14] A. Effendi, H. Gerhauser, A.V. Bridgwater, Production of renewable phenolic resins by thermochemical conversion of biomass: A review, *Renewable & Sustainable Energy Reviews* 12(8) (2008) 2092-2116.
- [15] A.E. Vithanage, E. Chowdhury, L.D. Alejo, P.C. Pomeroy, W.J. DeSisto, B.G. Frederick, W.M. Gramlich, Renewably sourced phenolic resins from lignin bio-oil, *Journal of Applied Polymer Science* 134(19) (2017) 10.
- [16] S.S. Kelley, X.-M. Wang, M.D. Myers, D.K. Johnson, J.W. Scahill, Use of biomass pyrolysis oils for preparation of modified phenol formaldehyde resins, in: B. A.V., B. D.G.B. (Eds.) *Developments in Thermochemical Biomass Conversion*, Springer·Science+Business Media, B. V., United Kingdom, 1997, pp. 557-574.

- [17] B. Li, Y. Wang, N. Mahmood, Z. Yuan, J. Schmidt, C. Xu, Preparation of bio-based phenol formaldehyde foams using depolymerized hydrolysis lignin, *Industrial Crops and Products* 97 (2017) 409-416.
- [18] H. Pan, Synthesis of polymers from organic solvent liquefied biomass: A review, *Renewable & Sustainable Energy Reviews* 15(7) (2011) 3454-3463.
- [19] C. Aouf, S. Benyahya, A. Esnouf, S. Caillol, B. Boutevin, H. Fulcrand, Tara tannins as phenolic precursors of thermosetting epoxy resins, *European Polymer Journal* 55 (2014) 186-198.
- [20] C. Aouf, C. Le Guerneve, S. Caillol, H. Fulcrand, Study of the O-glycidylation of natural phenolic compounds. The relationship between the phenolic structure and the reaction mechanism, *Tetrahedron* 69(4) (2013) 1345-1353.

Chapter 4

High performance cyanate esters from biomass pyrolysis oil

4.1. Introduction

Cyanate esters are a class of thermoset polymeric materials which have contributed to deliver high performance structures and products. With unique properties such as high glass transition temperature and modulus, radar transparency, low dielectric constant and moisture absorption, high adhesion to metals and resistance to ionizing radiation, cyanate esters are suitable materials for a wide range of applications including aerospace and microwave-transparent composites, electronic substrates, adhesives, coatings, radomes and photonics.[1-5] Figure 4.1 displays synthesis of bisphenol-A based cyanate ester monomer and its crosslinking. Cyanate ester monomers are crosslinked at elevated temperatures to yield crosslinked networks. Crosslinking agents are not required unlike conventional thermosets such as epoxides and polyurethanes since bifunctional and multi-functional cyanate esters can self-crosslink. Nonetheless, they can be co-crosslinked with epoxides,[6-8] benzoxazines,[9-12] and bismaleimides;[13, 14] thereby, expanding the opportunities of having versatility in the network structures and properties. As far as the performance is concerned, polycyanated materials have surpassed many thermosetting polymers and thus, have intrigued polymer chemists to continue developing cyanate ester-based materials.[15] Several high performance materials have been commercialized belonging to cyanate

ester chemistry, and have been used in specialty applications as outlined in Table 4.1.[2] However, they are derived from petroleum sources.

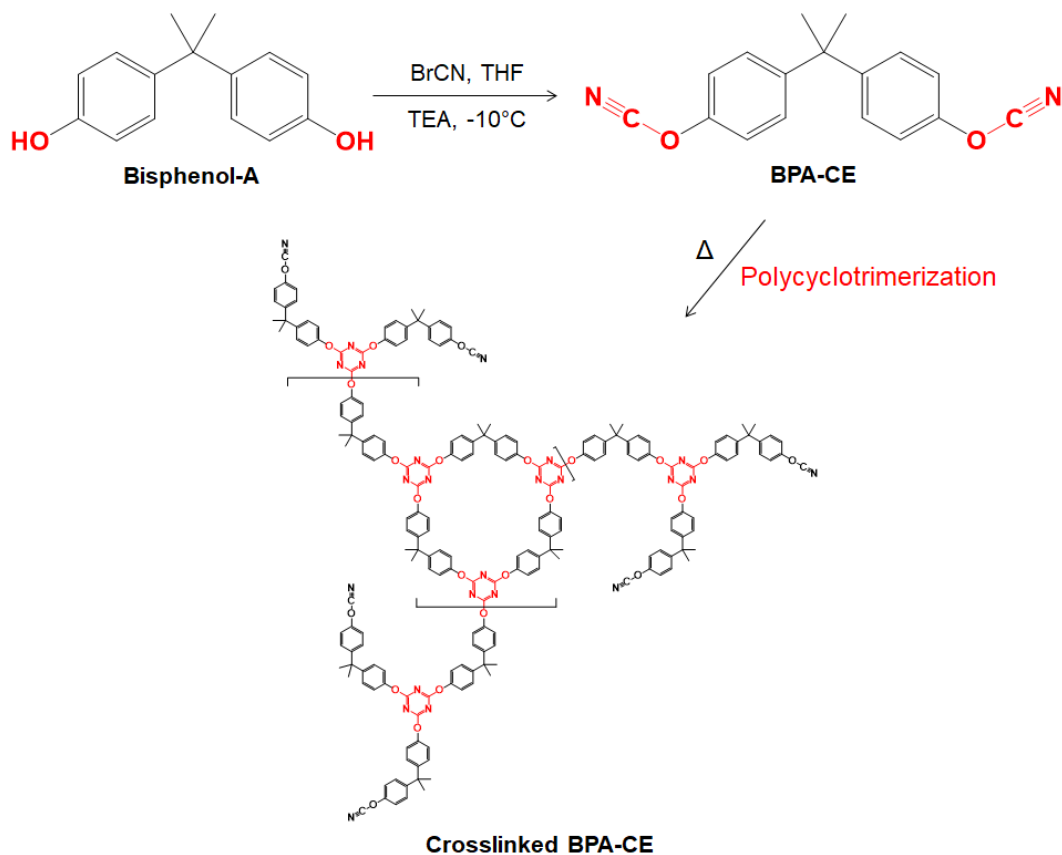
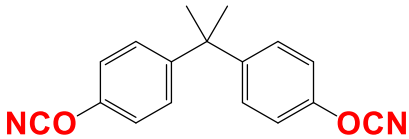
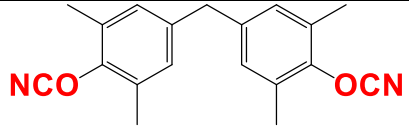
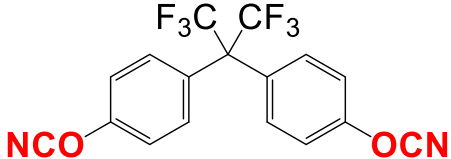
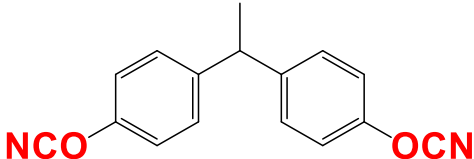
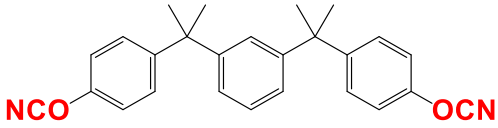
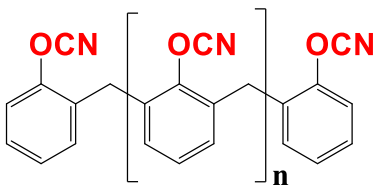
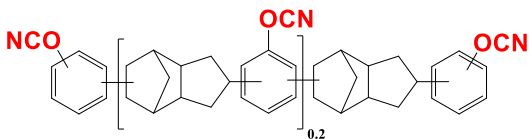


Figure 4.1: Synthesis of bisphenol-A based cyanate ester (BPA-CE) and its crosslinked network

Phenol and its derivatives, especially bisphenol-A and its further modifications, have been important precursors of cyanate ester resins.[2] Petroleum has been the boon for decades but its limited availability and impacts on the climate change have sought attention for considering alternate resources. Further, bisphenol-A is identified as a chemical compound with human hazard concerns.[16] Based on the previous mentioned factors, there is a substantial need for replacing bisphenol-A with less toxic and sustainable alternatives. Plant biomass serves as a resource that is both sustainable and less toxic as compared to the petroleum, but it puts forward challenges for

successful modifications. Recent developments in the bio-based monomers, polymers and thermoset networks have been documented,[17-19] but there have been limited studies in the field of cyanate esters. Previous researchers have developed cyanate esters from chemicals obtainable from renewable resources, including resveratrol,[20] eugenol,[21] carvacrol,[22] lignin-derived 4-n-propylguaiacol,[23] vanillin-based bisphenols,[24] creosol,[25] and trans-anethol.[26, 27] All of these cyanate esters possess bi- or trifunctionality, however, they are derived from compounds obtained from biomass resources. Often, it is difficult and economically cumbersome to selectively obtain specific compounds from biomass, that often has a complex assembly of natural macromolecules. Thermochemical processes have proved to be efficient in decomposing biomass to simpler organic compounds,[28] for example fast pyrolysis, a thermochemical process, which decomposes biomass to char, gases and condensable vapors. Condensation of vapors yields to a high amount of liquid mixture of hundreds of organic compounds – often called as bio-oil.[29-31] In the present study, the organic phase of bio-oil has been utilized as raw material of monomer synthesis. The organic phase of bio-oil is rich in phenolic compounds due to decomposition of lignin which is a natural, phenolic macromolecule.[32] Hence, a benefit of pyrolysis is that many biomass species containing lignin can be practically used for obtaining phenolic compounds. In our previous studies, bio-oil has been used for the synthesis of phenol-formaldehyde and epoxy polymers.[33-35] In this study, we focus on chemical transformation of the mixture of substituted phenols to a mixture of cyanate ester monomers. Further, since most compounds in the bio-oil are mono-phenolic, it is necessary to introduce bi- or multi-functionality similar to that explained in other bio-based cyanate ester research studies.[21-27, 36]

Table 4.1: Cyanate esters: Commercial products and properties [2]

Structure of cyanate ester (monomer)	Trade name/ Supplier	Melting Point (°C)	T _g (°C)	H ₂ O Absorption (%)	Dk (1 MHz)
	AroCy B/ Ciba-Geigy BT-2000/ Mitsubishi GC Lonsa	79	289	2.5	2.91
	AroCy M/ Ciba-Geigy	106	252	1.4	2.75
	AroCy F/ Ciba-Geigy	87	270	1.8	2.66
	AroCy L/ Ciba-Geigy	29	258	2.4	2.98
	XU-366/ Ciba-Geigy RTX-366	68	192	0.7	2.64
	Primaset PT/ Lonsa REX- 371/ Ciba-Geigy	Resinous	>350	3.8	3.08
	XU 71787.02L/ Dow Chemical	Resinous	244	1.4	2.80

An approach to synthesize organic biphenol from the bio-oil has also been emphasized in the current work. Depending on the phenolic compounds participating in the reaction, many isomeric biphenolic structures can be obtained, and hence a mixture of biphenolic monomers can be used as precursor for further cyanate ester synthesis. The effects of catalysts and reaction conditions on the structure of bisphenols obtained from creosol, have been studied earlier.[36] Our work demonstrates the replacement of bisphenol-A based cyanate ester by novel, bio-oil-based cyanated monomers as a promising pathway to increase sustainability while maintaining high performance and minimum process complexity. In addition, a detailed characterization of bio-oil and resulting cyanate esters is outlined as well.

4.2. Experimental Section

4.2.1. Materials

Bisphenol-A, chromium(III)acetyl acetonate, chloroform-d 99.8+ atom% D with 0.03 v/v% TMS, cyanogen bromide, dichloromethane, ethyl ether stabilized with BHT, hydrochloric acid 36.5 – 38.0 %, N-hydroxy-5-norbornene-2,3-dicarboximide (NHND), sodium sulfate anhydrous, tetrahydrofuran, toluene, triethylamine 99%, 1,3,5-trioxane 98% were ordered from VWR International, USA. 2-Chloro-4,4,5,5-tetramethyl-1,3,2-dioxaphospholane (TMDP) was purchased from Sigma Aldrich, USA. The organic phase of bio-oil was obtained from pine wood as per the procedure explained in the methods.

4.2.2. Methods

4.2.2.1. Fast pyrolysis of pine

An intermediate-scale auger-fed pyrolysis reactor was used to produce bio-oil from a clean pine wood feedstock (milled to a particle size of less than 4 mm) with a feed rate of 7.3 kg/hr and reaction temperature of 500 °C. The system was purged with N₂ at a flow rate of 50 L/min.

A detailed instrument description was reported previously.[37] The resulting biomass pyrolysis vapors were condensed to yield liquid bio-oil which was further separated into two phases – organic phase (ORG-bio-oil) and aqueous phase (AQ-bio-oil). The yield of bio-oil and biochar were measured gravimetrically, and the yield of non-condensable gases was calculated by difference. ORG-bio-oil was characterized by gas chromatography-mass spectrometry (GC-MS), ³¹P-nuclear magnetic resonance (³¹P-NMR), and Fourier transform infrared (FTIR) spectroscopy, and the density, acid value, water content and pH of bio-oils were measured. The bio-oil samples were stored in the freezer at -10 °C and ORG-bio-oil was used for monomer synthesis.

4.2.2.2. Characterization of ORG-bio-oil

GC-MS was used to measure the chemical composition of the produced ORG-bio-oil. The ORG-bio-oil was dissolved in 99.9 % pure MeOH (1 mL bio-oil in 9 mL MeOH), filtered with a PTFE syringe filter (0.20 µm), and a 1 µL aliquot was injected into the GC-MS system (Clarus 680 gas chromatograph and Clarus SQ 8C mass spectrometer, PerkinElmer, USA). The injection was performed at a split ratio of 80:1 and an injector temperature of 270 °C. An Elite 1701 MS capillary column (60 m x 0.25 mm ID by 0.25 µm film thickness) with a carrier gas (ultrahigh-purity helium, 99.9999%) flow rate of 1 cm³/min and pressure of 17.3 psi were used. The GC furnace was initially held at 50 °C for 4 min, then was ramped from to 280 °C at 5 °C/min, and held at 280 °C for 5

min. The MS was held at 270 °C with an ionization energy of 70 eV. Chromatogram peaks were extracted using TubroMass GC-MS software and peaks were identified with the National Institute of Standards and Technology (NIST) library.

The water content of the ORG-bio-oil was measured by Karl-Fisher titration (Metrohm 787 KF Titrino) following the American Society for Testing and Materials protocol (ASTM D4377-00).[38] The pH of ORG-bio-oil was measured using a pH meter after stirring 1 mL of ORG-bio-oil into 50 mL of DI water. The total acid number (TAN) was measured by dissolving 0.5 g of ORG-bio-oil in 25 mL of 1:1 isopropyl alcohol:water then titrating with 0.1 N KOH to a pH of 11 in accordance with ASTM D664.[39] The density of the ORG-bio-oil was determined using a 2 mL glass pycnometer according to ASTM D1475-13.[40] Analyses were performed in duplicate. For ³¹P-NMR spectroscopy, bio-oil samples were phosphorylated as per the procedure mentioned in the literature.[41] NHND and chromium(III)acetyl acetonate (20 mg each) were dissolved in the mixture of 3 mL pyridine and 2 mL deuterated chloroform to prepare the stock solution. 550 µL of stock solution was added to around 20 mg of bio-oil sample and stirred well. TMDP (150 µL) was then added to the mixture and stirred well to make the solution homogeneous. The prepared solution was then transferred to the NMR spectroscopy tube and the spectrum was acquired with a Bruker Avance II 250 MHz spectrometer using inverse gated decoupling pulse sequence, 90-degree pulse angle, 25 s pulse delay and 128 scans. The hydroxyl content of the samples was calculated by integrating relevant peaks compared to the internal standard NHND.

4.2.2.3. FTIR Spectroscopy

Fourier transform infrared analysis was performed on bio-oil samples and synthesized products using Thermo Scientific Nicolet 6700 FT-IR spectrophotometer equipped with attenuated total

reflection (ATR) accessory and OMNIC 7.3 software. IR spectra were collected in the wavenumber range 400 cm^{-1} to 4000 cm^{-1} at a resolution of 4 cm^{-1} and 64 scans.

4.2.2.4. Synthesis of ORG-biphenol

Using GC-MS analysis, it was observed that several monophenolic compounds were present in ORG-bio-oil. ORG-bio-oil was dissolved in toluene and washed with water. Toluene and water phases were allowed to separate in a separating funnel overnight. Toluene phase was heated at $80\text{ }^{\circ}\text{C}$ under vacuum using rotary evaporation to remove toluene, and the resultant, concentrated ORG-bio-oil was treated with 1,3,5-trioxane in acidic conditions to produce biphenolic compounds as per an adapted procedure.[22] Concentrated ORG-bio-oil and 1,3,5-trioxane (0.3 equiv/OH) were dispersed in water. Concentrated HCl was added to the dispersion in the amount adjusting the normality of reaction mixture at 2.5 N. The reaction mixture was heated at $80\text{ }^{\circ}\text{C}$ under stirring for six hours. After cooling down, the reaction mixture was added to dichloromethane and washed with water. The organic phase of the extraction was separated, and dichloromethane was distilled off with rotary evaporation under reduced pressure and at room temperature.

4.2.2.5. Synthesis of cyanate esters

Phenolic monomers: ORG-bio-oil, ORG-biphenol and bisphenol-A were cyanated as per the cyanation procedure[20, 22] to yield various cyanate ester resins. Phenolic monomer was dissolved in tetrahydrofuran in a jacketed, glass reactor equipped with mechanical stirrer. The reactor temperature was maintained at $-10\text{ }^{\circ}\text{C}$ with continuously flowing water/methanol:60/40 mixture through the jacket. After the reaction mixture achieved $-10\text{ }^{\circ}\text{C}$, cyanogen bromide (1.2 equiv/OH) was added. The mixture was stirred for five minutes and then dropwise addition of triethylamine

was initiated with the help of dropping funnel. Addition of triethylamine was continued for 30 minutes at -10 °C. After the addition was finished, the cooling was stopped, and the reaction mixture was stirred for 1 hour at room temperature. Tetrahydrofuran was distilled off with rotary evaporation. Diethyl ether and water were added to the remaining mixture, the solution was mixed well, and allowed to separate in separating funnel overnight. The diethyl ether fraction was dried over anhydrous sodium sulfate, filtered and then diethyl ether was removed by rotary evaporation under reduced pressure at room temperature. The cyanate esters from respective monomers were named as ORG-bio-oil-cyanate ester (ORG-bio-oil-CE), ORG-biphenol-cyanate ester (ORG-biphenol-CE) and bisphenol-A-cyanate ester (BPA-CE).

A schematic is represented in Figure 4.2 entailing the synthesis of ORG-biphenol and the cyanate esters from ORG-bio-oil and ORG-biphenol. ORG-biphenol represents two isomeric categories of compounds differentiated by the position of methylene bridge. This difference is possible due to the reaction mechanism driven by the influence of o,p-directing effects of OH and OCH₃ groups on the benzene rings.

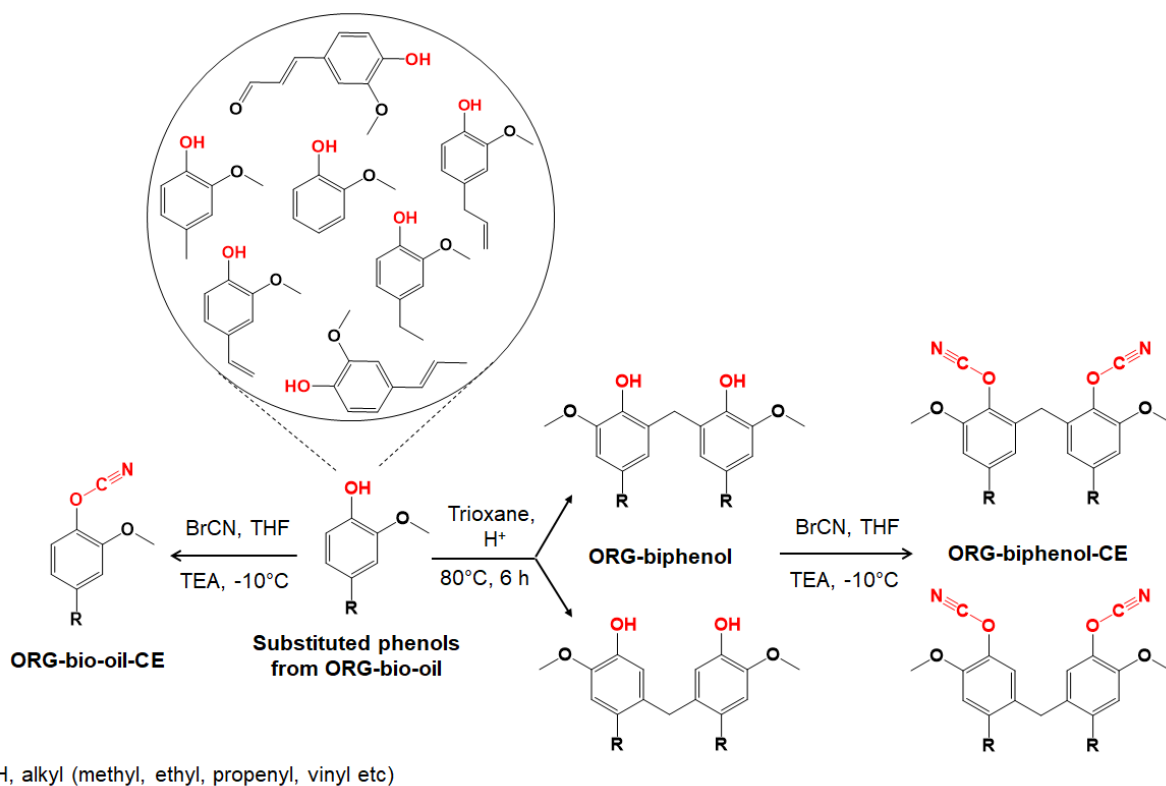


Figure 4.2: Synthesis of ORG-biphenol, ORG-bio-oil-CE and ORG-biphenol-CE

A catalyzed synthesis of similar compounds and their respective cyanate esters was discussed in the literature.[25, 36] Another important aspect for consideration in this study is the cyanate monomer functionality. ORG-bio-oil-CE is predominantly monocyanated mixture because it is derived directly from bio-oil that contains monophenolic compounds; whereas ORG-biphenol-CE provides bifunctionality similar to the conventional bisphenol-A-cyanate ester depicted in Figure 4.1. A continuous triazine network is possible if the cyanate esters bear bi- or multi-functionality; and hence, a similar crosslinked network is expected from ORG-biphenol-CE, with some differences arising from the pendant groups of aromatic rings. ORG-bio-oil-CE, on the other hand, might limit the crosslinking reactions due to monofunctionality.

4.2.2.6. Crosslinking of cyanate esters

BPA-CE and ORG-bio-oil-CE were blended in different proportions – 75:25, 50:50 and 25:75 (by wt%). All the cyanate esters (ORG-bio-oil-CE, ORG-biphenol-CE, BPA-CE and the blends) were heated at 150 °C for 3 hours followed by 200 °C for 3 hours under vacuum. The samples were further postcured at 300 °C for 1 hour in conventional furnace.

4.2.2.7. Dynamic mechanical analysis

Thermo-mechanical evaluation of polycyanate esters was performed using TA Instruments dynamic mechanical analyzer RSAIII. An oscillatory stress was applied at 1 Hz frequency on the horizontal specimen using three-point bending geometry to yield constant 0.1 % strain. The temperature was increased from at 5 °C/min during the test. The viscoelastic behavior was observed, especially during the glass transition.

4.2.2.8. Morphology

Crosslinked cyanate ester samples were immersed in liquid nitrogen and fractured. The samples were then sputter coated with gold plasma and the fractured surfaces were observed under scanning electron microscope.

4.2.3. Results and Discussion

4.2.3.1. Characterization of ORG-bio-oil, ORG-biphenol and the cyanate esters

The pyrolysis product yields and the properties of ORG-bio-oil are listed in Table 4.2. ORG-bio-oil was found to be acidic in nature due to its low pH and it had low water content.

Table 4.2: Properties of ORG-bio-oil

Fast Pyrolysis of Pine	
Bio-oil yield (%)	53.7 ± 0.0
Bio-char yield (%)	30.4 ± 0.0
Non-condensable gas yield (%)	15.9 ± 0.0
ORG-bio-oil	
Water content (%)	11.5 ± 0.5
Total acid number (mg KOH/g bio-oil)	100.6 ± 0.0
Density (g/mL)	1.15 ± 0.00
pH	3.0 ± 0.2

GC-MS analysis of ORG-bio-oil (Figure 4.3) revealed major peaks corresponding to substituted phenolic compounds. The presence of phenolic compounds is likely due to decomposition of lignin during pyrolysis, which is a polyphenolic macromolecule found in woody biomass.[42, 43]

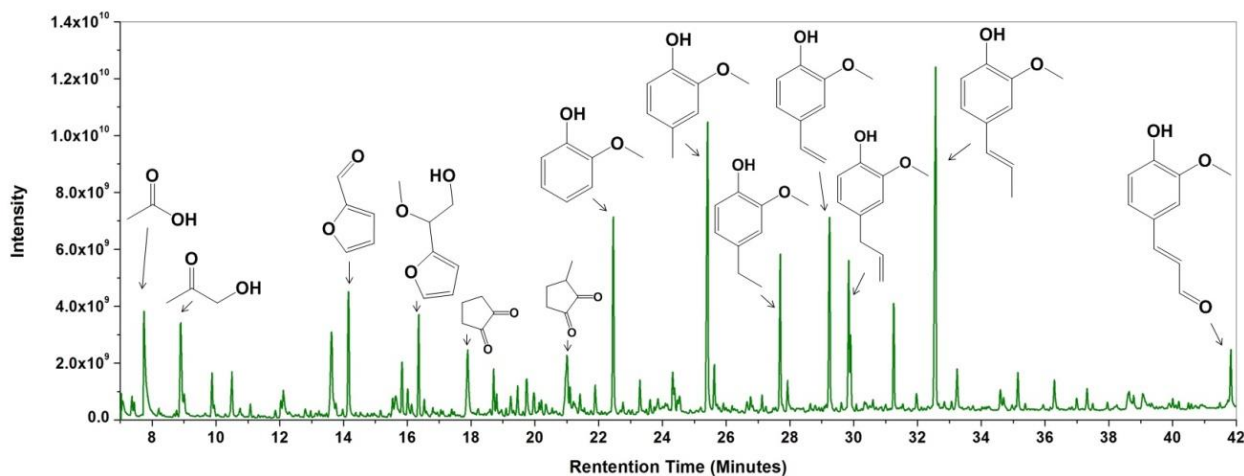


Figure 4.3: GC-MS analysis of ORG-bio-oil

^{31}P -NMR spectroscopy (Table 4.3) yielded quantitative information regarding the hydroxyl number, which was in agreement with GC-MS results. The amount of phenolic OH was observed to be the maximum among all kinds of OH groups. ORG-biphenol displayed greater content of phenolic OH, reduced quantity of acidic OH and an absence of aliphatic OH as compared to ORG-bio-oil. In Figure 4.4-(c), the FTIR spectra show that ORG-biphenol displayed a reduction in the peak at $3400 - 3300 \text{ cm}^{-1}$ corresponding to O-H stretch compared to ORG-bio-oil (Figure 4.4-(a)). This agrees with the total hydroxyl number obtained from ^{31}P -NMR spectroscopy indicated in Table 4.3. A slight increase in the intensity of peaks at 2928 cm^{-1} and 2855 cm^{-1} relating to sp^3 C-H stretch is probably due to a methylene (CH_2) bridge connecting two phenolic moieties in the biphenolic compounds in ORG-biphenol. Figure 4.4-(b) displays successful formation of cyanate ester monomers from ORG-bio-oil as evident by the appearance of peaks at 2256 cm^{-1} and 2201 cm^{-1} responsible for $\text{C}\equiv\text{N}$ stretch of cyanate ester groups. Another parallel observation of the reduced intensity of the O-H stretch peak in the range $3400 - 3300 \text{ cm}^{-1}$ indicated the consumption of hydroxyl groups. Similar changes were observed in case of ORG-biphenol-CE (appearance of $\text{C}\equiv\text{N}$ stretch at 2260 cm^{-1} and 2199 cm^{-1} in Figure 4.4-(d), and reduction in O-H stretch in the range $3400 - 3300 \text{ cm}^{-1}$) and BPA-CE (appearance of $\text{C}\equiv\text{N}$ stretch at 2276 cm^{-1} and 2242 cm^{-1} in Figure 4.4-(f), and reduction in O-H stretch in the range $3400 - 3300 \text{ cm}^{-1}$).

Table 4.3: ³¹P-NMR spectroscopy of ORG-bio-oil and ORG-biphenol

OH Type		Range (ppm)	ORG-bio-oil	ORG-biphenol		
Aliphatic OH		150 – 145.5	1.57	0		
Phenolic OH	C-5 substituted condensed phenolic OH	β-5	144.7 – 142.8	0.07	2.89 (54%) 2.35 (89%)	
		4-O-5	142.8 – 141.7	0.10		0.23
		5-5	141.7 – 140.2	0.28		0.24
	Guaiacyl phenolic OH	140.2 – 139.0	1.45	0.27		
	Catechol type OH	139.0 – 138.2	0.60	1.27		
	p-hydroxyphenyl OH	138.2 – 137.3	0.39	0.30		
Acidic OH		136.6 – 133.6	0.84	0.29		
TOTAL			5.30	2.64		

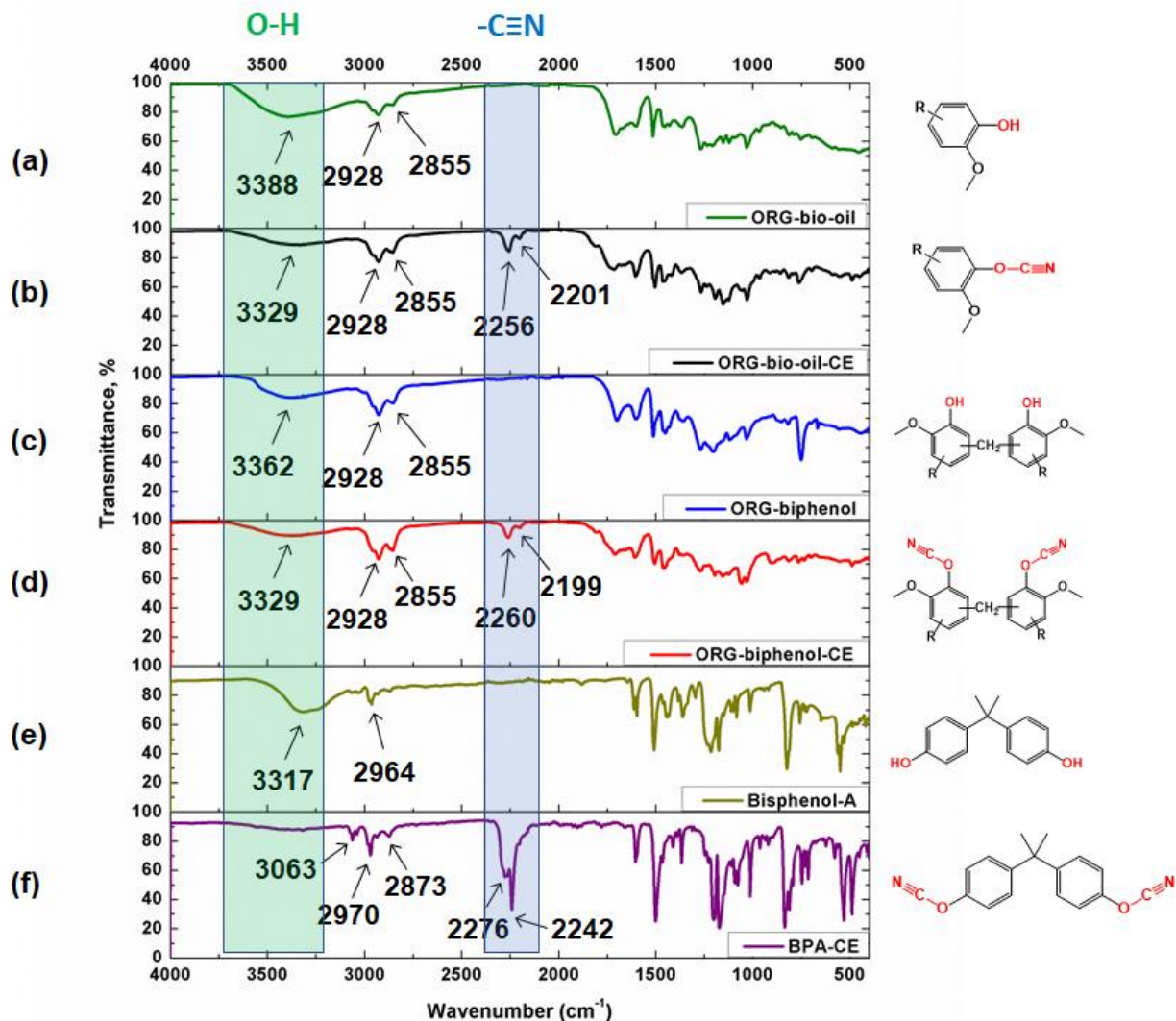


Figure 4.4: FTIR spectra of (a) ORG-bio-oil, (b) ORG-bio-oil-CE, (c) ORG-biphenol, (d) ORG-biphenol-CE, (e) bisphenol-A and (f) BPA-CE

4.2.3.2. Thermo-mechanical performance of cyanate esters

Dynamic mechanical analysis of ORG-bio-oil-CE and ORG-biphenol-CE yielded good thermo-mechanical properties in comparison with BPA-CE, yet considerable viscoelastic differences. In Figure 4.5-(a), crosslinked BPA-CE was observed to have a high storage modulus at room

temperature, with a value of 3 GPa. The BPA-CE sample showed an onset of glass transition at 190 °C, and a sharp decrease in storage modulus after 200 °C; whereas the peak in $\tan\delta$ was observed at 220 °C in Figure 4.5-(b).

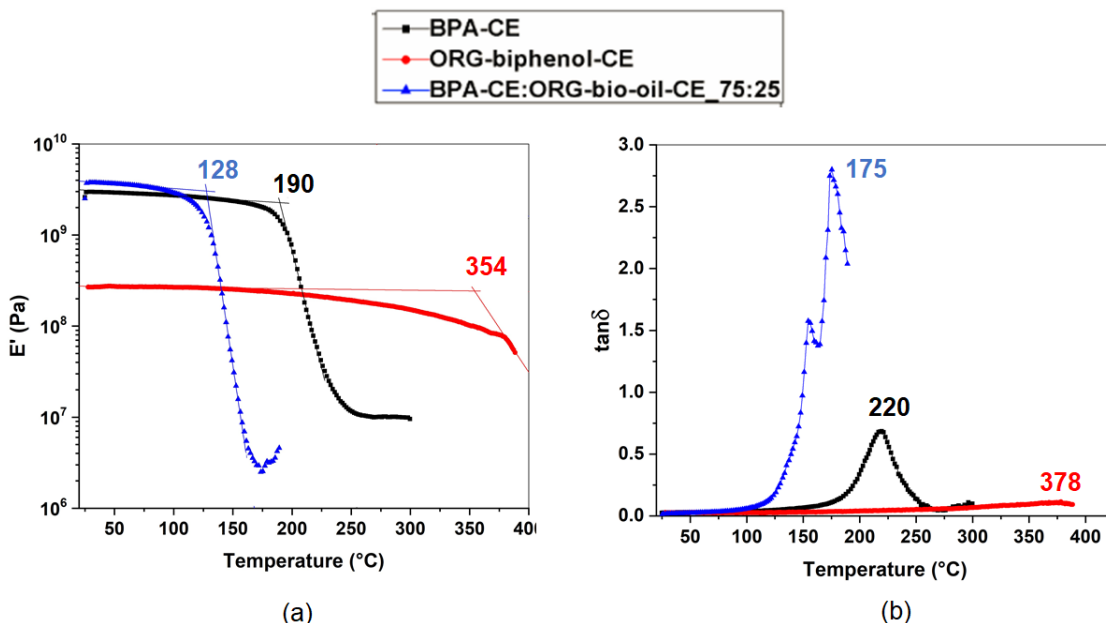


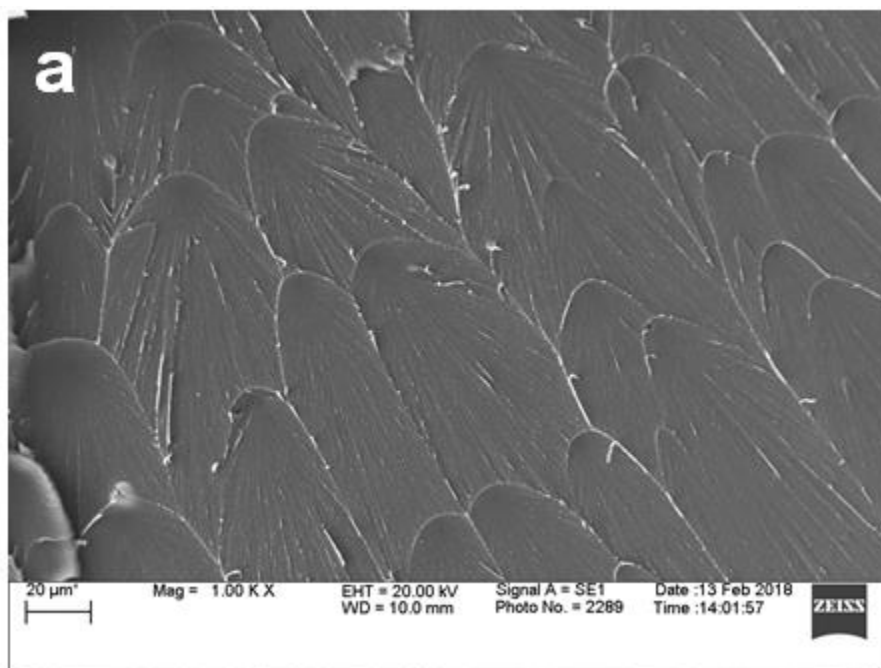
Figure 4.5: Thermo-mechanical properties of cyanate esters: (a) storage modulus, (b) $\tan\delta$

The crosslinked blend of BPA-CE:ORG-bio-oil-CE (75:25) displayed similar behavior, with an onset glass transition temperature at 128 °C, and the peak in $\tan\delta$ at 175 °C. Other blends of BPA-CE and ORG-bio-oil-CE (50:50 and 25:75) were too brittle to be analyzed with dynamic mechanical analysis and did not withstand the applied cyclic stress. A higher amount of ORG-bio-oil-CE might have caused a remarkable reduction in crosslinking density due to the monofunctionality and hence, resulting in brittle samples. In the case of BPA-CE and the 75:25 blend, a small plateau of storage modulus was observed after the glass transition region. Crosslinked ORG-biphenol-CE was characterized by a lower storage modulus (around 0.3 GPa) at room temperature and a gradual decline in the storage modulus over a wide range of temperature.

An onset temperature was observed at 354 °C and maximum value of $\tan \delta$ was found to be at 378 °C. Crosslinked ORG-biphenol-CE can be considered a material with crosslinks formed by triazine rings due to cyanate bifunctionality. Moreover, ORG-biphenol possessed substituent group on the aromatic rings due to presence of substituted phenols in ORG-bio-oil. The substituted groups could restrict the molecular mobility of the network, resulting in superior glass transition temperature as compared to BPA-CE which lacks phenolic ring substituents. A combination of triazine network and randomly crosslinked components is expected to occur in case of crosslinked ORG-biphenol-CE which might facilitate thermal transitions over a very broad range, and hence, the resulting behavior of the storage modulus observed in Figure 4.5-(a). A broad $\tan \delta$ peak is observed in the case of the crosslinked ORG-biphenol-CE sample (Figure 4.5-(b)), which supports this argument. It can be said that the glass transition temperature of crosslinked ORG-biphenol-CE lies in the range of 350 – 380 °C. In case of BPA-CE:ORG-bio-oil-CE_{75:25} sample, ORG-bio-oil-CE reduced the crosslinking density due to monofunctionality of ORG-bio-oil-CE and hence reduced the glass transition temperature range for the blend. Mono-cyanated esters limit the polymerization, thereby, producing materials with poor crosslinking. ORG-bio-oil also contains aliphatic hydroxyl compounds which, on cyanation, yield aliphatic cyanate esters. Aliphatic cyanate esters rearrange to aliphatic isocyanates that can react with water or moisture to produce carbamate derivatives. These products hinder crosslinking at elevated temperatures. A similar phenomenon of a reduction in glass transition temperature by monofunctional cyanate esters has been previously studied by other researchers.[44] Moreover, a probable heterogeneity leading to a phase separation between two different cyanate esters in the BPA-CE:ORG-bio-oil-CE_{75:25} sample led to two maxima in $\tan \delta$ curve (Figure 4.5-(b)).

4.2.3.3. Morphology of crosslinked cyanate esters

In Figure 4.6, a typical brittle fracture was observed in case of crosslinked BPA-CE. Curved fracture lines indicate the way material was fractured in cryogenic conditions. On the other hand, crosslinked ORG-bio-oil-CE displayed a remarkably smooth surface as compared to crosslinked BPA-CE. Non-cyanate crosslinks are not expected to impart strength to the material and thus, yielded a relatively softer material. ORG-biphenol-CE displayed a higher degree of randomness while undergoing fracture, indicating that cyanate crosslinks imparted brittleness and non-cyanate crosslinks provided smoothness, thereby creating a mixed system.



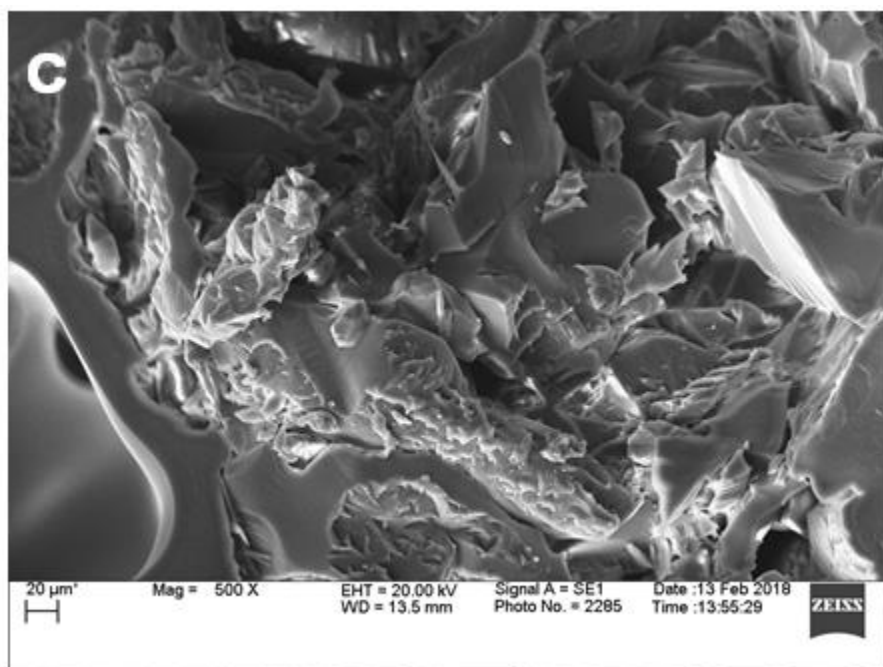
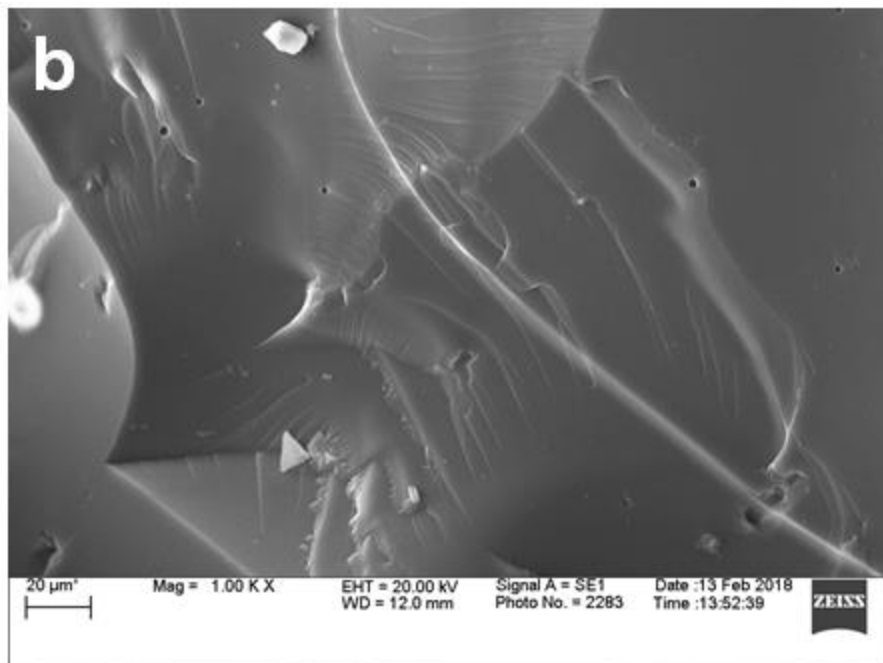


Figure 4.6: SEM photographs of fractured surface of crosslinked materials: (a) BPA-CE, (b) ORG-bio-oil-CE and (c) ORG-biphenol-CE

4.3. Conclusions

Lignocellulosic biomass, such as, wood can be utilized as feedstock for chemicals using fast pyrolysis. The organic phase of bio-oil contains a mixture of substituted phenolic compounds along with other organics as the decomposition products of fast pyrolysis process. Bio-oil derived phenolic hydroxyl compounds offer an opportunity for cyanation which leads to the synthesis of bio-oil based cyanate ester monomers. Nonetheless, ORG-bio-oil contains mono-phenolic compounds which produce mono-cyanated esters on direct cyanation. Monofunctional cyanate esters yield materials with less glass transition temperature. ORG-bio-oil can be successfully used to synthesize ORG-biphenol which resembles the structure of bisphenol-A, a traditional petrochemical based monomer for cyanate ester synthesis. ORG-biphenol has higher phenolic OH content as well as an absence of aliphatic hydroxyl compounds as compared to ORG-bio-oil. FTIR spectroscopy confirms the synthesis of cyanate ester resins. Crosslinked cyanate ester from ORG-biphenol yielded higher glass transition temperature than crosslinked cyanate esters derived from bisphenol-A. The morphology of crosslinked ORG-biphenol-CE was found to have greater heterogeneity than crosslinked BPA-CE. The present study was successful in preparing sustainable cyanate esters from bio-oil (ORG-bio-oil-CE and ORG-biphenol-CE), and 25 wt% of replacement of BPA-CE was possible by direct cyanation of ORG-bio-oil.

References

- [1] M.R. Kessler, Cyanate Ester Resins, in: L. Nicolais, A. Borzacchiello (Eds.) Wiley Encyclopedia of Composites, John Wiley & Sons, Inc., 2012, pp. 658-672.
- [2] C.P.R. Nair, D. Mathew, K.N. Ninan, Cyanate ester resins, recent developments, *New Polymerization Techniques and Synthetic Methodologies* 155 (2001) 1-99.
- [3] T. Fang, D.A. Shimp, Polycyanate esters - Science and applications, *Progress in Polymer Science* 20(1) (1995) 61-118.
- [4] G. Wang, G. Fu, T.L. Gao, H. Kuang, R.G. Wang, F. Yang, W.C. Jiao, L.F. Hao, W.B. Liu, Preparation and characterization of novel film adhesives based on cyanate ester resin for bonding advanced radome, *International Journal of Adhesion and Adhesives* 68 (2016) 80-86.
- [5] A. Inamdar, J. Cherukattu, A. Anand, B. Kandasubramanian, Thermoplastic-Toughened High-Temperature Cyanate Esters and Their Application in Advanced Composites, *Industrial & Engineering Chemistry Research* 57(13) (2018) 4479-4504.
- [6] A. Toldy, A. Szlancsik, B. Szolnoki, Reactive flame retardancy of cyanate ester/epoxy resin blends and their carbon fibre reinforced composites, *Polymer Degradation and Stability* 128 (2016) 29-38.
- [7] G.Z. Zhan, L. Zhao, S. Hu, W.J. Gan, Y.F. Yu, X.L. Tang, A novel biobased resin-epoxidized soybean oil modified cyanate ester, *Polymer Engineering and Science* 48(7) (2008) 1322-1328.

- [8] Y.X. Lei, M.Z. Xu, M.L. Jiang, Y.M. Huang, X.B. Liu, Curing behaviors of cyanate ester/epoxy copolymers and their dielectric properties, *High Performance Polymers* 29(10) (2017) 1175-1184.
- [9] A. Zegaoui, A.R. Wang, A.Q. Dayo, B. Tian, W.B. Liu, J. Wang, Y.G. Liu, Effects of gamma irradiation on the mechanical and thermal properties of cyanate ester/benzoxazine resin, *Radiation Physics and Chemistry* 141 (2017) 110-117.
- [10] K.S.S. Kumar, C.P.R. Nair, K.N. Ninan, Investigations on the cure chemistry and polymer properties of benzoxazine-cyanate ester blends, *European Polymer Journal* 45(2) (2009) 494-502.
- [11] Y.Q. Wang, G.L. Wu, K.C. Kou, C. Pan, A.L. Feng, Mechanical, thermal conductive and dielectrical properties of organic montmorillonite reinforced benzoxazine/cyanate ester copolymer for electronic packaging, *Journal of Materials Science-Materials in Electronics* 27(8) (2016) 8279-8287.
- [12] S. Ohashi, J. Kilbane, T. Heyl, H. Ishida, Synthesis and Characterization of Cyanate Ester Functional Benzoxazine and Its Polymer, *Macromolecules* 48(23) (2015) 8412-8417.
- [13] L. Wan, X. Zhang, G.L. Wu, A.L. Feng, Thermal conductivity and dielectric properties of bismaleimide/cyanate ester copolymer, *High Voltage* 2(3) (2017) 167-171.
- [14] I. Hamerton, High-performance thermoset-thermoset polymer blends: A review of the chemistry of cyanate ester-bismaleimide blends, *High Performance Polymers* 8(1) (1996) 83-95.
- [15] R.J. Iredale, C. Ward, I. Hamerton, Modern advances in bismaleimide resin technology: A 21st century perspective on the chemistry of addition polyimides, *Progress in Polymer Science* 69 (2017) 1-21.
- [16] F.F. Ng, G. Couture, C. Philippe, B. Boutevin, S. Caillol, Bio-Based Aromatic Epoxy Monomers for Thermoset Materials, *Molecules* 22(1) (2017) 48.

- [17] A. Llevot, E. Grau, S. Carlotti, S. Grelier, H. Cramail, From Lignin-derived Aromatic Compounds to Novel Biobased Polymers, *Macromolecular Rapid Communications* 37(1) (2016) 9-28.
- [18] J.M. Raquez, M. Deleglise, M.F. Lacrampe, P. Krawczak, Thermosetting (bio)materials derived from renewable resources: A critical review, *Progress in Polymer Science* 35(4) (2010) 487-509.
- [19] Y. Jiang, D.C. Ding, S. Zhao, H.Y. Zhu, H.I. Kenttamaa, M.M. Abu-Omar, Renewable thermoset polymers based on lignin and carbohydrate derived monomers, *Green Chemistry* 20(5) (2018) 1131-1138.
- [20] L.R. Cambrea, M.C. Davis, M.D. Garrison, T.J. Groshens, R.E. Lyon, N. Safronava, Processable Cyanate Ester Resin from Cis Resveratrol, *Journal of Polymer Science Part a-Polymer Chemistry* 55(6) (2017) 971-980.
- [21] B.G. Harvey, A.J. Guenther, G.R. Yandek, L.R. Cambrea, H.A. Meylemans, L.C. Baldwin, J.T. Reams, Synthesis and characterization of a renewable cyanate ester/polycarbonate network derived from eugenol, *Polymer* 55(20) (2014) 5073-5079.
- [22] B.G. Harvey, A.J. Guenther, T.A. Koontz, P.J. Storch, J.T. Reams, T.J. Groshens, Sustainable hydrophobic thermosetting resins and polycarbonates from turpentine, *Green Chemistry* 18(8) (2016) 2416-2423.
- [23] S.F. Koelewijn, S. Van den Bosch, T. Renders, W. Schutyser, B. Lagrain, M. Smet, J. Thomas, W. Dehaen, P. Van Puyvelde, H. Witters, B.F. Sels, Sustainable bisphenols from renewable softwood lignin feedstock for polycarbonates and cyanate ester resins, *Green Chemistry* 19(11) (2017) 2561-2570.

- [24] B.G. Harvey, A.J. Guenther, H.A. Meylemans, S.R.L. Haines, K.R. Lamison, T.J. Groshens, L.R. Cambrea, M.C. Davis, W.W. Lai, Renewable thermosetting resins and thermoplastics from vanillin, *Green Chemistry* 17(2) (2015) 1249-1258.
- [25] H.A. Meylemans, B.G. Harvey, J.T. Reams, A.J. Guenther, L.R. Cambrea, T.J. Groshens, L.C. Baldwin, M.D. Garrison, J.M. Mabry, Synthesis, Characterization, and Cure Chemistry of Renewable Bis(cyanate) Esters Derived from 2-Methoxy-4-Methylphenol, *Biomacromolecules* 14(3) (2013) 771-780.
- [26] M.C. Davis, A.J. Guenther, C.M. Sahagun, K.R. Lamison, J.T. Reams, J.M. Mabry, Polycyanurate networks from dehydroanethole cyclotrimers: Synthesis and characterization, *Polymer* 54(26) (2013) 6902-6909.
- [27] M.C. Davis, A.J. Guenther, T.J. Groshens, J.T. Reams, J.M. Mabry, Polycyanurate networks from anethole dimers: Synthesis and characterization, *Journal of Polymer Science Part a-Polymer Chemistry* 50(19) (2012) 4127-4136.
- [28] B. Kamm, M. Gerhardt, S. Leiß, The Biorefinery Concept - Thermochemical Production of Building Blocks and Syngas, in: M. Crocker (Ed.), *Thermochemical Conversion of Biomass to Liquid Fuels and Chemicals*, Royal Society of Chemistry, Cambridge, UK, 2010, pp. 46-62.
- [29] A.V. Bridgwater, D. Meier, D. Radlein, An overview of fast pyrolysis of biomass, *Organic Geochemistry* 30(12) (1999) 1479-1493.
- [30] D. Mohan, C.U. Pittman, P.H. Steele, Pyrolysis of wood/biomass for bio-oil: A critical review, *Energy & Fuels* 20(3) (2006) 848-889.
- [31] A.V. Bridgwater, Review of fast pyrolysis of biomass and product upgrading, *Biomass & Bioenergy* 38 (2012) 68-94.

- [32] K. Jacobson, K.C. Maheria, A.K. Dalai, Bio-oil valorization: A review, *Renewable & Sustainable Energy Reviews* 23 (2013) 91-106.
- [33] M. Barde, S. Adhikari, B.K. Via, M.L. Auad, Synthesis and Characterization of Epoxy Resins from Fast Pyrolysis Bio-oil, *Green Materials* (2018) 1-9.
- [34] Y. Celikbag, S. Meadows, M. Barde, S. Adhikari, G. Buschle-Diller, M.L. Auad, B.K. Via, Synthesis and Characterization of Bio-oil-Based Self-Curing Epoxy Resin, *Industrial & Engineering Chemistry Research* 56(33) (2017) 9389-9400.
- [35] B. Sibaja, S. Adhikari, Y. Celikbag, B. Via, M.L. Auad, Fast pyrolysis bio-oil as precursor of thermosetting epoxy resins, *Polymer Engineering and Science* (2017) 1-12.
- [36] H.A. Meylemans, T.J. Groshens, B.G. Harvey, Synthesis of Renewable Bisphenols from Creosol, *Chemsuschem* 5(1) (2012) 206-210.
- [37] P. Kim, S. Weaver, K. Noh, N. Labbe, Characteristics of Bio-Oils Produced by an Intermediate Semipilot Scale Pyrolysis Auger Reactor Equipped with Multistage Condensers, *Energy & Fuels* 28(11) (2014) 6966-6973.
- [38] ASTM D4377-00, Standard Test Method for Water in Crude Oils by Potentiometric Karl Fischer Titration, ASTM International, West Conshohocken, PA, 2011.
- [39] ASTM D664-11a, Standard Test Method for Acid Number of Petroleum Products by Potentiometric Titration, ASTM International, West Conshohocken, PA, 2011.
- [40] ASTM D1475-13, Standard Test Method for Density of Liquid Coatings, Inks, and Related Products, ASTM International, West Conshohocken, PA, 2013.
- [41] H.X. Ben, A.J. Ragauskas, NMR Characterization of Pyrolysis Oils from Kraft Lignin, *Energy & Fuels* 25(5) (2011) 2322-2332.

- [42] K. Sipila, E. Kuoppala, L. Fagernas, A. Oasmaa, Characterization of biomass-based flash pyrolysis oils, *Biomass & Bioenergy* 14(2) (1998) 103-113.
- [43] P.K. Kanaujia, Y.K. Sharma, M.O. Garg, D. Tripathi, R. Singh, Review of analytical strategies in the production and upgrading of bio-oils derived from lignocellulosic biomass, *Journal of Analytical and Applied Pyrolysis* 105 (2014) 55-74.
- [44] K.I. Papathomas, D.W. Wang, Triazine networks modified with monofunctional reactive cyanate ester monomers, *Journal of Applied Polymer Science* 44(7) (1992) 1267-1274.

Chapter 5

Crosslinked acrylic polymers from aqueous phase of biomass pyrolysis oil and acrylated epoxidized soybean oil

5.1. Introduction

Plant biomass has been widely accepted as an alternate and renewable resource of chemicals and fuels. Depending on the species, plant biomass can be remarkably different in its components and is characterized by great complexity at the molecular level. Lignocellulosic biomass is one of the main plant biomass types and is comprised of lignin, cellulose and hemi-cellulose biopolymers bound together.[1] Breakdown of complex macromolecules in the biomass to smaller compounds has been a general approach to obtain chemicals. This can be achieved by employing various chemical, thermochemical and biochemical processes such as gasification, pyrolysis,[2, 3] liquefaction,[4, 5] torrefaction, and fermentation. Biomass can be subjected to fast pyrolysis process to efficiently produce high yields of liquid fraction often called biomass pyrolysis oil or bio-oil.[6] The fast pyrolysis process often yields bio-oil liquids into separated phases – a useful, organic-rich phase and an aqueous phase which is mostly regarded as a waste stream.[7] The aqueous phase of bio-oil can have water content as high as 80% and the remaining appearing as polar organic compounds which are degradation products of cellulose and hemi-cellulose.[8, 9] Since the aqueous phase generally has high water content, it renders useless to be used as conventional fuel. Upgrading aqueous phase to liquid fraction with higher heating value can be

technically as well as economically cumbersome. Several attempts have been documented about utilization of the aqueous phase of bio-oil for producing hydrogen by steam reforming [10-16] and supercritical water reforming.[17] Nevertheless, the bio-oil aqueous phase has not been successfully used for producing functional chemicals, monomers and polymers which are highly value-added applications. On the other hand, bio-oil organic phase has been extensively used for synthesis of monomers and polymers such as phenol-formaldehyde,[18, 19] epoxy,[20-22] polyurethane[23, 24] etc.

In the current study, we focus on utilization of waste aqueous bio-oil to develop acrylic polymers. Conventionally, most commonly used acrylic polymers are obtained from acrylate and/or methacrylate monomers such as methyl methacrylate, ethyl acrylate, n-butyl acrylate etc. Polyacrylates are used in many applications including coatings, adhesives, composites, super-absorbent materials etc. Typical acrylate and methacrylate monomers are alkyl esters of acrylic acid and methacrylic acid respectively, which are derived from petrochemicals. Acrylic monomers have been synthesized from a few biomass resources in the past, such as soybean oil,[25] vanillin,[26] lignin[27] etc. Acrylated epoxidized soybean oil (AESO) has been successfully used for copolymerization in several studies. The approach of this study is to exploit aliphatic hydroxyl compounds available in the aqueous bio-oil to produce methacrylate monomers and subsequent polymers. We have also employed acrylated epoxidized soybean oil in varying proportions to develop crosslinked polymers with improved thermo-mechanical properties.

5.2. Experimental sections

5.2.1. Materials

Acetone, acrylated epoxidized soybean oil, benzoyl peroxide 100%, chloroform, chromium(III)acetyl acetonate, deuterated chloroform, dichloromethane, N-hydroxy-5-norbornene-2,3-dicarboximide (NHND), methacryloyl chloride 97%, triethylamine 99% were ordered from VWR International, USA. 2-Chloro-4,4,5,5-tetramethyl-1,3,2-dioxaphospholane (TMDP) was purchased from Sigma Aldrich, USA. The aqueous phase of bio-oil was obtained from pine wood as per the procedure described in methods.

5.2.2. Methods

5.2.2.1. Fast pyrolysis of pine

Clean pine wood with particles less than 4 mm were fed into an auger-fed pyrolysis reactor at 7.3 kg/hr and with the reactor temperature raised to 500 °C and N₂ purge flow rate at 50 L/min. A detailed instrument description was reported previously.[28] Product vapors of pyrolyzed biomass were condensed to yield a liquid bio-oil which was further separated into two phases – aqueous phase (AQ-bio-oil) and organic phase (ORG-bio-oil). The yield of bio-oil and biochar were measured gravimetrically, and the yield of non-condensable gases was calculated by difference. AQ-bio-oil was characterized by gas chromatography-mass spectroscopy (GC-MS), ³¹P-nuclear magnetic resonance (³¹P-NMR) spectroscopy, Fourier transform infrared (FTIR) spectroscopy, density, acid value, water content and pH. The bio-oil samples were stored in the freezer at -10 °C. AQ-bio-oil was heated at 80 °C for 15 minutes under reduced pressure using a rotary evaporator to concentrate the bio-oil phase. The concentrated AQ (c-AQ-bio-oil) was characterized and used for chemical modification.

5.2.2.2. Characterization of AQ-bio-oil

GC-MS was used to measure the chemical composition of the produced AQ-bio-oil. The AQ-bio-oil was dissolved in 99.9 % pure MeOH (1 mL bio-oil in 9 mL MeOH), filtered with a PTFE syringe filter (0.20 μm), and a 1 μL aliquot was injected into the GC-MS system (Clarus 680 gas chromatograph and Clarus SQ 8C mass spectrometer, PerkinElmer, USA). The injection was performed at a split ratio of 80:1 and an injector temperature of 270 °C. An Elite 1701 MS capillary column (60 m x 0.25 mm ID by 0.25 μm film thickness) with a carrier gas (ultrahigh-purity helium, 99.9999%) flow rate of 1 cm^3 per min and pressure of 17.3 psi were used. The GC furnace was initially held at 50 °C for 4 min, then was ramped from to 280 °C at 5 °C/min, and held at 280 °C for 5 min. The MS was held at 270 °C with an ionization energy of 70 eV. Chromatogram peaks were extracted using TubroMass GC-MS software and peaks were identified with the National Institute of Standards and Technology (NIST) library.

The water content of the bio-oils was measured by Karl-Fisher titration (Metrohm 787 KF Titrino) following the American Society for Testing and Materials protocol – ASTM D4377-00.[29] The pH of bio-oil samples was measured using a pH meter after stirring 1 mL of bio-oil into 50 mL of DI water. The total acid number (TAN) was measured by dissolving 0.5 g bio-oil in 25 ml of 1:1 isopropyl alcohol:water then titrating with 0.1 N KOH to a pH of 11 in accordance with ASTM D664-11a.[30] The density of the bio-oil samples was determined using a 2 mL glass pycnometer according to ASTM D1475-13.[31] Analyses were performed in duplicate.

For ^{31}P -NMR spectroscopy, the bio-oil phases were phosphorylated as per the procedure mentioned in the literature.[32] NHND and chromium(III)acetyl acetonate (20 mg each) were dissolved in the mixture of 3 mL pyridine and 2 mL deuterated chloroform to prepare the stock solution. 550 μL of stock solution was added to around 20 mg of desired bio-oil sample and stirred well. TMDP (150 μL) was then added to the mixture and stirred well to make the solution homogeneous. The prepared solution was then transferred to the NMR spectroscopy tube and the spectrum was acquired with a Bruker Avance II 250 MHz spectrometer using inverse gated decoupling pulse sequence, 90-degree pulse angle, 25 s pulse delay and 128 scans. The hydroxyl content of the bio-oil phases was calculated by integrating relevant peaks compared to the internal standard NHND.

Fourier transform infrared spectroscopy was performed on bio-oil samples and synthesized products using Thermo Scientific Nicolet 6700 FT-IR spectrophotometer equipped with attenuated total reflection (ATR) and OMNIC 7.3 software. IR spectra were collected in the wavenumber range 400 cm^{-1} to 4000 cm^{-1} at a resolution of 4 cm^{-1} and 64 scans.

5.2.2.3. Synthesis and characterization of methacrylated aqueous bio-oil (MeABO)

Methacrylation procedure was adapted from literature[33] and used with modifications. Around 38 g c-AQ-bio-oil was dissolved in 150 mL acetone in a jacketed, glass reactor equipped with mechanical stirrer. Triethylamine (1.2 equiv/OH) was added to the reactor with stirring. Water-methanol coolant was circulated through jacket to reduce the temperature of the reaction mixture to $0\text{ }^{\circ}\text{C}$. Methacryloyl chloride (1.2 equiv/OH) dissolved in acetone was added dropwise to the reaction mixture over 30 minutes. After the addition was completed, the mixture was stirred for 6 hours and the cooling was turned off. The reaction product was heated at $40\text{ }^{\circ}\text{C}$ under reduced

pressure to remove acetone and was further mixed in chloroform. The chloroform phase was washed with water to remove salts. Chloroform was distilled off using rotary evaporator and the product, named as methacrylated aqueous bio-oil (MeABO), was characterized by FTIR spectroscopy, $^1\text{H-NMR}$ spectroscopy and $^{31}\text{P-NMR}$ spectroscopy. $^1\text{H-NMR}$ spectra were collected with Bruker Avance II 600 MHz spectrometer using 64 scans. Deuterated chloroform was used as the solvent with tetramethylsilane added as the reference. Figure 5.1 depicts methacrylation of AQ-bio-oil and further polymerization. Theoretically, it is expected to obtain a mixture of chemically similar compounds predominantly appearing as alkyl methacrylates and aryl methacrylates.

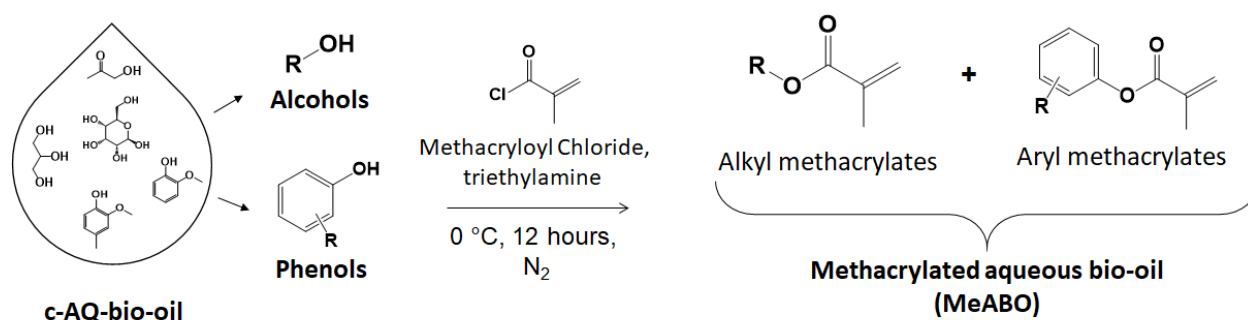


Figure 5.1: Methacrylation of c-AQ-bio-oil

5.2.2.4. Polymerization of methacrylated monomers with AESO

MeABO and AESO were mixed in the proportions explained in Table 5.1. Initiator benzoyl peroxide was ground and added (3 wt%) to each monomer blend. All monomer blends were poured in Teflon cavity mold and heated at 40 °C in a conventional oven and vacuum oven for 1 day each to remove any residual solvent. The samples were heated at 70 °C for 12 hours, 90 °C for 6 hours and 120 °C for 6 hours under vacuum. After the heating program, the samples were allowed to cool down and then taken for further characterization and analysis. The typical reactions and

structures of polymeric systems are described in Figure 5.2, 5.3 and 5.4. R represents alkyl group; whereas Ar stands for aryl group. R can be any group contributed by the hydroxyl compounds present in the original bio-oil. Due to a range of possible, different monomers, it is expected to have a random structure for poly(MeABO) and its crosslinked systems with AESO.

Table 5.1: Preparation of MeABO/AESO blends

Sample Name	Amount of MeABO in the sample	Amount of AESO in the sample	Samples After polymerization
MeABO	100%	--	poly(MeABO)
75:25A	75%	25%	poly(75:25A)
50:50A	50%	50%	poly(50:50A)
25:75A	25%	75%	poly(25:75A)
AESO	--	100%	poly(AESO)

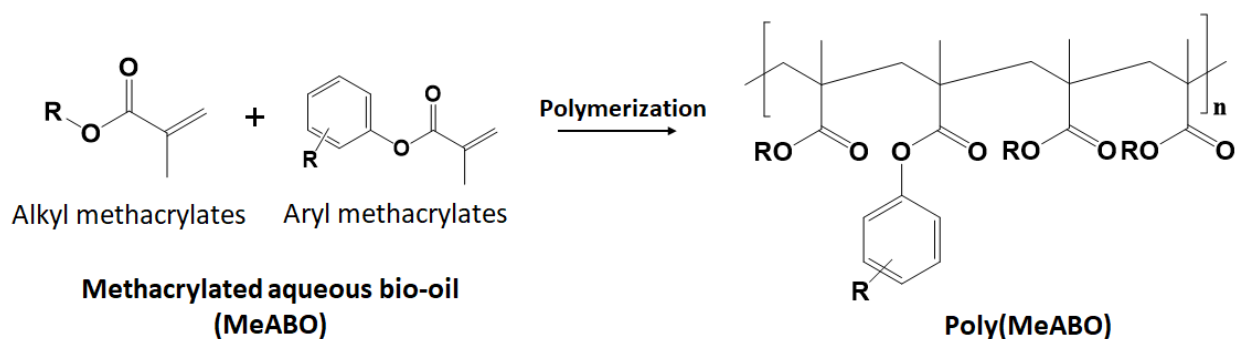


Figure 5.2: Polymerization of MeABO

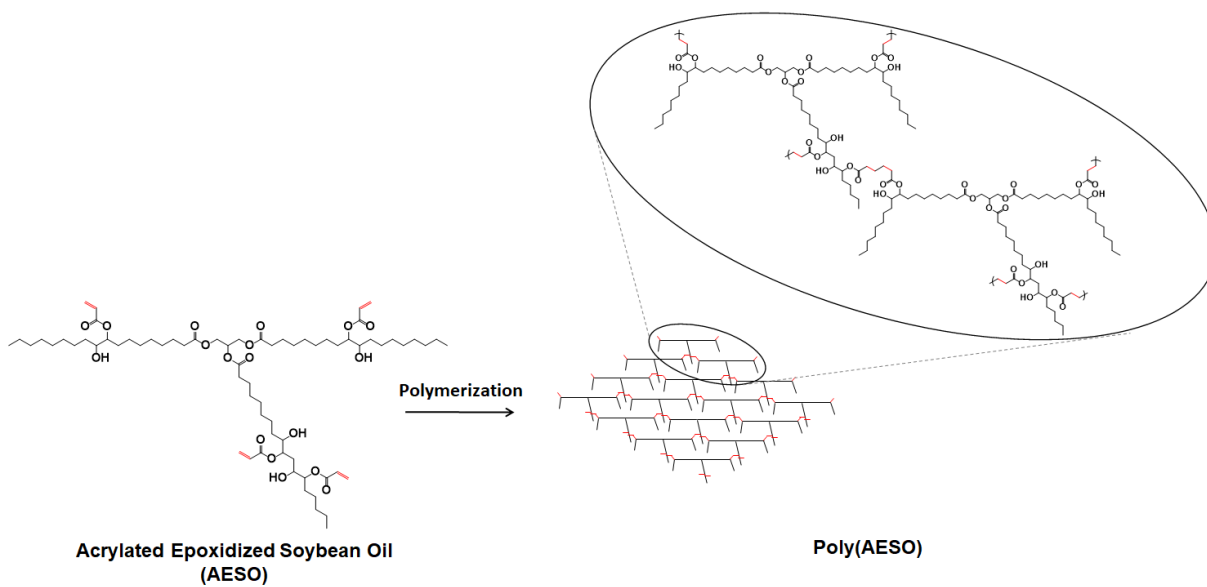


Figure 5.3: Polymerization of AESO

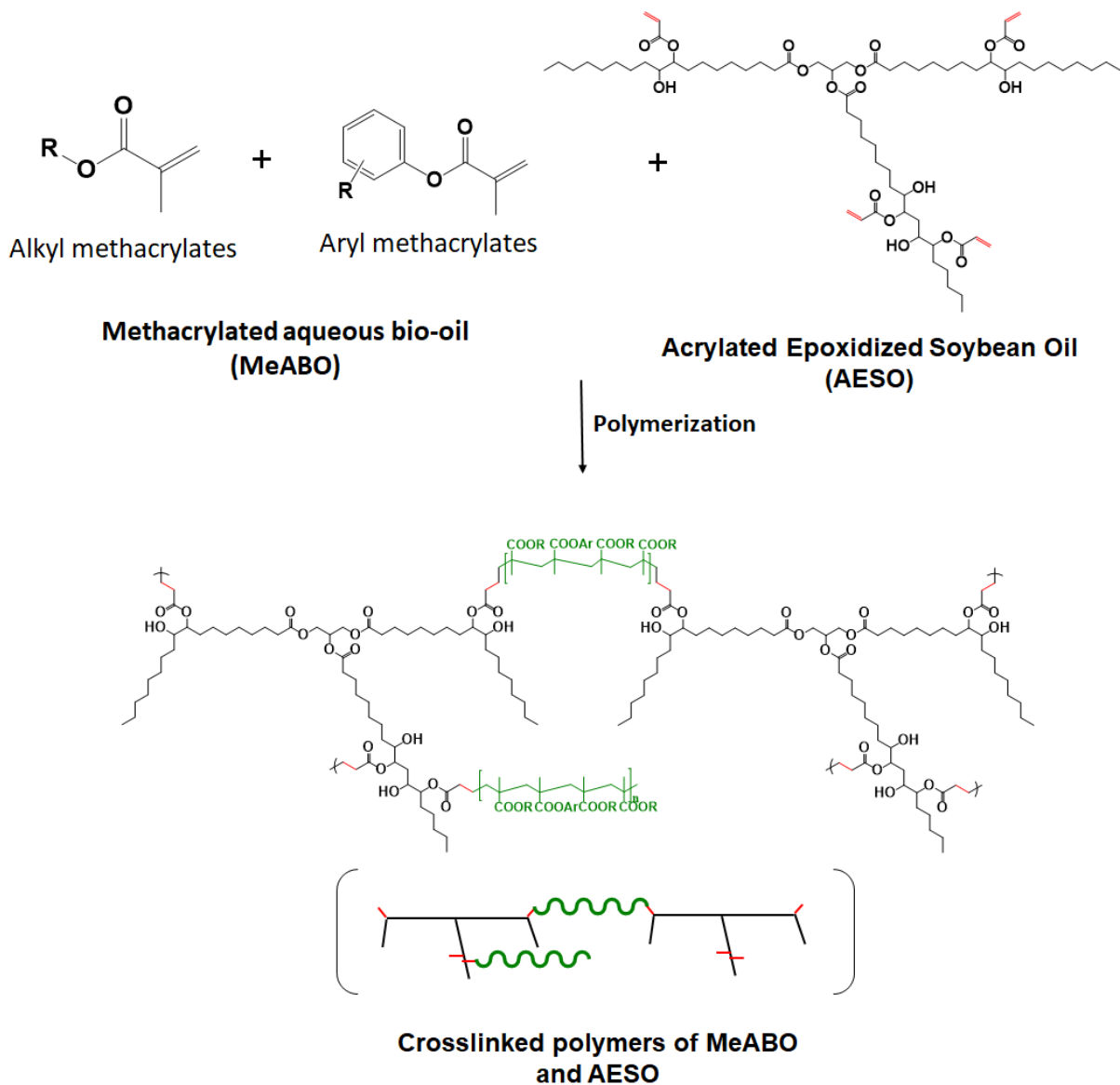


Figure 5.4: Polymerization of MeABO and AESO

5.2.2.5. Soxhlet extraction

The polymer samples were subjected to Soxhlet extraction by refluxing 200 mL dichloromethane for 24 hours using Soxhlet extraction apparatus. After the extraction, the insoluble solids were

dried, and the mass retained for each polymeric system was reported per cent of the initial sample weight.

5.2.2.6. Morphology

Cross-sectional surface morphology of the polymer samples was observed using a scanning electron microscope. The samples were submerged in liquid nitrogen and fractured before coating with gold plasma.

5.2.2.7. Dynamic mechanical analysis

Mechanical and thermo-mechanical evaluation of polymer samples was performed using TA Instruments dynamic mechanical analyzer RSAIII. In first method, tensile analysis was carried out on the specimens with 10 mm initial length and extension rate 10 mm/min at room temperature using the rectangular tensile geometry. Tensile modulus was reported for all the samples. In second method, a cyclic stress is applied at 1 Hz frequency on the horizontal specimen using three-point bending geometry to yield constant 0.1 % strain. The temperature was increased from -100 °C to 100 °C at 5 °C/min. The glass transition temperature, storage modulus and active chains density were reported.

5.2.3. Results and Discussion

5.2.3.1. Characterization of AQ-bio-oil

Pyrolysis process results and the properties of AQ-bio-oil are listed in Table 5.2.

Table 5.2: Properties of AQ-bio-oil

Fast Pyrolysis of Pine	
Bio-oil yield (%)	53.7 ± 0.0
Bio-char yield (%)	30.4 ± 0.0
Non-condensable gas yield (%)	15.9 ± 0.0
AQ-bio-oil	
Water content (%)	49.0 ± 2.6
Total acid number (mg KOH/g bio-oil)	131.3 ± 1.4
Density (g/mL)	1.12 ± 0.00
pH	2.7 ± 0.0

GC-MS analysis of AQ-bio-oil (depicted in Figure 5.5) revealed the major peaks corresponding to the aliphatic compounds. Most of the detected aliphatic compounds can be classified into alcohols, carboxylic acids, aldehydes, ketones and sugars. Substituted phenols and furans were also detected in AQ-bio-oil.

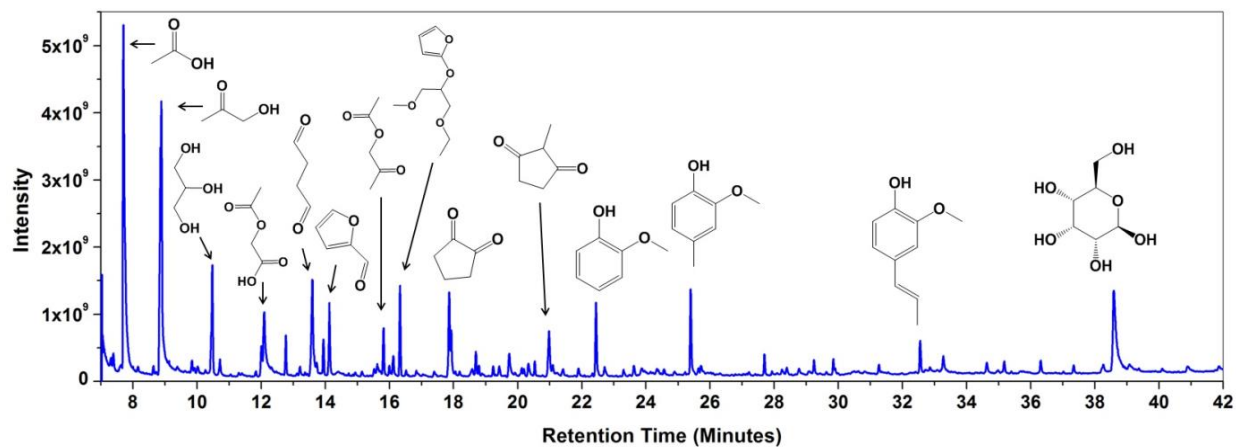


Figure 5.5: Chromatogram of AQ-bio-oil

^{31}P -NMR spectroscopy yielded quantification of hydroxyl number which was in agreement with GC-MS results. The amount of aliphatic OH was observed to be the maximum among all kinds of OH groups. After concentrating AQ-bio-oil by rotary evaporation, it was observed that all organic hydroxyl groups showed higher amount per gram of bio-oil as shown in Figure 5.6. This is due to the removal of a significant amount of water from AQ-bio-oil

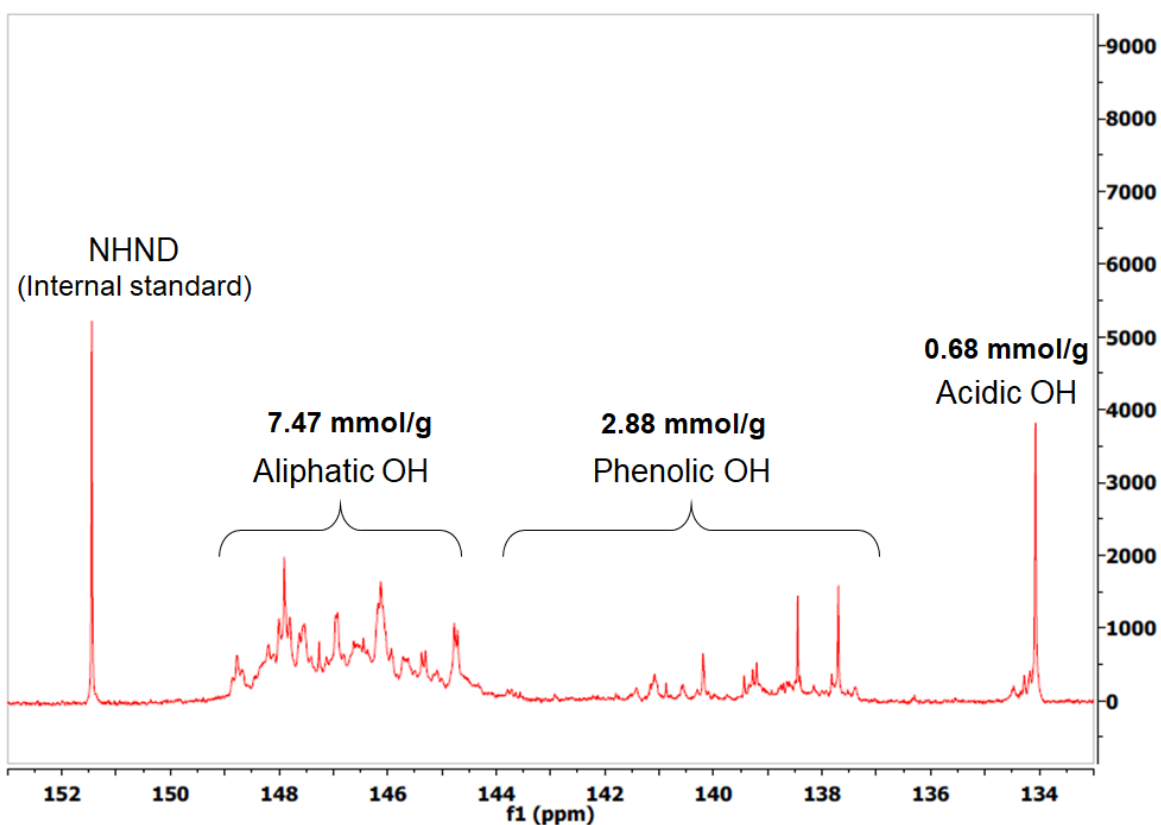


Figure 5.6: ^{31}P -NMR spectra of c-AQ-bio-oil

5.2.3.2. Characterization of MeABO

In the FTIR spectrum of MeABO in Figure 5.7-(b), a peak was observed at 1677 cm^{-1} which was due to the stretching vibration of $\text{C}=\text{C}$ incorporated by methacrylation reaction. A weak stretching

vibration of $sp^2 =C-H$ was also observed near 2983 cm^{-1} . Another important observation was the reduction of broad peak at 3383 cm^{-1} related to O-H stretch. Other peaks present in Figure 5.7-(b) can be assigned to their respective groups: 2928 cm^{-1} for $sp^3\text{ C-H}$, 1722 cm^{-1} for $C=O$, 1150 cm^{-1} for C-O bonded to carbonyl group and 1031 cm^{-1} for C-O on the alcohol side of the ester group.

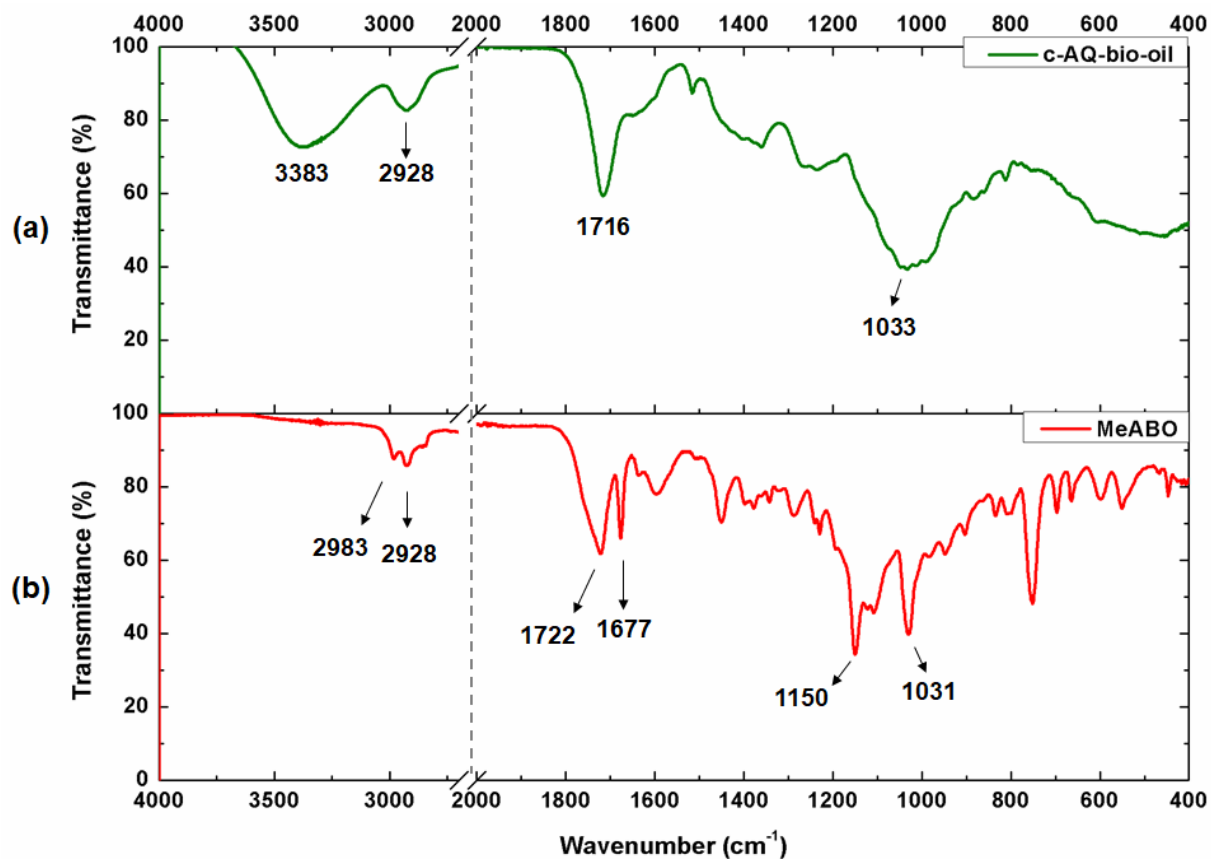


Figure 5.7: FTIR spectra of (a) c-AQ-bio-oil (b) MeABO (Note: all numbers are in cm^{-1})

In Figure 5.8-(a), $^1\text{H-NMR}$ spectrum of MeABO reflected the appearance of peaks at 5.51 and 6.08 ppm due to the protons de-shielded by $C=C$ group. Protons on the $-CH_3$ group adjacent to $C=C$ also caused the appearance of a peak at 1.94 ppm.

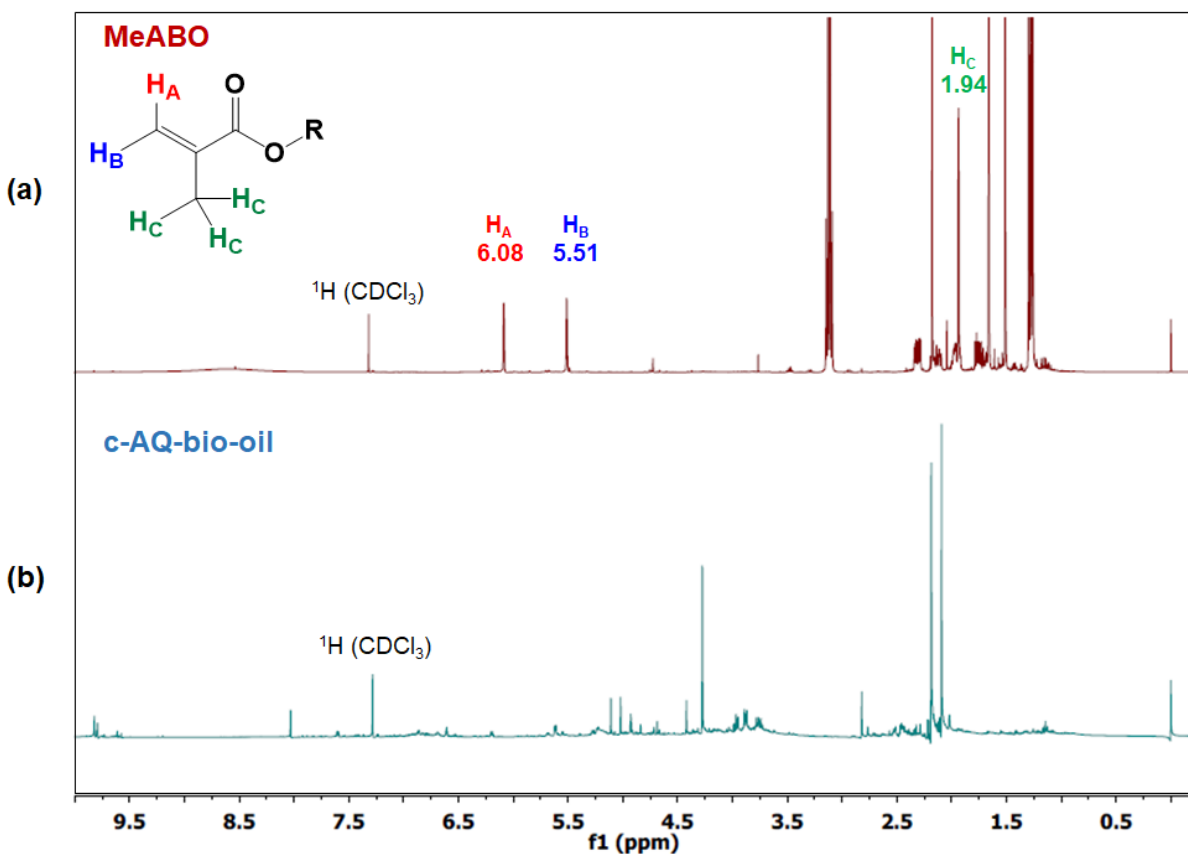


Figure 5.8: ^1H -NMR spectra of (a) MeABO, (b) c-AQ-bio-oil (Note: all numbers are in ppm)

Both FTIR and ^1H -NMR spectroscopy confirmed the presence of olefin functionality in the synthesized methacrylated phase. Quantification of hydroxyl groups by ^{31}P -NMR spectroscopy before and after the modification of AQ-bio-oil is presented in Table 5.3. Methacrylation of c-AQ-bio-oil consumed the most aliphatic OH and all phenolic OH groups. The presence of higher acidic OH value can be attributed to the conversion of methacryloyl chloride to methacrylic acid which is also a methacrylic monomer.

Table 5.3: ³¹P-NMR spectroscopy of AQ-bio-oil, c-AQ-bio-oil and MeABO

OH Type		Range (ppm)	AQ-bio-oil	c-AQ-bio-oil	MeABO	
Aliphatic OH		150 – 145.5	3.95	7.47	0.26	
Phenolic OH	C-5 substituted condensed phenolic OH	β-5	144.7 – 142.8	0.01	0.70	0
		4-O-5	142.8 – 141.7	0	0.11	0
		5-5	141.7 – 140.2	0.14	0.48	0
	Guaiacyl phenolic OH		140.2 – 139.0	0.04	0.54	0
	Catechol type OH		139.0 – 138.2	0.13	0.52	0
	p-hydroxyphenyl OH		138.2 – 137.3	0.06	0.54	0
	Acidic OH		136.6 – 133.6	0.34	0.68	1.58
TOTAL			4.67	11.04	1.84	

5.2.3.3. FTIR spectroscopy of polymers

In Figure 5.9-(a), FTIR spectroscopy of all monomer blends confirmed the presence of C=C peak at 1677 cm⁻¹ coming from MeABO and at 1633 cm⁻¹ coming from AESO. After the polymerization

(Figure 5.9-(b)), the peaks corresponding to C=C disappeared indicating the reaction of C=C functionalities by free radical formed by thermal, homolytic cleavage of peroxide group of benzoyl peroxide initiator. The FTIR spectroscopy proved the exploitation of olefins to carry out the polymerization.

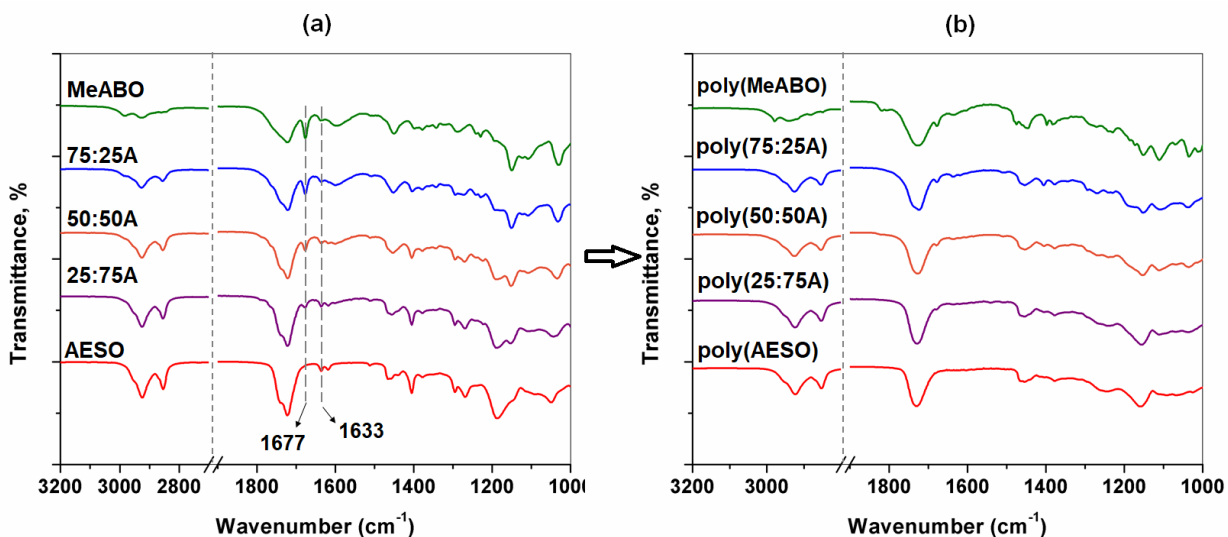


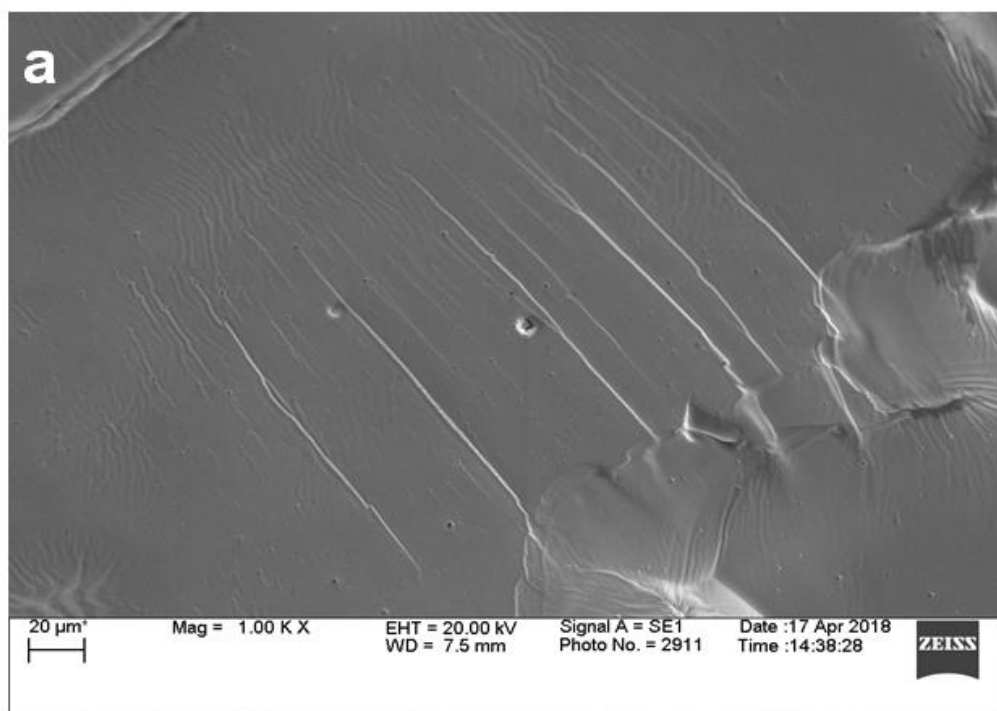
Figure 5.9: FTIR spectroscopy of (a) monomer blends of MeABO and AESO, (b) polymeric systems of MeABO and AESO

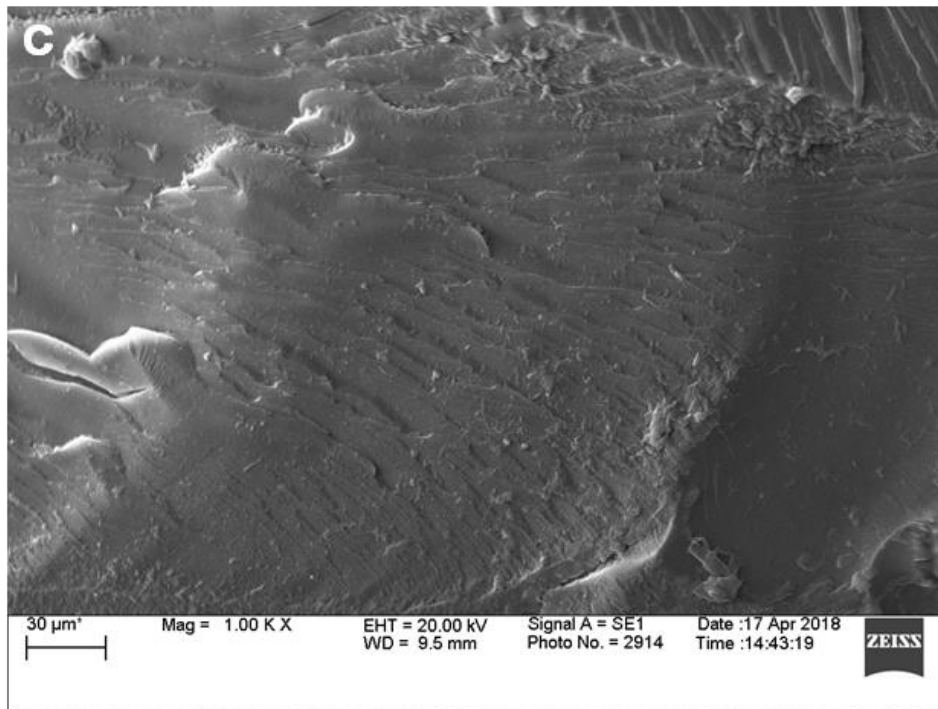
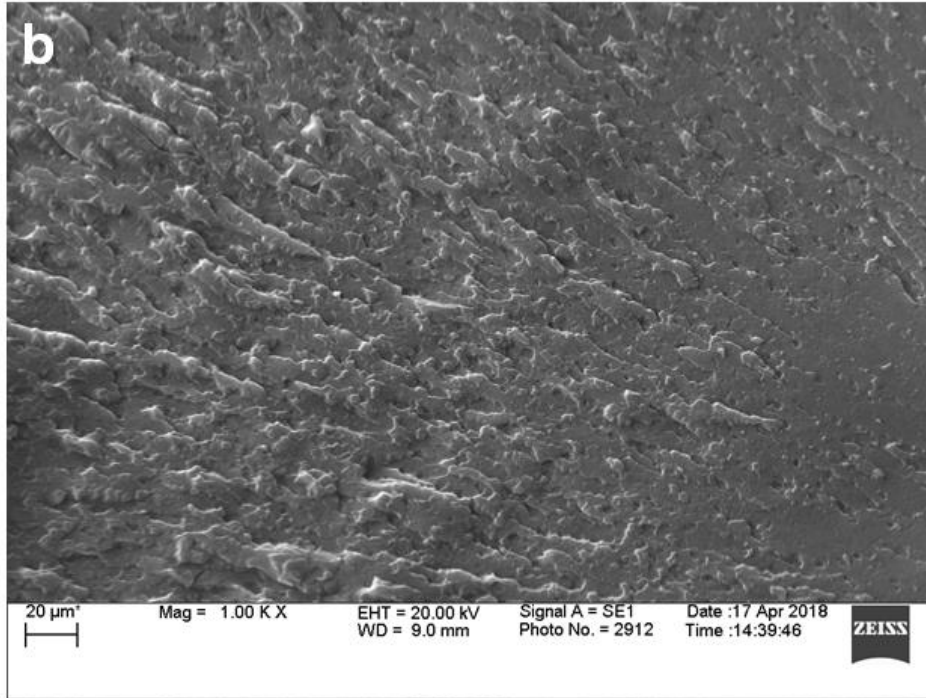
5.2.3.4. Soxhlet extraction

The mass retained after performing Soxhlet extraction with dichloromethane for 24 hours, was observed to increase by raising the amount of AESO. (Table 5.4) Greater amount of AESO produces denser networks which resist the solubilization by dichloromethane. For poly(AESO), highest mass retention was observed with very small amount being solubilized. Increasing the amount of MeABO yields polymer domains with less crosslinking and helps better solubilization.

5.2.3.5. Morphology

As displayed in Figure 5.10, the fracture surfaces of polymeric samples were observed for comparing relative soft/brittle domains, homogeneity and effect of varying ratios of acrylates on them. Cross-sectional surface of Poly(MeABO) appeared to be the smoothest and revealed minute fracture lines. Poly(AESO) and its crosslinked mixtures indicated brittle nature of the polymers. All samples were observed to be considerably homogeneous and had no phase separation.





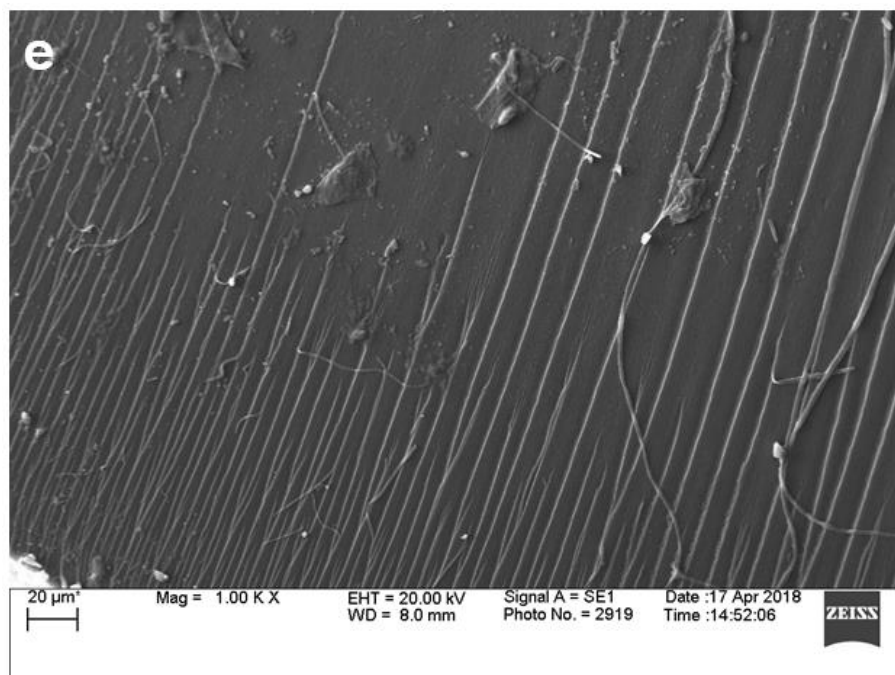
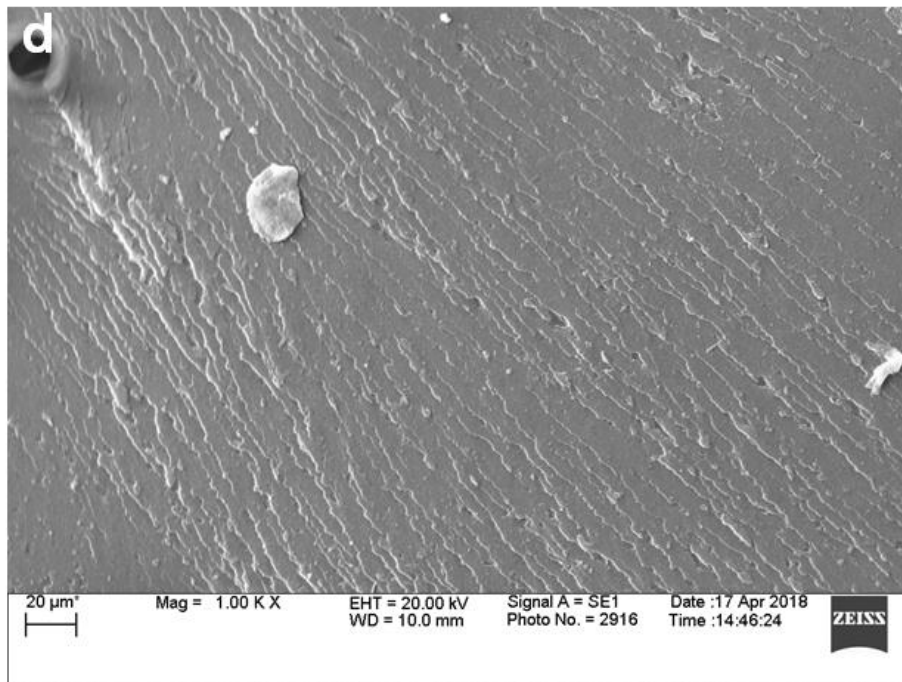


Figure 5.10: Morphology by scanning electron microscopy (a) poly(MeABO), (b) poly(75:25A), (c) poly(50:50A), (d) poly(25:75A) and (e) poly(AESO)

5.2.3.6. Dynamic mechanical analysis of polymers

The tensile modulus of all the polymers is listed in Table 5.4 and was observed to increase with increasing AESO content. This is due to the higher stiffness imparted by higher crosslink density as a result of increasing amount of AESO.

Table 5.4: Thermo-mechanical properties of crosslinked polyacrylate samples

Polymer sample	Tensile Modulus at 25 °C (MPa)	Glass Transition Temperature, T _g (°C)	Storage Modulus, E' (MPa)		Active Chains Density, n (mol/m ³)	Mass Retention (%) by Soxhlet Extraction
			at 25 °C	at 80 °C		
poly(MeABO)	0.6	-29.6 ± 0.0	14.3	N/A	N/A	45
poly(75:25A)	6.2	-21.4 ± 1.4	59.0	5.9	670	61
poly(50:50A)	17.6	-24.2 ± 2.0	53.0	17.7	2007	72
poly(25:75A)	23.4	-24.4 ± 2.1	61.8	21.2	2409	86
poly(AESO)	41.9	-25.5 ± 1.9	113.3	38.7	4380	93

Dynamic analysis with three-point bending revealed the change in storage modulus (real component of the modulus relating to the elastic nature), loss modulus (complex component of the

modulus relating to the viscous nature) and $\tan \delta$ (ratio of loss to storage modulus) with respect to the temperature. Storage moduli at ambient conditions (at 25 °C) and in the rubbery plateau (at 80 °C) and the glass transition temperature (considered at maximum of $\tan \delta$) are reported in Table 5.4. For Poly(MeABO), the rubbery plateau was not observed after a sharp decline in storage modulus. Poly(MeABO) does not have AESO crosslinks and is expected to behave more like a linear, random copolymer. The storage moduli of crosslinked samples increased with increasing AESO content and this phenomenon can be explained by the higher crosslink density of the network. The active chains density (n) of all the samples was calculated by the following equation:

$$n = \frac{E'}{3RT}$$

where E' is storage modulus from the rubbery plateau (at 80 °C), T is the temperature at which corresponding value of modulus is taken and R is the universal gas constant. All quantities bear SI units. The increase in the value of active chains density with increase in AESO content was due to the multi-acrylate functionality of AESO. Figure 5.3 depicts a schematic of a crosslinked structure of poly(AESO) with crosslinking points between the molecular segments; and can be considered to be having higher crosslinking points than that of the polymer structure depicted in Figure 5.4. Two major phenomena affecting glass transition temperature can be considered for the crosslinked polymers presented in the current study – effect of crosslinking by multi-functional acrylates and effect of long, linear aliphatic chains of AESO. Longer the alkyl chain of the acrylate monomer, higher is the plasticizing effect which results in more decline in the glass transition temperature of the polymer.[34] Same effect was observed in the case of polymethacrylates too.[34, 35] As AESO quantity is increased, long aliphatic chains of AESO occupy more volume and space out the polymer chains, imparting a plasticizing effect. Thus, increasing the amount of crosslinkable, multi-functional acrylate with long, aliphatic structure can enhance the modulus by crosslinking

but reduce the glass transition temperature due to the competing, plasticizing effect. Similar observations have been reported earlier in other studies which utilized AESO,[25, 26, 36] soy protein,[37] PEGDMA[38] etc. in the development of polyacrylates. A thorough analysis of the varying effects on the glass transition temperature has been carried out in case of crosslinking and copolymerization of methyl methacrylate and glycol dimethacrylates.[39, 40]

In present study, effect of copolymerization has been assessed by using Fox equation. As discussed earlier, poly(MeABO) resembles a linear copolymer structurally, but poly(AESO) is a crosslinked system. The plasticizing effect of poly(AESO) on glass transition temperature was predicted by estimating the theoretical glass transition temperature of linearly homopolymerized AESO using the group contribution scheme proposed as per the following equation.[41]

$$T_{g_{poly}} = \frac{1}{\sum(M_i + M_j)} \left[\sum_{i=1}^n (T_{g_i} M_i) + \sum_{j=1}^m (T_{g_j} M_j) \right]$$

where, T_{g_i} and M_i are the glass transition temperature and molecular weight of the groups in the main chain; whereas T_{g_j} and M_j are the glass transition temperature and molecular weight of the groups in the side chain of the polymer structure. The effect of crosslinking contribution has been analyzed with the help of Fox and Loshaek model.[42, 43]

$$T_{g_{Total}} = T_{g_{Fox}} + \frac{K}{M_c}$$

where, K/M_c factor represents the crosslinking effect. M_c is the molecular weight of fragments between the crosslinking points and was calculated with the help of experimental values of density of sample and active chains density. The total effect of two effects was studied and compared with the experimental values. The value of K was taken as 5200 K g/mol.[42, 44] The total effect of

crosslinking and plasticizing segments is denoted in Figure 5.11 and was found to be closer to experimental values.

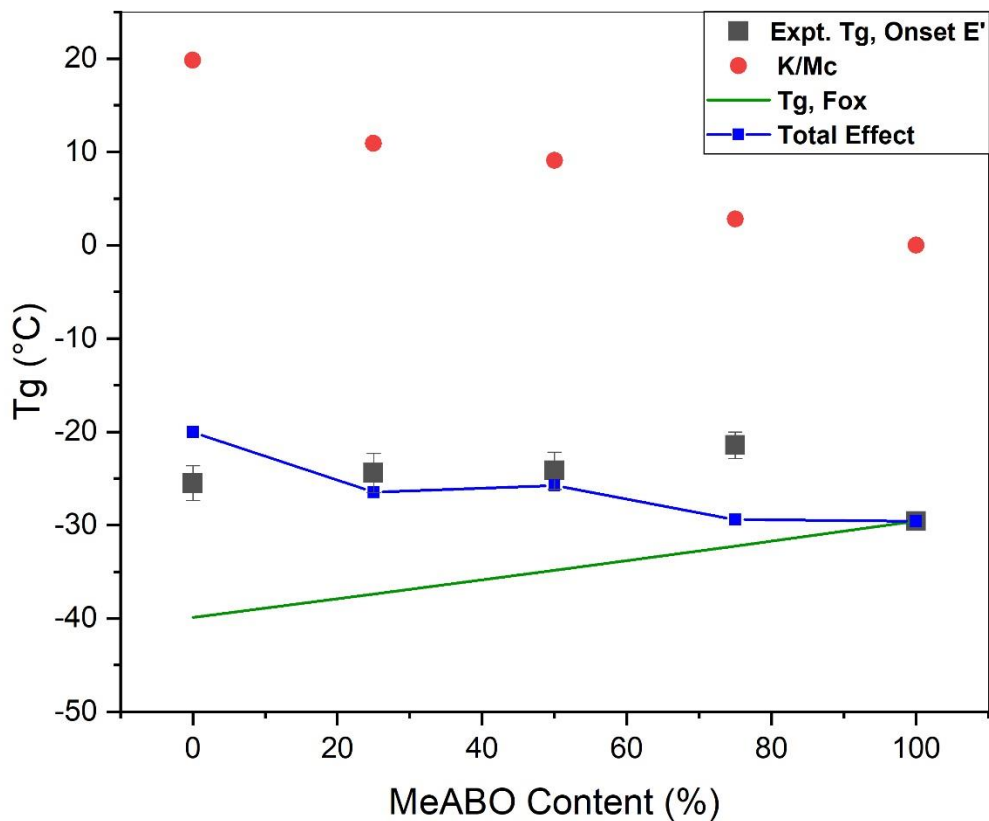


Figure 5.11: Glass transition temperature of crosslinked acrylates: Effects of copolymerization and crosslinking

5.3. Conclusions

Aqueous phase of bio-oil contains modifiable hydroxyl compounds which can be transformed into methacrylic monomers by methacrylation reaction. The methacrylated aqueous bio-oil is a mixture of methacrylic monomers synthesized from corresponding alcohols and phenols present in the

aqueous bio-oil. Free radical polymerization of methacrylated aqueous bio-oil is possible and yields a predominantly non-crosslinked copolymer. The mechanical properties of methacrylated bio-oil are improved by crosslinking with acrylated epoxidized soybean oil; however, the glass transition temperature is reduced due to the plasticizing effect of long, aliphatic chains of the fatty acid portion present in acrylated epoxidized soybean oil. The effect of crosslink density of polymeric samples is evident from the measured values of tensile modulus, storage modulus, active chains density and mass retention by Soxhlet extraction. The experimental values of glass transition temperature can be fitted with the help of Fox and Loshaek model. Morphological characteristics are similar in case of all polymeric samples with differences appearing in the brittle fracture in case of crosslinked polymers. Utilization of aqueous bio-oil and soybean oil, both of which are biomass-derived, tend to enhance sustainability of the crosslinked polymers which can be used in the applications of elastomers, packaging materials and composites.

References

- [1] N. Terashima, K. Kitano, M. Kojima, M. Yoshida, H. Yamamoto, U. Westermark, Nanostructural assembly of cellulose, hemicellulose, and lignin in the middle layer of secondary wall of ginkgo tracheid, *Journal of Wood Science* 55(6) (2009) 409-416.
- [2] S.C. Capareda, Pyrolysis, in: S.C. Capareda (Ed.), *Introduction to Biomass Energy Conversions*, CRC Press, Boca Raton, 2014, p. 346.
- [3] A.V. Bridgwater, D. Meier, D. Radlein, An overview of fast pyrolysis of biomass, *Organic Geochemistry* 30(12) (1999) 1479-1493.
- [4] S.C. Capareda, Biomass Liquefaction, in: S.C. Capareda (Ed.), *Introduction to Biomass Energy Conversions*, CRC Press, Boca Raton, 2014, pp. 439-470.
- [5] F. Behrendt, Y. Neubauer, M. Oevermann, B. Wilmes, N. Zobel, Direct liquefaction of biomass, *Chemical Engineering & Technology* 31(5) (2008) 667-677.
- [6] T. Bridgwater, Challenges and Opportunities in Fast Pyrolysis of Biomass: Part I Introduction to the technology, feedstocks and science behind a promising source of fuels and chemicals, *Johnson Matthey Technology Review* 62(1) (2018) 118-130.
- [7] F.J. Campanario, F.J.G. Ortiz, Techno-economic assessment of bio-oil aqueous phase-to-liquids via Fischer-Tropsch synthesis and based on supercritical water reforming, *Energy Conversion and Management* 154 (2017) 591-602.

- [8] R.J. Evans, T.A. Milne, Molecular characterization of the pyrolysis of biomass. 1. Fundamentals, *Energy & Fuels* 1(2) (1987) 123-137.
- [9] L. Garcia, R. French, S. Czernik, E. Chornet, Catalytic steam reforming of bio-oils for the production of hydrogen: effects of catalyst composition, *Applied Catalysis a-General* 201(2) (2000) 225-239.
- [10] T. Bridgwater, Challenges and Opportunities in Fast Pyrolysis of Biomass: Part II Upgrading options and promising applications in energy, biofuels and chemicals, *Johnson Matthey Technology Review* 62(2) (2018) 150-160.
- [11] E.C. Vagia, A.A. Lemonidou, Thermodynamic analysis of hydrogen production via steam reforming of selected components of aqueous bio-oil fraction, *International Journal of Hydrogen Energy* 32(2) (2007) 212-223.
- [12] E.C. Vagia, A.A. Lemonidou, Thermodynamic analysis of hydrogen production via autothermal steam reforming of selected components of aqueous bio-oil fraction, *International Journal of Hydrogen Energy* 33(10) (2008) 2489-2500.
- [13] C.F. Yan, F.F. Cheng, R.R. Hu, Hydrogen production from catalytic steam reforming of bio-oil aqueous fraction over Ni/CeO₂-ZrO₂ catalysts, *International Journal of Hydrogen Energy* 35(21) (2010) 11693-11699.
- [14] F. Bimbela, M. Oliva, J. Ruiz, L. Garcia, J. Arauzo, Hydrogen production via catalytic steam reforming of the aqueous fraction of bio-oil using nickel-based coprecipitated catalysts, *International Journal of Hydrogen Energy* 38(34) (2013) 14476-14487.
- [15] J.A. Medrano, M. Oliva, J. Ruiz, L. Garcia, J. Arauzo, Hydrogen from aqueous fraction of biomass pyrolysis liquids by catalytic steam reforming in fluidized bed, *Energy* 36(4) (2011) 2215-2224.

- [16] S.M. Liu, M.Q. Chen, L. Chu, Z.L. Yang, C.H. Zhu, J. Wang, M.G. Chen, Catalytic steam reforming of bio-oil aqueous fraction for hydrogen production over Ni-Mo supported on modified sepiolite catalysts, *International Journal of Hydrogen Energy* 38(10) (2013) 3948-3955.
- [17] F.J.G. Ortiz, F.J. Campanario, P. Ollero, Supercritical water reforming of model compounds of bio-oil aqueous phase: Acetic acid, acetol, butanol and glucose, *Chemical Engineering Journal* 298 (2016) 243-258.
- [18] B.S. Hernandez, M. Barde, B. Via, M.L. Auad, Sustainable products from bio-oils, *Mrs Bulletin* 42(5) (2017) 365-370.
- [19] A. Effendi, H. Gerhauser, A.V. Bridgwater, Production of renewable phenolic resins by thermochemical conversion of biomass: A review, *Renewable & Sustainable Energy Reviews* 12(8) (2008) 2092-2116.
- [20] M. Barde, S. Adhikari, B.K. Via, M.L. Auad, Synthesis and Characterization of Epoxy Resins from Fast Pyrolysis Bio-oil, *Green Materials* (2018) 1-9.
- [21] B. Sibaja, S. Adhikari, Y. Celikbag, B. Via, M.L. Auad, Fast pyrolysis bio-oil as precursor of thermosetting epoxy resins, *Polymer Engineering and Science* (2017) 1-12.
- [22] Y. Celikbag, S. Meadows, M. Barde, S. Adhikari, G. Buschle-Diller, M.L. Auad, B.K. Via, Synthesis and Characterization of Bio-oil-Based Self-Curing Epoxy Resin, *Industrial & Engineering Chemistry Research* 56(33) (2017) 9389-9400.
- [23] H.W. Li, N. Mahmood, Z. Ma, M.Q. Zhu, J.Q. Wang, J.L. Zheng, Z.S. Yuan, Q. Wei, C. Xu, Preparation and characterization of bio-polyol and bio-based flexible polyurethane foams from fast pyrolysis of wheat straw, *Industrial Crops and Products* 103 (2017) 64-72.

- [24] Y.H. Wang, J.P. Wu, F. Yu, P. Chen, R. Ruan, I&EC 62-Preparation of polyurethane foam from microwave pyrolytic bio-oils, Abstracts of Papers of the American Chemical Society 234 (2007).
- [25] L. Jong, Z. Liu, Biobased Composites From Crosslinked Soybean Oil and Thermoplastic Polyurethane, *Polymer Engineering and Science* 57(3) (2017) 275-282.
- [26] C.Q. Zhang, M.G. Yan, E.W. Cochran, M.R. Kessler, Biorenewable polymers based on acrylated epoxidized soybean oil and methacrylated vanillin, *Materials Today Communications* 5 (2015) 18-22.
- [27] B. Podkoscielna, M. Goliszek, O. Sevastyanova, New approach in the application of lignin for the synthesis of hybrid materials, *Pure and Applied Chemistry* 89(1) (2017) 161-171.
- [28] P. Kim, S. Weaver, K. Noh, N. Labbe, Characteristics of Bio-Oils Produced by an Intermediate Semipilot Scale Pyrolysis Auger Reactor Equipped with Multistage Condensers, *Energy & Fuels* 28(11) (2014) 6966-6973.
- [29] ASTM D4377-00, Standard Test Method for Water in Crude Oils by Potentiometric Karl Fischer Titration, ASTM International, West Conshohocken, PA, 2011.
- [30] ASTM D664-11a, Standard Test Method for Acid Number of Petroleum Products by Potentiometric Titration, ASTM International, West Conshohocken, PA, 2011.
- [31] ASTM D1475-13, Standard Test Method for Density of Liquid Coatings, Inks, and Related Products, ASTM International, West Conshohocken, PA, 2013.
- [32] H.X. Ben, A.J. Ragauskas, NMR Characterization of Pyrolysis Oils from Kraft Lignin, *Energy & Fuels* 25(5) (2011) 2322-2332.

- [33] S. Wang, A.W. Bassett, G.V. Wieber, J.F. Stanzione, T.H. Epps, Effect of Methoxy Substituent Position on Thermal Properties and Solvent Resistance of Lignin-Inspired Poly(dimethoxyphenyl methacrylate)s, *Acs Macro Letters* 6(8) (2017) 802-807.
- [34] F. Fleischhaker, A.P. Haehnel, A.M. Misske, M. Blanchot, S. Haremza, C. Barner-Kowollik, Glass-Transition-, Melting-, and Decomposition Temperatures of Tailored Polyacrylates and Polymethacrylates: General Trends and Structure-Property Relationships, *Macromolecular Chemistry and Physics* 215(12) (2014) 1192-1200.
- [35] S.S. Rogers, L. Mandelkern, Glass formation in polymers. 1. The glass transition of the poly-(n-alkyl methacrylates), *Journal of Physical Chemistry* 61(7) (1957) 985-990.
- [36] S. Oprea, Properties of polymer networks prepared by blending polyester urethane acrylate with acrylated epoxidized soybean oil, *Journal of Materials Science* 45(5) (2010) 1315-1320.
- [37] F.P. Wang, J.F. Wang, C.P. Wang, F.X. Chu, X.H. Liu, J.Y. Pang, Fabrication of soybean protein-acrylate composite mini-emulsion toward wood adhesive, *European Journal of Wood and Wood Products* 76(1) (2018) 305-313.
- [38] M.J. Barwood, C. Breen, F. Clegg, C.L. Hammond, The effect of organoclay addition on the properties of an acrylate based, thermally activated shape memory polymer, *Applied Clay Science* 102 (2014) 41-50.
- [39] S. Loshaek, T.G. Fox, Cross-linked Polymers. I. Factors influencing the efficiency of cross-linking in copolymers of methyl methacrylate and glycol dimethacrylates, *Journal of American Chemical Society* 75(14) (1953) 3544-3550.
- [40] S. Loshaek, Crosslinked Polymers. II. Glass temperatures of copolymers of methyl methacrylate and glycol dimethacrylates, *Journal of Polymer Science Part A: General Papers* 15(80) (1955) 391-404.

- [41] C. Camacho-Zuniga, F.A. Ruiz-Trevino, A new group contribution scheme to estimate the glass transition temperature for polymers and diluents, *Industrial & Engineering Chemistry Research* 42(7) (2003) 1530-1534.
- [42] B. Sibaja, J. Sargent, M.L. Auad, Renewable Thermoset Copolymers from Tung Oil and Natural Terpenes, *Journal of Applied Polymer Science* 131(23) (2014) 7.
- [43] M.L. Auad, M. Aranguren, J. Borrajo, Epoxy-based divinyl ester resin styrene copolymers: Composition dependence of the mechanical and thermal properties, *Journal of Applied Polymer Science* 66(6) (1997) 1059-1066.
- [44] J. La Scala, R.P. Wool, Property analysis of triglyceride-based thermosets, *Polymer* 46(1) (2005) 61-69.

General Conclusions

Wood, a lignocellulosic biomass, was pyrolyzed using fast pyrolysis process for producing liquid bio-oil. Bio-oil was utilized as raw material for the synthesis of monomers and polymers. Using GC-MS, ³¹P-NMR spectroscopy and FTIR spectroscopy, the chemical characterization of bio-oil yielded compositional information and confirmed the presence of specific functional groups including hydroxyl, phenolic, carboxyl, etc. The functional groups were reacted with reagents to produce desired monomeric structures. Monomers were polymerized/co-crosslinked to construct bio-based crosslinked polymer networks with high performance.

In chapter 2, bio-oil was co-reacted with phenol and formaldehyde to synthesize phenol-formaldehyde resin – BioNovolac. Phenol was replaced by 10 wt% and 50 wt% of bio-oil during synthesis of BioNovolac resins which were then interpenetrated with α -resorcylic-based epoxy resin (GDGB) to develop semi-interpenetrating polymer networks (semi-IPN). Crosslinking of GDGB was carried out using 4-DMAP in immediate presence of BioNovolac resin. Dynamic mechanical analysis proved that the semi-IPNs of BioNovolac and GDGB displayed high glass transition temperature and modulus. As 4-DMAP was used as anionic initiator, the quantity of 4-DMAP needed for polymerization was typically less, indicating an overall reduction in consumption of petrochemicals during the developments of crosslinked polymers with high performance. BioNovolac/GDGB semi-IPNs can be potentially used as the polymeric matrices for composite applications.

In chapter 3, the treatment of bio-oil and BioNovolac with epichlorohydrin led to the synthesis of varying epoxy resins that could be crosslinked with amine crosslinking agents. FTIR spectroscopy, ^{31}P -NMR spectroscopy and measurement of epoxy equivalent weight by HBr/acetic acid titration proved the successful formation of epoxide rings. Epoxy resins were crosslinked by Jeffamine T-403 hardener at elevated temperature. All epoxy, and epoxy-novolac thermoset systems displayed comparable glass transition temperature and storage modulus to petroleum-based analogues as assessed by dynamic mechanical analysis and differential scanning calorimetry. Crosslinked systems possessing novolac backbone showed higher thermo-mechanical performance and crosslinking density. Bio-oil and BioNovolac based epoxy resins could find applications in coatings, adhesives and composites.

In chapter 4, the organic phase of bio-oil was reacted with cyanogen bromide in basic medium for synthesizing cyanate ester monomers which were heated at elevated temperature under vacuum to yield crosslinked cyanate esters. For inducing multi-functionality, organic phase of bio-oil was reacted with 1,3,5-trioxane in acidic medium to form ORG-biphenol which chemically resembled bisphenol-A. Cyanation was carried out with ORG-biphenol followed by curing program to develop cyanate ester materials with superior thermo-mechanical performance. FTIR spectroscopy confirmed the presence of $\text{O}-\text{C}\equiv\text{N}$ groups after cyanation reaction. Excellent glass transition temperature upto $378\text{ }^{\circ}\text{C}$ was recorded for cyanate ester derived from ORG-biphenol and surpassed bisphenol-A based cyanate ester.

In the last chapter, the aqueous phase of bio-oil was used to obtain methacrylic monomers by methacrylation reaction. Methacrylated aqueous bio-oil was polymerized in presence of acrylated epoxidized soybean oil by benzoyl peroxide to yield crosslinked polyacrylate materials. Polyacrylates were found to have low glass transition temperatures ideal for elastomeric and

packaging applications. Crosslinking and plasticizing effects of acrylated epoxidized soybean oil on the glass transition temperatures were studied with Fox and Loshaek model. Group contribution scheme was employed for the prediction of theoretical glass transition temperature of homopolymerized AESO.

In general, it can be concluded that the organic compounds from the bio-oil can be transformed into monomers and can be successfully polymerized to yield crosslinked thermosetting polymers. The performance of bio-oil-derived thermosetting polymers was observed to be on par with their petrochemical-based analogues. Minimum separation and purification of bio-oil was performed, indicating the reduction in process complexity. Further, the bio-oil-based polymers proved to have good compatibility with other bio-based systems as observed in the case of α -resorcylic acid-based epoxy and acrylated epoxidized soybean oil. Utilization of aqueous phase of bio-oil helped to add value to the aqueous phase often considered as a waste stream. Pyrolysis of lignocellulosic biomass can be employed for efficient production of bio-oil that serves to be reservoir of chemicals for developing high performance crosslinked polymers with increased bio-content and hence, the sustainability.